EFFECT OF BAGASSE ASH AND SISAL FIBER ON STRENGTH AND COMPRESSIBILITY PROPERTIES OF EXPANSIVE SOIL: IN CASE OF DUKEM TOWN

Kerima Hussen Ebrahim

A Thesis Submitted to the Department of Civil Engineering,
School of Civil Engineering and Architecture

Presented in Partial Fulfillment of the Requirement for the Degree of Master's in Civil Engineering (Specialization in Geotechnical Engineering)

Office of Graduate Studies
Adama Science and Technology University

June 2022

Adama, Ethiopia

EFFECT OF BAGASSE ASH AND SISAL FIBER ON STRENGTH AND COMPRESSIBILITY PROPERTIES OF EXPANSIVE SOIL: IN CASE OF DUKEM TOWN

Kerima Hussen Ebrahim
Advisor: Srikanth Vadlamudi (Ph.D.)

A Thesis Submitted to the Department of Civil Engineering,
School of Civil Engineering and Architecture

Presented in Partial Fulfillment of the Requirement for the Degree of Master's in Civil Engineering (Specialization in Geotechnical Engineering)

Office of Graduate Studies

Adama Science and Technology University

June 2022
Adama, Ethiopia

DECLARATION

I hereby declare that this Master Thesis entitled “Effect of Bagasse Ash and Sisal Fiber on Strength and Compressibility Properties of Expansive Soil: In Case of Dukem Town" is my original work. That is, it has not been submitted for the award of any academic degree, diploma or certificate in any other university. All sources of materials that are used for this thesis have been duly acknowledged through citation.

Kerima Hussen	____________________	____________________
Name of the student	Signature	Date

RECOMMENDATION

I, the advisor of this thesis, hereby certify that I have read the revised version of the thesis entitled “Effect of Bagasse Ash and Sisal Fiber on Strength and Compressibility Properties of Expansive Soil: In Case of Dukem Town” prepared under my guidance by Kerima Hussen submitted in partial fulfillment of the requirements for the degree of Mater’s of Science in Civil Engineering (specialization in Geotechnical Engineering). Therefore, I recommend the submission of revised version of the thesis to the department following the applicable procedures.

____________________	________________________	________________
Advisor	Signature	Date

APPROVAL PAGE

I, the advisor of this thesis entitled "Effect of Bagasse Ash and Sisal Fiber on Strength and Compressibility Properties of Expansive Soil: In Case of Dukem Town" and developed by Kerima Hussen, hereby certify that the recommendation and suggestions made by the board of examiners are appropriately incorporated into the final version of the thesis.

______________________ ______________________ ___________________

Advisor Signature Date

We, the undersigned, members of the Board of Examiners of the thesis by Kerima Hussen have read and evaluated the thesis entitled "Effect of Bagasse Ash and Sisal Fiber on Strength and Compressibility Properties of Expansive Soil: In Case of Dukem Town" and examined the candidate during open defense. This is, therefore, to certify that the thesis is accepted for partial fulfillment of the requirement of the degree of Master of Science in Civil Engineering (specialization in Geotechnical Engineering).

______________________________ ________________________ _________________

Chairperson Signature Date

______________________________ ________________________ _________________

Internal Examiner Signature Date

______________________________ ________________________ _________________

External Examiner Signature Date

Finally, approval and acceptance of the thesis is contingent upon the submission of its final copy to the Office of Postgraduate Studies (OPGS) through the Department Graduate Council (DGC) and School Graduate Committee (SGC).

______________________________ ____________________ _____________________

Department Head Signature Date

______________________________ _____________________ _____________________

School Dean Signature Date

______________________________ _____________________ ____________________

Office of Postgraduate Studies, Dean Signature Date

ACKNOWLEDGEMENT

I would like to thank God for granting me the courage, strength, and health to finish this research. I am grateful to my organization Adama Science and Technology University providing scholarship opportunities.

I would like to express my deepest gratitude to my advisor Dr. Srikanth Vadlamudi his valuable advice, and critical comments during my research work. My special thanks to Oromia engineering corporation and ASTU geotechnical laboratory for letting me use and carry out relevant tests in their laboratory with special supervision and guidance.

Finally, I would like to extend my heartfelt thanks to my mother Toyba Oumer for her unlimited support and initiation for this work, and also, thank my beloved family for their help.

TABLE OF CONTENTS

LIST OF TABLES

LIST OF FIGURES

LIST OF ABBREVIATIONS

AASHTO	American Association of State Highway and Transportation Officials
ASTM	American Standard of Testing Materials
BA	Bagasse ash
CBR	California Bearing Ratio
CH	Inorganic Highly Plastic Clays
CL	Inorganic Clays of Low Plasticity
FA	Fly ash
FS	Free Swell
FSI	Free swell index
IS	Indian standard
LL	Liquid Limit
MDD	Maximum Dry Density
MH	Inorganic Silt of High Plasticity
ML	Inorganic Silt of Low Plasticity
NMC	Natural Moisture Content
ODFS	Oriented distributed fiber-reinforced soil
OMC	Optimum Moisture Content
OH	Organic Silts and Organic Clays of High Plasticity
OL	Organic Silts and Organic Clays of Low Plasticity
PI	Plasticity Index
PL	Plastic Limit
RDFS	Randomly Distributed Natural Fiber reinforcement
SF	Sisal fiber
SCBA	Sugarcane bagasse ash
TP	Test Pit
UCS	Unconfined Compressive Strength
USCS	Unified Soil Classification System
WAC	Water absorption capacity
XRD	X - ray diffraction

LIST OF SYMBOLS

a_v - Coefficient of compressibility

C_c - Compression Index

C_r - Recompression index

C_u - Undrained cohesion

C_v - Coefficient of consolidation

e_o - Initial void ratio

e -Void ratio

H_s - Height of solid soil sample

m_v - Coefficient of volume change

P – Pressure

q_u - Unconfined compressive stress

t_{50}- Time at 50% of primary consolidation

t_{90} - Time at 90% of primary consolidation

σ_1 - Normal stress

ABSTRACT

Expansive soils have a large volume change potential when the moisture content changes and cause foundation damage when wetting-drying cycles. Proper application of soil stabilization methods can significantly reduce the damage that results from expansive soil problems. In an attempt to make these poor soils more appropriate for use in engineering projects, different stabilization techniques were applicable. In this study, the combined effect of bagasse ash and sisal fiber was investigated. First bagasse ash was mixed with expansive soil in varying proportions of 0%,3%,6%, and 9% the effect of bagasse ash on the expansive soil was investigated by performing Atterberg limit, free swell, compaction, and unconfined compressive strength for un cured and 7 days cured condition. The results of these test have shown that the bagasse ash can reduce plasticity index, and free swell, and improves the unconfined compressive strength value on both uncured and 7 days cured condition. Trial mixes showed that the use of 6% bagasse ash gave better results. The effect of sisal fiber on the bagasse ash stabilized soil was also investigated by taking the optimum content of bagasse ash (6%). the expansive soil stabilized with optimum bagasse ash was further stabilized with 0.5 %, 1%, and 1.5% by dry weight of soil and varying the lengths (10mm,20mm, and 30mm). The compaction test and unconfined compressive strength test were conducted to see the effects of sisal fiber on bagasse ash stabilized expansive soil. The results showed that when increasing the fiber length and fiber content the maximum dry density decreases and the optimum moisture content increases. The unconfined compressive strength was improved, when 6% bagasse ash stabilized soil mixed with 1 % and 20mm length of Sisal fiber. The effect of bagasse ash and sisal fiber on the consolidation characteristics of soil such as coefficient of consolidation, coefficient of volume compressibility, compression and recompression index, and void ratio of the samples were studied by varying the percentages of bagasse ash (0%,3%,6%, and 9%.) and bagasse ash stabilized soil with different percentages of sisal fiber with optimum length selected based on strength value 20mm (0.5%,1%, and 1.5%). The analysis of results showed that bagasse ash considerably increases the coefficient of consolidation of the expansive soil up to 6% addition by dry mass of soil. and the compression index and re-compression index decreased when soil is stabilized with bagasse ash only and reinforced with sisal fiber up to the addition of 6% bagasse ash and 20 mm 1% sisal fiber. Coefficient of volume compressibility decreases with increasing of bagasse ash alone and reinforcing with sisal fiber on the expansive soil. So, these two stabilizing materials can be used for ground improvement. The combination of Bagasse ash and sisal fiber is more effective than the addition of bagasse ash alone for the strength improvement of expansive soil and for controlling the consolidation characteristics. The combination of 6% bagasse ash and 20 mm 1% sisal fiber gave a better result.

Keywords*: Sisal fiber, Bagasse ash, Expansive soil, Compressibility, Strength improvement*

1 INTRODUCTION

1.1 Background

Expansive soils exhibit massive volume change against fluctuations of moisture content. Shrinkage and expansion of soil can commonly take place near the ground surface, where it is directly subjected to seasonal and environmental variations. Construction of civil engineering structures on expansive soils is highly risky, as this type of soil is susceptible to seasonal drying and wetting cycles, causing significant deformations. Frequent soil movements can generate cracks and damage residential buildings, roads, and other civil structures directly placed on this type of problematic soil (Dang, 2019).

The stability and durability of pavements and buildings are largely dependent on the characteristics of the soil underneath. The soil mass might vary from non-expansive to highly expansive and when the expansive soils are encountered it poses problems unless and otherwise proper improvement measures are taken for proper treatment of expansive soils, it is important to adequately identify and understand the characteristics of expansive soils and materials used for soil treatment. Proper treatment procedures should also be adopted for successful characteristic improvement of expansive soil (Asres, 2017). Several research works are being carried out to study the behavior of expansive soil, it is known that when structures built over expansive soil cause serious damage due to its alternative swelling and shrinkage behavior. To protect the structures, build over the expansive soil, from damage and to increase their design life, it is necessary to modify the geotechnical properties of natural soil.

When the soil beneath the lightweight structure is expansive, it has to be avoided to construct on it before improving its strength properties. so, it should be replaced by another soil having good properties that meet the strength requirement, to achieve economy in construction. If the appropriate soil is not available in the nearby areas to replace the expansive soil, it has to be transported from a long distance, these may cause an increase in cost and time of construction. Hence, there is a need for soil improvement by using locally available materials.

Proper application of soil stabilization methods can significantly reduce the damage that results from expansive soil problems. In an attempt to make these poor soils more appropriate for use in engineering projects, different stabilization techniques are applicable now like cement, lime, and fly ash, and soil reinforcement using natural and artificial fibers. However, some of them are associated with environmental challenges and are not cost-effective. This leads researchers to find out for environmentally friendly, low-cost, and sustainable stabilizers, such as bagasse ash, fly ash, rice husk ash, and without and with combination of lime or cement as stabilizing agents for improving the engineering properties of problematic soil (Argaw, A. & Patra, N. R., 2016), and (Dinke ,2015).

The waste materials available in Ethiopia include a large amount of bagasse ash and many natural fibers also available like Sisal fiber, Katcha fiber, and Enset. A considerable amount of research work has been done concerning the stabilization of soil using bagasse ash and sisal fiber independently and in combination with other stabilizing materials. various researches have been performed on the effect of bagasse ash stabilization on the properties of expansive soil. Based on their test results, they indicated that bagasse ash admixture can have used the improvement on the engineering properties of expansive soil. (Bekele, 2022),(Khan et al., 2019),(Osinubi, 2009),(Kharade et al., 2014) , and (Surjandari et al., 2017). The researchers have investigated most of the engineering properties of bagasse ash stabilized soil but limited investigations were done on the effects of the stabilizing materials on the consolidation characteristics of expansive soil. They gave a different optimum amount of bagasse ash mainly based on the improvement in the unconfined compressive strength (UCS) and California bearing ratio (CBR) value. It has been seen from these researches' bagasse ash is pozzolanic material with a high amount of silica and calcium oxide in proportion to other chemicals and it can improve the property of the soil since the chemical composition of bagasse ash meets the requirement for the pozzolanic property. However, some of them concluded bagasse ash cannot fulfill the strength required to become a stabilizer alone and they recommended that it has to be mixed with other stabilizers to make it an effective stabilizer for construction purposes (Worku, 2015), and (Wubshet & Tadesse, 2014).

The natural fiber reinforcement causes significant improvement in shear strength, and other engineering properties of the clay soil (Maja, 2018). The function of the reinforcements in the soil matrix is to increase the strength (shearing resistance) and reduce the deformation. Sisal fibers are cellulose-rich (> 65%) and show tensile strength. Sisal is a natural fiber material, cheap, easy laying in the field, and biodegradable. Sisal fiber has low moisture absorption, excellent durability, and high initial tensile strength. When the fiber-reinforced soil is loaded, the fibers mobilize tensile resistance, which in turn imparts greater strength to the soil (Gowthaman et al., 2018). The researchers studied the effect of applicability of sisal fibers in geotechnical properties of problematic soil implying that the addition of sisal fibers improved the properties of loose soil (Narayana Reddy, 2019),(Haimanot, 2020),and (Dubey and Tegar, 2018). The combined effect of chemical admixture and natural fibers on soil properties is not widely investigated. Although a large number of studies were established about bagasse ash stabilization its effect on the compressibility of soil was limited. Consolidation characteristics are prime considerations for any structure constructed above clay soil. This behavior of soil is mainly responsible for the settlement of a clay layer.

Therefore, in this thesis, the combined effect of bagasse ash and sisal fiber on the strength characteristics of expansive soil was investigated by conducting Atterberg limit tests, free swell, specific gravity, compaction test, and UCS for uncured and 7 days cured to evaluate their effectiveness as soil stabilizer. The effect of bagasse ash and sisal fiber on consolidation characteristics which are (coefficient of consolidation, coefficient of volume compressibility, void ratio and compression index, and recompression index was done.

1.2 Statement of The Problem

A large part of the current study area, i.e. Dukem town, is covered with soils that have high swelling potential (Tamrat, 2013). The stability of many lightweight structures, residential buildings, and roads in this area is affected by expansive soil and is exhibiting structural cracks. Most of the structures failed before the completion of their design life. Therefore, the strength improvement of such type of soil is needed. Nowadays replacing the expansive soil with selected material is used. This leads to higher construction costs and delays in construction, so, to reduce transportation of selected material costs and to reduce damages caused by problematic soil using soil stabilization methods was investigated. The application of locally available materials and waste materials is effective in terms of cost and environmental benefits. Sisal fiber, a locally available plant-based fibrous material, and bagasse ash, a sugar industry byproduct, were used for this study. Limited research has been done on the stabilization of expansive soil using the above-said combination. Although the bearing capacity is depending on compressibility and settlement of soil, studies on the effect of these two stabilizers on consolidation characteristics of expansive soil were limited. Therefore, in this thesis, the combined effect of sisal fiber and bagasse ash on the strength and consolidation characteristics of the expansive soil was investigated.

1.3 Research Questions

1. What are the effects of bagasse ash and sisal fiber on expansive soil?
2. Are properties of expansive soil improved by addition of bagasse ash and sisal fiber?
3. What is the optimum content of the stabilizing materials?

1.4 Objective

1.4.1 General objective

The main objective of this research work was to investigate the effect of bagasse ash and sisal fiber on the strength and compressibility properties of expansive soil.

1.4.2 Specific objective

The specific objectives of this thesis are:

- To determine the basic properties of the expansive soil.
- To determine the optimum content of bagasse ash and sisal fiber needed to stabilize the expansive soil.
- To make a comparison between stabilized and un stabilized expansive soil.

1.5 Significance of The Study

To characterize and study the use of locally available industrial waste and natural fiber (i.e., Bagasse ash and sisal fiber) in the improvement of the engineering properties of problematic soil. To make it a suitable foundation material that meets the strength requirement by avoiding the cut, disposal, and fill material price and protecting the environment from disposal of bagasse ash on the environment and the effect on the society. To use the natural fibers for future use in engineering purposes.

1.6 Scope and Limitation of The Study

In this study, samples of expansive soil were collected from Dukem town. To take sample soils, the area where expansive soils are found was identified by reviewing previous research on this area. By field identification, three test pits were excavated for soil sampling. Different laboratory tests were conducted as per the ASTM manual and IS manual. The most problematic soil of all three test pits was selected to be stabilized with bagasse ash and sisal fiber.

The study covers improving the strength characteristics of expansive soil using sisal fiber and bagasse ash using different mix proportions. First, soil samples with different contents of bagasse ash (3%, 6%, and 9%) were prepared. Then, Atterberg limits, specific gravity test, free swell test, free swell index, free swell ratio, standard proctor compaction test, and unconfined compressive strength test (uncured and 7 days cured) were conducted on soil- bagasse ash mixtures. The UCS test result has been selected to identify the optimum bagasse ash.

The water absorption capacity of uncoated and kerosene-coated sisal fiber was determined. The bagasse ash stabilized soil also reinforced with different percent (0.5 %,1 %,1.5 %) and different length (10mm,20mm,30mm) of kerosene coated sisal fiber. Compaction and UCS tests were conducted for soil-bagasse ash-coated sisal fiber mix. Then optimum sisal fiber content and length were identified. Additionally, the effect of bagasse ash and sisal fiber on consolidation characteristics of expansive soil was discussed. by conducting a one-dimensional consolidation test. expansive soil and different percentages of bagasse and taking optimum sisal fiber length with different percentages (0.5%,1%, and 1. 5%). The curing time for bagasse ash stabilized soil was limited to 7 days to determine the unconfined compressive strength of samples.

1.7 Organization of The Study

The thesis includes five chapters. In the first chapter the background, statement of the problem, objectives, research questions, significance of the study, scope, and limitations of the work is presented. The second chapter deals with a brief literature review comprising a study on previous similar works that are important to this study about expansive soil, soil stabilization techniques natural fiber, and industrial wastes. In the third chapter the method, description of the study area, the material used, procedures to be followed, and tools and techniques performed in the laboratory to achieve the objectives are presented. The fourth chapter presents the analysis and results obtained from the experimental work. Finally, in the fifth chapter conclusions and recommendations are made from the findings of the study.

2 LITERATURE REVIEW

2.1 Expansive Soils

Expansive soils are fine-grained soil or decomposed rocks that show huge volume changes when exposed to the fluctuations of moisture content. Swelling-shrinkage behavior is likely to take place near the ground surface where it is directly subjected to seasonal and environmental variations (Dang et al., 2018). Most soil classification systems arbitrarily define clay particles as having an effective diameter of two microns (0.002mm) or less. Particle size alone doesn't determine clay minerals. Probably the most important grain property of fine-grained soils is the mineralogical composition. For small size particles, the electrical forces acting on the surface of the particles are much greater than the gravitational force. These particles are in a colloidal state. The colloidal particles consist primarily of clay minerals that were derived from parent rock by weathering (Chen, 1975). The origin of expansive soils is related to a combination of conditions and processes that result in the formation of clay minerals having a particular chemical makeup that, when in contact with water, expands. Variations in the conditions and processes may also form other clay minerals, most of which are non-expansive. The conditions or processes, which determine the clay mineralogy, include the composition of the parent material and the degree of physical and chemical weathering to which the materials are subjected (Asres, 2017).

The parent materials of expansive soils may be classified into two groups (Chen, 1975). The first group comprises basic igneous rocks. Here feldspar and pyroxene minerals of the parent rocks decompose to form montmorillonite - the predominant mineral of expansive soil - and other secondary minerals. The second group comprises sedimentary rocks that contain montmorillonite (Chen, 1975). The expansive soils of Ethiopia are derived from both groups (Alemayehu Teferra and Solomon, 1986). Expansive soils are clay soils with high plasticity. As the name of the soils suggests, these soils are known for their peculiar nature of expanding or shrinking when exposed to moisture changes. commonly they are known as black clays or in some regions as black cotton soil. the name black cotton came from the fact that the soils are found favorable in some regions for growing cotton (Alemayehu Teferra, and Mesfin, 1999).

Expansive soils are mostly found in the arid and semi-arid regions of the world. The presence of montmorillonite clay in these soils imparts them high swell–shrink potentials (Chen, 1988).

2.2 Clay Mineralogy

Clay minerals are complex aluminum silicates composed of two basic units these are silica tetrahedron and alumina octahedron. Each tetrahedron unit consists of four oxygen atoms surrounding a silicon atom Clay minerals are formed by sandwiching tetrahedral and octahedral layer sand sheets together. A tetrahedron sheet can be considered as a layer of silicon ions between a layer of oxygen and a layer of hydroxyl ions (Das and Roy, 2014). This also is called a gibbsite sheet sometimes magnesium replaces the aluminum atoms in the octahedral units; in this case, the octahedral sheet is called a Brucite sheet. Absorption of water by clays leads to expansion From the mineralogical standpoint, the magnitude of expansion depends on the kind and amount of clay minerals present, their exchangeable ions, electrolyte content of the aqueous phase, and the internal structure (Chen, 1975). There are three types of clay minerals. In order of increasing their expansiveness, they are listed as Kaolinite, Illite, and Montmorillonite.

Kaolinite: consists of repeating layers of elemental silica-gibbsite sheets in a 1:1 lattice (Das, 2014). Kaolinite is stable and water is unable to penetrate between the layers. It shows little swelling during wetting.

Montmorillonite: - Montmorillonite is the clay mineral that presents most of the expansive soil problems. Its basic structure consists of an alumina sheet sandwiched between two silica sheets. The basic Montmorillonite units are stacked with one on top of the other but the bond between individual units is relatively weak so water can easily penetrate between the sheets and separation of them produces swelling. It is extremely active and its activity decreases as the adsorbed cation exchanges in the order of Sodium, Lithium, Potassium, Calcium, Magnesium, and Hydroxyl (Alemayehu Teferra and Mesfin, 1999).

Illite: consists of a gibbsite sheet bonded to two silica sheets one at the top and another at the bottom. It is sometimes called clay mica. The illite layers are bonded by potassium ions. The negative charge to balance the potassium ions comes from the substitution of aluminum for some silicon in the tetrahedral sheets (Das, 2014). The illite units are stable and so the mineral swells less than montmorillonite (Alemayehu Teferra and Mesfin, 1999).

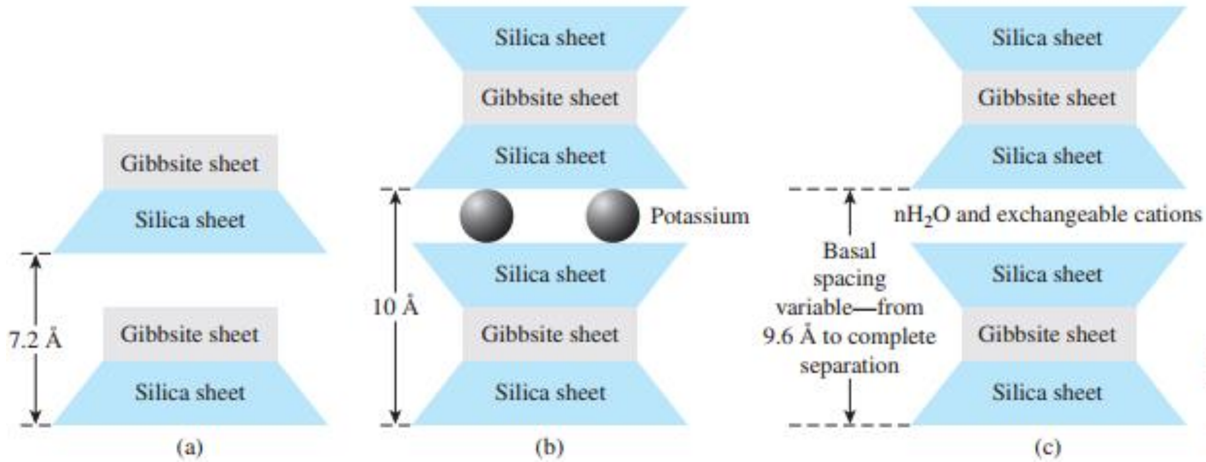

Figure 2.1 The structures of (a) kaolinite (b) illite (c) montmorillonite (Das, 2014)

2.3 Distribution of Expansive Soils in Ethiopia

Expansive soils are mostly found in the arid and semi-arid regions of the world. The presence of montmorillonite clay in these soils imparts them high swell–shrink potentials (Chen, 1988). In Ethiopia, expansive soils covered nearly 40% surface area of the country (Molenaar., 2005). Expansive soils are observed in areas such as central Ethiopia, following the major trunk road like Addis Ababa - Ambo, Addis Ababa - Weliso, Addis Ababa – Debere Berehan, Addis Ababa- Gohatsion, and Addis Ababa - Mojo. Also covers the area like Mekelle, Bahirdar, Gambela, Arba Minch, and the most Southern, South-west and southeast part of the capital Addis Ababa area in which the most major recent construction is being carried out (Bantayehu, 2017) The black and gray soils found in the eastern and southern part of Addis Ababa are highly expansive (Alemayehu Teferra & Yohannes., 1986).

2.4 Identification of Expansive Soil

Soil deposits can be recognized in the field through visual inspection. In the field, expansive clays can be recognized in the dry season by the deep cracks of roughly polygonal patterns (Das, 2014). The expansive soils show a polygonal pattern of surface cracks having 2.5 cm wide and over 1 m in depth is not uncommon in the dry season. The cracks close down after the rainy season. A shiny surface is also easily obtained when a partially dry piece of the soil is polished with a smooth object such as the top of a fingernail. The wet samples of the soil are sticky and it will be relatively difficult to clean the soil with your hands.

They are very hard when dry and they usually have a color of black or gray. One can also easily recognize expansive soil areas by simply looking at the failures of lightly loaded buildings as shown in Figure 2.4. Swelling soils lift lightly loaded foundations and frequently cause distress in floor slabs, and vertical and horizontal cracks develop in the walls. Diagonal cracks that develop below the windows are indications of swelling movement (Kassahun, 2006).

The black and gray soils found in the eastern and southern parts of Addis Ababa are highly expansive and the percentage of montmorillonite present in the black and gray soils ranges from 45 to 87 percent (Alemayehu Teferra and Solomon, 1986).

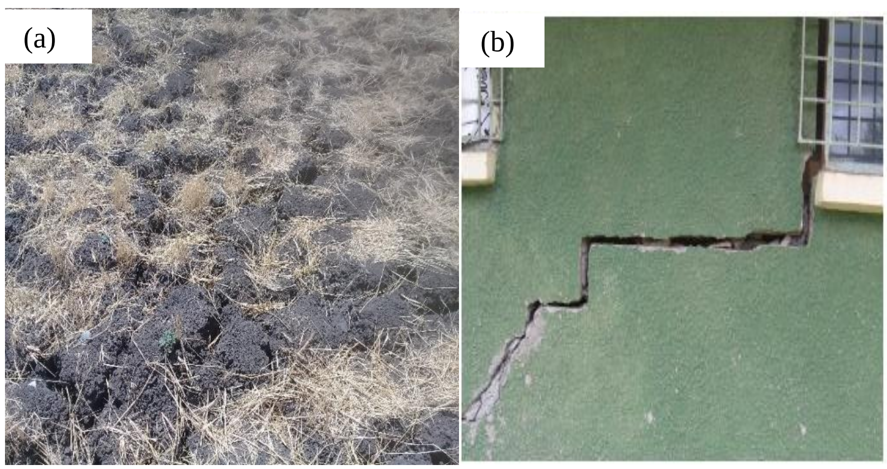

Figure 2.2 Typical crack on expansive soil during the dry season(a) Diagonal cracks that develop below windows (b) (Kassahun, 2006)

Expansive soil can be identified by conducting several laboratory tests. these can be categorized as mineralogical identification and direct and indirect methods. Mineralogical identification can be useful in the evaluation of the material but is not sufficient in itself when dealing with natural soils. The various method of mineralogical identification is important in a research laboratory in exploring the basic properties of clays, but are impractical and uneconomical for practicing engineers. (Chen, 1988). The five techniques which may be used are for mineralogical identification are differential thermal analysis-ray diffraction, dye adsorption., Chemical analysis and Electron microscope resolution. Due to their property of time consumption, expensiveness, and need for skilled technicians for result interpretation, these tests cannot be considered routine tests (Chen, 1988).

Indirect Methods for the identification of expansive soil

It includes simple soil property tests that a practicing engineer resorts to using for identifying expansive soil. Such tests are easy and can be performed in most soil mechanics laboratories, and yield excellent indices of expansive properties. The various tests under these methods are:

i. **Atterberg limit tests**

The Atterberg limit defines the moisture content boundaries between states of consistency of fine-grained soils. The plasticity index and liquid limit are used to characterize soils and useful indices for the identification of swelling of expansive soils. The plasticity index can be used as a preliminary indication of the swelling characteristics of most clay. Expansive soils are characterized by a PI >30%, a liquid limit > 50%, and a high swelling potential (Chen, 1975). The relation between the degree of expansion and the plasticity index is given in Table 2.1.

Table 2.1 Relation between degree of expansion and Atterberg limits (Alemayehu Teferra and Mesfin , 1999)

No	Degree of expansion	Liquid limit (%)	Shrinkage limit (%)	Plastic index (%)
1	Very high	60-70	>30	>35
2	High	40-60	20-30	20-35
3	Medium	30-40	10-20	10-20
4	Low	20-30	<10	<10

Daksanamurthy and Raman (1973) also presented a single index method for identifying expansive soils using only liquid limits. They suggested four classes of clays according to their liquid limits as shown in Table 2.2. USBR Method is developed by Holtz and Gibbs; it is based on a direct correlation of observed volume change (degree of expansion) with colloid content, plastic index, and shrinkage limit. The classification is as given in Table 2.3.

Table 2.2 Relation between the swelling potential of clays and the liquid limit Daksanamurthy and Raman (1973)

Swelling potential	Low	Medium	High	Very high
Liquid limit	20<LL<=35	35<LL<=50	50<LL<=70	LL>70

Table 2.3 Classification based on bureau of reclamation method (Chen ,1988)

Colloid content (%)	Plasticity index (%)	Shrinkage limit (%)	Probable expansion (%)	Degree of expansion (%)
<15	<18	>15	<10	Low
13-23	15-28	10-16	10-20	Medium
20-31	25-41	7-12	20-30	High
>28	>35	<11	>30	Very high

ii. Linear shrinkage

Linear shrinkage is the change in length of a soil sample as it dries to the shrinkage limit, SL, expressed as a percentage of the original length. This test also in combination with other tests is used for the classification of expansive soil (Alemayehu Teferra and Mesfin, 1999).

The swell potential is presumed to be related to the opposite property of linear shrinkage measured in a very simple test. In theory, it appears that the shrinkage characteristics of the clay should be a consistent and reliable index to the swelling potential (Chen, 1975).

Table 2.4 Potential expansiveness for various values of shrinkage limits and linear shrinkage (Altmeyer, 1955)

Shrinkage limit as a percentage	Linear shrinkage as a percentage	Degree of expansion
Less than 10	Greater than 8	Critical
10-1 2	5- 8	Marginal
Greater than 12	0-5	Non-critical

iii. Free swell

This test is a simple test conducted in the laboratory for the determination of the degree of expansiveness. Free swell tests consist of placing a known volume of dry soil in water and noting the swelled volume after the material settles, without any surcharge, to the bottom of a graduated cylinder. The difference between the final and initial volume, expressed as a percentage of the initial volume, is the free swell value. The swell test is very crude and was used in the early days when refined testing methods were not available. Experiments conducted by (Holtz & Gibbs, 1956)indicated that a good grade of high swelling commercial bentonite will have a free swell value of from 1200 to 2000 percent. Holtz suggested that soils having a free swell value as low as 100 percent can cause considerable damage to lightly loaded structures, and soils having a free swell value below 50 percent seldom exhibit appreciable volume change even under very light loading (Chen, 1975).

$$\text{Free Swell (\%)} = \left(\frac{\text{final volume} - \text{initial volume}}{\text{initial volume}}\right) * 100 \qquad (2,1)$$

Table 2.5 Degree of expansiveness and free swell (Chen, 1975)

Degree of expansiveness	DFS (%)
Low	<20
Moderate	20-35
High	35-50
Very high	>50

iv. Free swell index

A free swell index is one of the most commonly used simple tests to estimate the swelling potential of expansive clay. The procedure involves taking two oven-dried soil samples passing through a 425µm sieve and 10ml of each was placed separately in two 100ml graduated cylinders. One cylinder is filled with kerosene oil and the other is filled with distilled water. Both of the samples are stirred and left undisturbed for a minimum of 24 hours after which the final volumes of soils in the cylinders are noted. The free swell index is calculated as:

$$\text{Free Swell (\%)} = \left(\frac{\text{final volume in water} - \text{final volume in kerosene}}{\text{final volume in kerosene}}\right) * 100 \qquad (2,2)$$

v. Activity index

Atterberg limits and clay contents have been combined in a single parameter called activity ratio sometimes called activity index (A) developed by Skempton (1953). It is Skepton's method of clay soil classification which is based on their activity. Montmorillonite clay (expansive clay) is defined as active. Based on Skepton: Colloidal Activity (A) = $\frac{I_p}{C}$ where C is the percent of clay fraction finer than 2µ and I_p is the plasticity index.

Table 2.6 Skepton's Method of clay Soil Classification based on activity

Degree of activity	activity
In active clay	<0.75
Normal clay	0.75-1.25
Active clay	>1.25

Direct Methods

These methods offer the most useful data by direct measurement, and tests are simple to perform and do not require complicated equipment. Testing should be performed on several samples to avoid erroneous conclusions. Direct measurement of expansive soils can be achieved by the use of a conventional one-dimensional consolidometer (Chen, 1975).

Table 2.7 Relationship between swelling potential and % of expansion in oedometer

Swell potential	% Expansion in oedometer (Holtz and Gibbs, 1956)	% Expansion in oedometer (seed et al.,1962)
Low	<10	0-1.5
Medium	10-20	1.5-5
High	20-30	5-25
Very high	>30	>25

2.5 Classification of Soils

Most of the soil classification systems that have been developed for engineering purposes are based on simple index properties such as particle-size distribution and plasticity. Although several classification systems are now in use, none is totally definitive of any soil for all possible applications because of the wide diversity of soil properties. In general, there are two major categories into which the classification systems developed in the past can be grouped.

1 The textural classification is based on the particle-size distribution of the percent of sand, silt, and clay-size fractions present in a given soil.

2 The other major category is based on the engineering behavior of soil and takes into consideration the particle-size distribution and the plasticity (i.e., liquid limit and plasticity index). Under this category, there are two major classification systems in extensive use now:

a. The AASHTO classification system, and

b. The Unified classification system.

2.5.1 The textural classification

By making use of the grain size limits for sand, silt, and clay, a triangular classification chart has been developed as shown in Figure 2.3 for classifying mixed soils. This method of classification does not reveal any properties of the soil other than grain-size distribution. Because of its simplicity, it is widely used by workers in the field of agriculture. The gradation of the black cotton soils varies considerably. There is little or no gravel size in most black cotton soils and those that have shown percentages of less than 8 %. The amount of sand varies between 2 % and 50 % and silt from 11 % to 58 %. The clay size contents also range from 40 % to 75 %. The soils classify as clay, sandy clay, and silty-clay in the U.S.

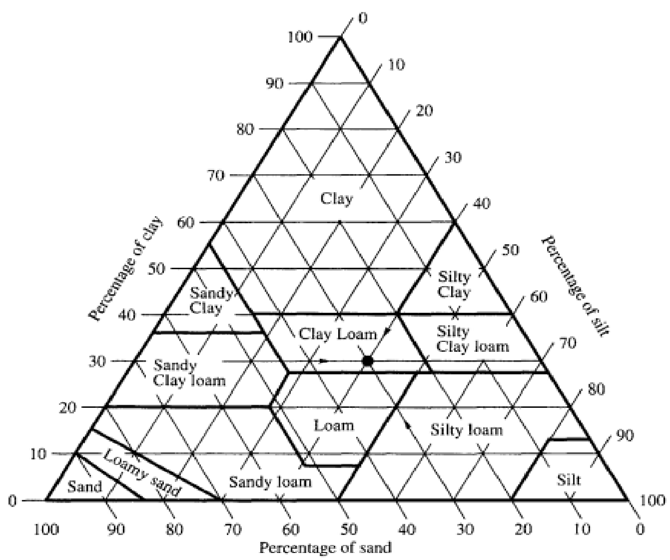

Figure 2.3 U.S department of agriculture textural classification (Murthy, 2002)

2.5.2 AASHTO soil classification

This system is known as the AASHTO (American Association of State Highway and Transportation Officials) System. The revised system comprises seven groups of inorganic soils, A-l to A-7 with 12 subgroups in all. The system is based on Particle-size distribution, Liquid Limit, and Plasticity Index. To evaluate the quality of soil as a highway subgrade material group index (GI) is an important parameter and it can be given by the equation below.

$$GI = (F200 - 35)[0.2 + 0.005(LL - 40)] + 0.01(F200 - 35)(PI - 10) \quad (2,3)$$

Where F200 is percentages passing through sieve No.200 and LL & PI are liquid limit and plasticity index respectively.

Table 2.8 Chart for use in the AASHTO soil classification system (Murthy, 2002)

General classification	Granular materials (35 percent or less of total sample passing N0,200							Silt –clay materials (more than 35 percent of total samples passing No,200)			
Group classification	A-1		A3	A-2				A-4	A-5	A-6	A-7
	A-1-a	A-1-b		A-2-4	A-2-5	A-2-6	A-2-7				A-7-5 A-7-6
Sieve analysis percentpassing											
No.10	50 max										
No.40	30 max	50max	51 min								
No.200	15 max	25 max	10 max	35 max	35 max	35 max	35 max	35 max	35 max	35 max	35 max
Characteristics of fraction passing No.40											
liquid limit				40max	40 min	40 max	41 min	40 max	41 min	40 max	41 min
plastic index	6 max		N.P	10 max	10max	11 min	11 max	10 max	10 max	11 min	11 min
Usual types of significant constituent	Stone fragments – gravel and sand		Fine sand	Silty or clayey gravel and sand				Silty soils		Clayey soils	
General rating as subgrade	Excellent to good			Fair to poor							

2.5.3 Unified soil classification system

The USCS is the most widely used system for determining the suitability of soils for general use based on particle size distribution and plasticity. According to this system, the soils are classified into three major groups; coarse-grained, fine-grained, and highly organic (peat). The soils are grouped as coarse-grained if more than 50% of the soil is retained on the No.200 (0.075mm) sieve and fine-grained if more than 50% of the soil passes the No.200 sieve.

Table 2.9 Correlation between swell potential and unified soil classification

Category	Little or no expansion	Moderate expansion	High volume change	No rating
Soil classification system	GW, GP, GM, SW, SP, SM	GW, SC, ML, MH	CL OL, CH, OH	Pt

In the above classification soils rated as CL or OH may be considered potentially expansive.

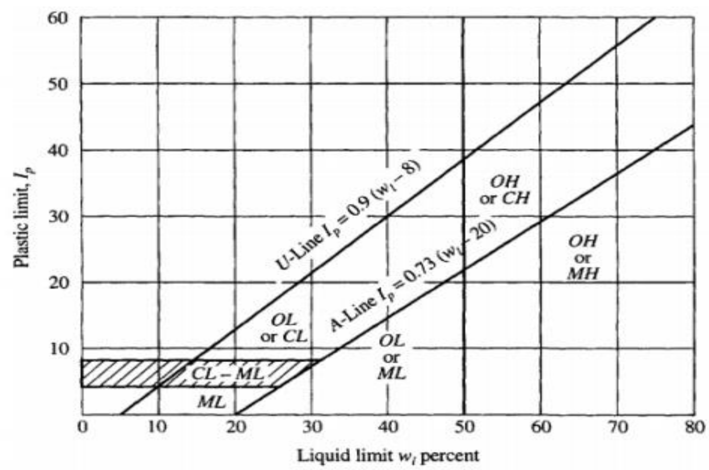

Figure 2.4 Plasticity chart for fine-grained soils (Murthy, 2002)

2.6 Theories of Consolidation and Compression

In the natural process of deposition, fine-grained soils undergo the process of consolidation by the layer of soil deposited above. After some time, a state of equilibrium is reached and compression ceases. Due to the application of external pressure on saturated clay excess pore water pressure develops. This induced excess pore water pressure initially takes up the applied external pressure. The process of consolidation consists of a gradual transfer of stress from pore water pressure to the soil skeleton. As the pore water pressure decreases the effective stress increases. In the process of consolidation, the extent to which the transfer of stress has progressed is known as the degree of consolidation (Sissay, 2011).

Any structure built on the ground causes an increase of pressure on the underlying soil layers. The soil layers being confined by the surrounding soil strata adjust to the new pressure mainly through deformation. Soil may be considered to be a skeleton of solid grains enclosing voids that may be filled with gas, liquid, or a combination of liquid and gas. The vertical compression of the soil under increased pressure is thus made up of a compression of solid mater which under usual loading is account for very small compression, compression of the pore fluid, which may be considered where the pores contain air, but negligible when the pore is completely filled with water. Reduction of the pore space by the expulsion of pore fluid forms the major component of the compression (Alemayehu Teferra, and Mesfin, 1999).

A stress increase caused by the construction of foundations or other loads compresses soil layers. The compression is caused by the deformation of soil particles, relocations of soil particles, and expulsion of water or air from the void spaces. In general, the soil settlement caused by loads may be divided into three broad categories: these are elastic settlement, primary settlement, and secondary settlement. Elastic settlement (or immediate settlement), which is caused by the elastic deformation of dry soil and moist and saturated soils without any change in the moisture content, primary consolidation settlement, which is the result of a volume change in saturated cohesive soils because of the expulsion of the water that occupies the void spaces and secondary consolidation settlement, which is observed in saturated cohesive soils and organic soil and is the result of the plastic adjustment of soil fabrics. It is an additional form of compression that occurs at constant effective stress (Das, 2014).

2.6.1 One-dimensional consolidation

The standard one-dimensional consolidation test is carried out on a saturated specimen using an Odometer. The soil specimen is placed inside a metal ring with two porous stones, one at the top of the specimen and another at the bottom. The load on the specimen is applied through a lever arm, and compression is measured by a micrometer dial gauge. The specimen is kept under water during the test. Each load usually is kept for 24 hours. After that, the load usually is doubled, which doubles the pressure on the specimen, and the compression measurement is continued. At the end of the test, the dry weight of the test specimen is determined (Fikadu, 2015). The consolidation characteristics of a soil which are compression index (C_c) and recompression index (C_r), coefficient of consolidation (C_v), and volume of compressibility(m_v) are determined from the one-dimensional oedometer test. The compression index relates to how much consolidation or settlement will take place. The coefficient of consolidation relates to how long it will take for an amount of consolidation to take place. The results of the typical odometer test are usually presented in the form of an e-P, e-log(P), and dial reading-time plots.

Compression index (C_c)

Consolidation index Cc is numerically equal to the slope of the straight portion of the void ratio versus the log pressure plot from the e-log P curve. Its value is constant beyond the range of the recompression since beyond this point the plot of e against log P is a straight line. C_c is an important index used to calculate the ultimate settlement of a foundation founded on a clay layer. The compression index (C_c) is an important parameter used in geotechnical engineering as it is related to the amount of anticipated consolidation settlement that a soil stratum will experience when introduced to loads that are greater than experienced in the past. The slope of the linear portion of the e -log p curve is designated as the C_c (Fattah & Jaber, 2014).

$$Cc = \frac{e_1 - e_2}{\log\left(\frac{p_2}{P_1}\right)} \quad (2,4)$$

Where:

C_c-Compression Index

e -Void ratio

p - Pressure in log scale

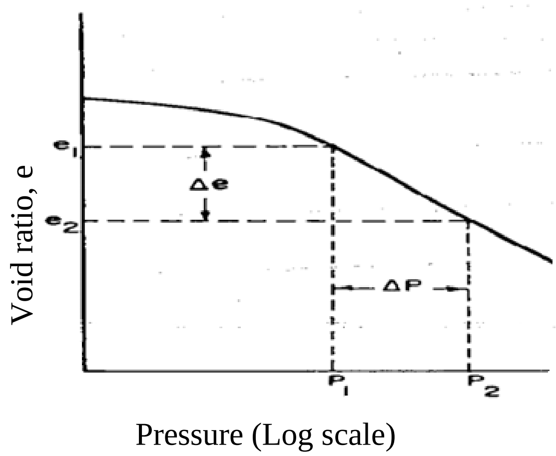

Figure 2.5 Determination of consolidation index (Chen, 1975)

Coefficient of consolidation, C_v

The coefficient of consolidation is the measure of the rate at which the consolidation takes place for a certain increase in stress (Ali et al., 2022). C_v may be found experimentally from conventional laboratory one-dimensional consolidometer test results. Both Casagrande and Taylor's methods have been determined as follows.

The coefficient of consolidation C_v as determined by Casagrande's semi-logarithmic plot method is:

$$C_v = \frac{0.197 * H^2}{t_{50}} \qquad (2,5)$$

C_v = coefficient of consolidation, in cm^2/sec

H = equivalent specimen thickness, in cm

t_{50} = time at 50 percent of primary consolidation, in sec

The coefficient of consolidation C_v value as determined by Taylor's square root of time fitting method is (0.848).

$$C_v = \frac{0.848 * H^2}{t_{90}} \qquad (2,6)$$

C_v = Coefficient of consolidation of stratum, in cm^2/sec

H = Equivalent specimen thickness, in cm

t_{90} = Time at 90 percent of primary consolidation, in sec

Two methods are available for the evaluation of C_v from consolidometer test data. The first called the square root of time fitting method is due to Taylor & the second called the logarithm of time fitting method is due to Casagrande. The two methods are based on the comparison of the laboratory and theoretical time curves. Since the natural scale doesn't offer the best representation of time, the square root & the logarithm of time are used.

2.7 Damages Caused by Expansive Soil

In the dry state, the expansive soils exhibit a high bearing capacity which is gradually lost with an increase in moisture content. If prevented from swelling following exposure to moisture, the soils exert high swelling pressure. the pressure is usually build-up is usually responsible for cracking of buildings, distortion of pavement surfaces, and damage to other structures (Alemayehu Teferra and Mesfin, 1999).

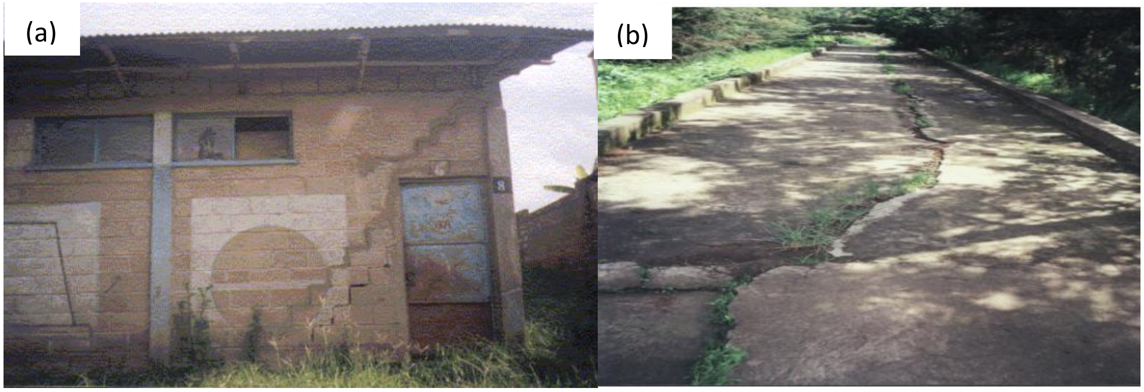

Figure 2.6 Sever diagonal crack (a) Crack of a walkway(b) (Afewerk, 2004)

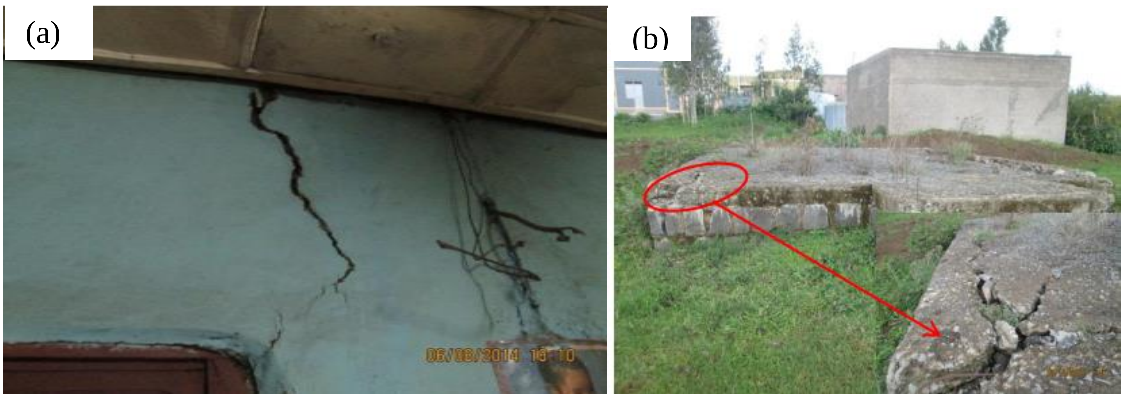

Figure 2.7 Typical damages due to soil swelling and shrinking characteristics show distress on lightweight structures(a,b) (Tibebu, 2015).

Damage due to expansive soils could occur on any type of building, road, and other civil engineering constructions that are not properly designed and/or constructed. However light structures like one or two-story buildings, warehouses retaining walls, and buried facilities are more vulnerable to damage because these structures couldn't exert a heavy pressure to counteract the uplift pressure from the expansive soils (Chen, 1975). Different researches have shown the damages caused by expansive soil in some parts of Ethiopia.

Teklu D. (2003) examined the swelling pressure of Addis Ababa area expansive soil. So many damages were reported as a result of expansive soil. Such damages occur when the pressure exerted by the soils is greater than the foundation pressure. Consequently, assessing the swelling pressure is an important step in designing a foundation on expansive soil.

Afewerk (2004) assessed the damage that occurred on buildings that are constructed on expansive soil areas by taking ninety-six randomly selected houses in the city of Addis Ababa. The houses are located in Bole, Olympia, Nifasilk, Lafto, Old Airport, Mekanisa, Gergi, and Bole bulbula localities of the city. The study showed that 64 % of the houses suffered heavy damage, 8 % of the houses were slightly damaged and 28% of the houses showed no damage He found that drainage is the most critical initiating factor for building damages. 84 % of the damaged buildings do not have a proper drainage system or the drainage system provided is adequate.

Tibebu (2015) Out of randomly visited 78 buildings 68 of them are damaged due to swelling and shrinkage cycle of the soil, which is 87%. In most cases, more than one building component is affected. The building component which is highly susceptible to damage due to expansive soil is the walkway around the building. The extent of damage decreases as we proceed to walls, floors, and foundations in their respective orders.

2.8 Review On Soil Stabilization

Soil stabilization is the process of alteration of one or more soil properties to create an improved soil material possessing the desired engineering properties. Soil stabilization can be classified into two broad categories as mechanical and chemical stabilization. Mechanical stabilization can be defined as a process of improving the stability and shear strength characteristics of the soil without altering the chemical properties of the soil. The main methods of mechanical stabilization can be categorized into compaction, mixing or blending of two or more gradations, applying geo-reinforcement, and mechanical remediation (Sumi & Unnikrishnan, 2015).Chemical stabilization depends on a chemical reaction between stabilizer and soil minerals to achieve the desired effect. Chemical stabilization is the mixing of soil with one or a combination of admixtures of powder, slurry, or liquid to improve or control its stability, strength, swelling, permeability, and durability. Chemical stabilization can achieve improvement of soil through three chemical reactions (Asres, 2017).

i) Cation Exchange- Cation exchange is the interchange between a cation on the surface of any negatively charged particle (clay particle) and the stabilizer. The ease of replacement or exchange of cations depends on several factors, primarily the valence of the cation. Higher valence cations easily replace cations of lower valence. The size of the hydrated ion becomes important for ions of the same valence.

A typical replaceability series is

$Na^{+} < Li^{+} < K^{+} < Rb^{+} < Cs^{+} < Mg^{2+} < Ca^{2+} < Ba^{2+} < Cu^{2+} < Al^{3+} < Fe^{3+} < Th^{4+}$

An example of the cation exchange;

$Ca^{2+} + Na^{+\,-}Clay \rightarrow Ca^{2+}\text{-}Clay + Na^{+}$

The thickness of the diffused double layer decreases as replacing the divalent ions (Ca^{2+}) from stabilizers with monovalent ions (Na^{+}) of clay. Thus, swelling potential decreases.

ii) Flocculation and Agglomeration: Cation exchange results in a change in the electrical charge around the clay particles, therefore, an increase in the inter-particle attraction causes flocculation and agglomeration. This leads to the reduction of clay-sized particles and hence the soil surface area, which accounts for the reduction in plasticity and swelling of the soil (Asres, 2017).

iii) Pozzolanic Reactions: Time-dependent pozzolanic reactions play a major role in the stabilization of the soil since they are responsible for the improvement of the various soil properties. Pozzolanic constituents produce calcium silicate hydrate (CSH) and calcium aluminate hydrate (CAH).

$Ca^{2+} + 2(OH)^{-} + SiO_2$ (Clay Silica) $\rightarrow$ CSH, $Ca^{2+} + 2(OH)^{-} + Al_2O_3$ (Clay Alumina) $\rightarrow$ CAH

The calcium silicate gel formed initially coats and binds lumps of clay together. The gel then crystallizes to form an interlocking structure which increases the soil strength (Aschalew, 2021).

2.8.1 Bagasse ash stabilization

Bagasse ash stabilization is grouped under the chemical stabilization technique. It is a waste product from the sugar industry from sugar cane processing. Sugarcane processing is focused on the production of cane sugar from sugarcane. Other products of the processing include bagasse, molasses, and filter cake. Bagasse is a fibrous dry pulpy residue obtained after crushing to extract juice from sugarcane or sorghum stalks. After extracting the juice from the sugarcane, the bagasse is kept for drying the dried bagasse is then burnt to generate heat in the boiler to convert water into steam. This steam is then used to rotate a turbine-generator system at high pressure to produce electricity. From the combustion process, bagasse ash is generated. That has a gray-black color (Khan et al., 2019). About 40-45% of this fibrous residue is left which is reused in the same industry as fuel boiler for heat generation leaving behind 8-10% ash as waste. This ash is known as sugarcane bagasse ash (SCBA) and is deposited in stockpiles which are normally dumped in waste landfills and constitute environmental problems to the society. Bagasse ash has a problem with the environment due to its disposal. When bagasse is left in the open, it ferments and decays; this brings about the need for the safe disposal of the pollutant. It can be blown away by wind and inhaled and can create health problems (Worku, 2015).

2.8.1.1 Chemical composition of bagasse ash from different literature

Bagasse ash is a pozzolanic material that is very rich in the oxides of, silica and aluminum, and sometimes calcium. Pozzolans usually require the presence of water for silica to combine with calcium hydroxide to form stable calcium silicate, possessing cementitious properties. It is a fibrous material with the presence of silica (SiO_2) and it can be made used to improve the existing properties of black cotton soil.(Mathew & Raneesh, 2016). High silica in the SCBA could be due to the absorption of silicic acid from the soil and deposit in an amorphous state in the plant. Besides the main oxides, SCBA also contains carbon and water expressed by loss of ignition(Gupta et al., 2021). Srinivasan (2010) reported the three-oxide components (SiO_2, Al_2O_3, Fe_2O_3) found in bagasse ash account for more than 75% of the total mineral content and the loss of ignition (LOI) was within the limit indicated in the ASTM C 618-00 manual (Srinivasan, 2010). As per ASTM C618 Standard Specification for Natural Pozzolans, the loss on ignition (LOI) content of a maximum of 10% is allowed for class N and 6% maximum for classes C and F. (Bersisa & Zekaria, 2021) Conducted a complete silica analysis experiment for bagasse ash. the composition of SiO_2, Al_2O_3, and Fe_2O_3 was 83.18%. It is greater than 75 %. The bagasse ash possessed higher silica content, and it is grouped under Class-F pozzolanic material (Bersisa & Zekaria, 2021).

Based on the chemical compositions of bagasse ash studied by different kinds of literature at different times bagasse ash can achieve the requirement given for pozzolanic property given by ASTM C 618–05 in Table 2.10.

Table 2.10 Chemical Requirements for Pozzolanic Property (ASTM C 618–05)

	Class		
	N	F	C
Silicon dioxide (SiO_2) + aluminum oxide (Al_2O_3) + iron oxide (Fe_2O_3), min, %	70.0	70.0	50.0
Sulfur trioxide (SO_3), max, %	4.0	5.0	5.0
Moisture content, max, %	3.0	3.0	3.0
Loss on ignition, max, %	10.0	6.0	6.0

2.8.1.2 Bagasse ash in Ethiopia

Sugar production in Ethiopia started in 1954/55. The commercial cultivation of sugarcane for sugar production started in 1954 at Wonji and in 1962 at Shoa (together named as Wonji-Shoa), in 1969 at Metahara, and in 1998 at Finchaa. Currently, eight factories are producing sugar in Ethiopia these include Wonji-shewa, Metahara, Fincha, Kessem, Tendaho, Arjo, Omo kuraz II, and Omo kuraz III. In addition, five factories which are Omo kuraz I, Omo kuraz V, Tana abeles I, Tana abeles II and wolkaite are at their construction phase. According to the Ethiopian Sugar Corporation, the countries sugar production has increased from 2.5 million quintals in 2019 to 3.2 million quintals in 2020 (ESC,2021). For every 10 tons of sugarcane crushed, a sugar factory produces nearly 3 tons of wet bagasse.

Table 2.11 The amount of sugarcane bagasse generated at the Ethiopian sugar factories (ESC, 2019)

Produced sugarcane bagasse (ton)								
Year	Wonji shewa	Metehara	Fencha	Tendaho	Kessem	Arjo-dedesa	Omo-kuraz ii	Omokuraz iii
2014	269,492	235,035	332,696					
2015	278,560	375,834	382,582		118,011	12,914		
2016	275,373	213,467	316,74	22,131	173,827	39,140		
2017	327,127	318,599	406,830	63,677	124,240	20,405	43,376	
2018	278,286	271,031	346,089	40,586	91,256	23,305	39,140	78,008

2.8.2 Soil reinforcement

Soil reinforcement can be defined as a technique of improving the engineering characteristics and behavior of soil by introducing materials comprised of desired properties. The prime objective of reinforcing soil mass is to enhance its stability that is, shear capacity and bearing capacity, thereby reducing deformations of soils. Fiber reinforcement involves mixing natural or synthetic fibers with soil, where the fibers act as tensile resisting elements that improve soil strength. The primary advantages of natural fibers are that they are cheap, abundantly available, and biodegradable(Torio-kaimo et al., 2020). The reinforcement acts as a tensile member coupled to the soil fill material by friction, adhesion, interlocking, or confinement, and thus improves the stability of the soil mass. The primary objective of reinforcing a soil mass is to enhance its stability, increase its bearing capacity, and thereby reduce settlement and lateral deformation of soils (Hejazi et al., 2012).

Based on their method of application: Fiber-reinforced soil can be classified into (i) Oriented distributed fiber-reinforced soil (ODFS) and randomly distributed fiber-reinforced soil (RDFS). Oriented distributed fiber-reinforced soil (ODFS) is one of the reinforcement mechanisms where fibers can be introduced by planner systems in vertical, horizontal, or both directions. The reinforcement material is put in layers and then the soil is compacted in a direction parallel to the shear plane (Gowthaman et al., 2018). It is the inclusion of planar sheets such as strips, fabrics, bars, grids, etc. into several layers of soil. It should be noted that the soil is first compacted to the required density, then the reinforcement material is placed and the sequence is repeated until the required thickness is achieved. Oriented distributed fiber-reinforced soil develops supplementary frictional strength along the fiber-reinforced planes whereas unreinforced zones provide survival by their strength and there is a possibility to generate failure planes through weaker unreinforced zones. This type of reinforcement mechanism is similar to traditional geo-synthetic approaches in which materials were introduced to weaker planes of the soil as geo-grids, geo-cells, geo-mats, or geotextiles (Gowthaman et al., 2018).

Randomly Distributed Natural Fiber reinforcement (RDFS) is a well-recognized soil improvement technique in which fibers comprised of desired property and quantity are assorted randomly and compacted in situ and are commonly differentiated as natural fibers (coir, sisal, bamboo, palm, jute, cane, etc.) and synthetic fibers (polypropylene, polyethylene, polyester, etc.), Geosynthetics, such as geogrid, geotextile, geonet, and geocell, are traditional reinforcement materials. And they can be varied in forms like strips, bars, grids, sheets, etc., and in mechanical properties, texture, stiffness, and density and also, they are often introduced to structures in different layers with a predetermined orientation. However, potential weak planes can develop along with the geo synthetics-soil interface due to lower interfacial shear strength. Compared with traditional geosynthetic reinforcement methods, soil reinforced with discrete short fibers is easier to prepare and can maintain strength isotropy without introducing the potential of a weak plane (Wang & Guo, 2017).

Generally, natural fibers are advantageous than synthetic fiber because its relatively inexpensive Cheap, locally and widely available, eco-friendly, easy to process, and renewable, natural fibers such as sisal fiber have high tensile strength and modulus. It can enhance the soil strength and reduce the swelling and shrinkage properties, it is also not significantly affected by weather conditions, compared to cement, lime and other chemical stabilization techniques construction by using fibers can take place in any weather condition and Good dimensional stability, anti-slip nature, high moisture absorption, and biodegradability (Sumi & Unnikrishnan, 2015)**.**

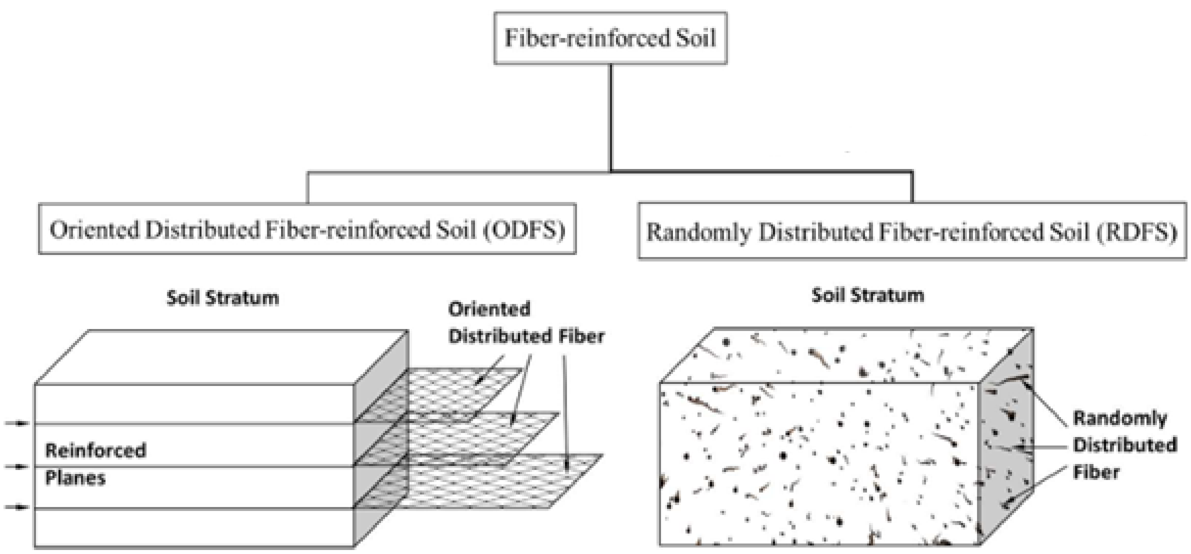

Figure 2.8 Classification and illustration of Fiber reinforcement mechanism of soil (Gowthaman et al., 2018).

Hejazi et al.(2012) concluded that as the length increases the local aggregation (clumping) and folding of fibers (balling) are two problems concerned with fiber–soil composites. In this way, fiber lengths beyond 51 mm were not found to significantly improve soil properties and proved more difficult to work within both laboratory and field experiments. So using a length beyond 5cm is not effective (Hejazi et al., 2012).

2.8.2.1 Sisal fiber reinforcement

Microstructurally natural fiber structures consist of cellulose, hemicellulose, lignin, pectin, and waxes. However, cellulose is more predominant of all the compositions, due to this reason the structure of the natural fiber is of lingo cellulosic fibrils embedded in the lignin matrix (Fuqua et al., 2012). The cellulose fibril is a natural polymer made of the chained cellulose molecule, identified in plants as slender like crystalline micro fibrils along the length of the fiber that affect the reinforcing effect of natural fiber. Cellulose provides higher mechanical strength (tensile and flexural strength) in addition to providing rigidity due to its crystalline nature (Fuqua et al., 2012). Sisal fiber is composed of numerous elongated fiber cells that tapper towards each end these fiber cells are linked together using middle lamella which consists of cellulose, hemicellulose, lignin, and pectin (Maya et al., 2017).

Natural fibers are good reinforcing materials. among the various natural fibers, sisal fiber is of particular interest since its composites have high impact strength besides having moderate tensile and flexural properties compared to other lingo-cellulosic fibers. Sisal fiber is a promising reinforcement for use in composites on account of its low cost, low density, high specific strength and modulus, no health hazards, easy availability, and renewability (Maya et al., 2017).

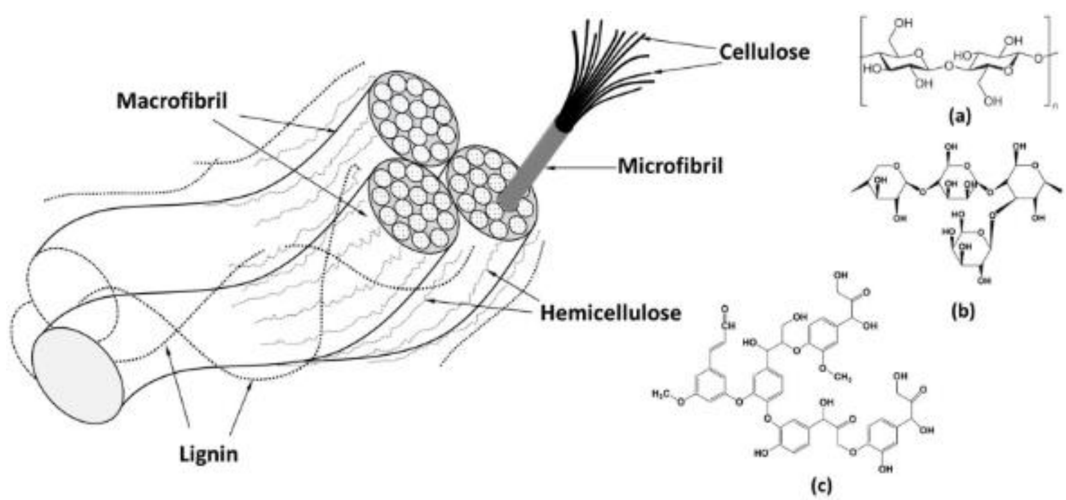

Figure 2.9 Fibril matrix structure of plant fiber and the chemical composition of (a) Cellulose, (b) Hemicellulose; and (c) Lignin (Gowthaman et al., 2018)

2.8.2.2 The chemical composition of sisal fiber

Different researchers reported chemical compositions of sisal fiber. Benítez-Guerrero et al.(2017) Founded sisal fiber contains 43%-88% cellulose, 10%-15% hemicellulose, 4%-20% lignin, (0.8-10), pectin, (1-4) water soluble, 0.15-2 fat and wax 10%-22% moisture content Fuqua et al. (2012) found that sisal fiber contains 56.5%-78% cellulose, 5.6%- 16.5% hemicellulose and 8%-14% lignin. Naveen et al. (2019) founded sisal fiber contains 65%-68% cellulose, 10%-22% hemicellulose, 9.9%-14% lignin and 10%-22% moisture content.

These large variations in the chemical composition of sisal fiber are due to different measurement methods, sources, and ages. Sisal fibers are cellulose-rich (> 65%) and show tensile strength. Sisal is a natural fiber material, cheap, easy laying in the field, and biodegradable. Sisal has low moisture absorption, excellent durability, and high initial tensile strength. The distributed fibers subjected to tension contribute to the increase in strength of specimens (Khan et al., 2019).

Table 2.12 Properties of sisal fiber studied by previous literature

Author	Density (g/cm^3)	Diameter (μm)	Ultimate tensile strength (MPa)	Young's Modulus (GPa)
Maya et al. (2017)	1.45	50-200	400-700	9-12
Naveen et al. (2019)	1.33-1.5	25-400	400-700	9-38
Khan et al. (2019)	1.58	80-.200	385-728	-
Arulsurya et al. (2019)	1.47	25	407.4	-
Tamilvendan et al. (2020)	1.5	15-30	510-635	9-22

Among the various natural fiber composites, sisal fiber-reinforced composites produce superior impact strength with moderate tensile and flexural properties making them potential alternatives for applications that require good impact strength. Currently, sisal fiber has been used as a reinforcement in a variety of thermoset, thermoplastic, and bio-degradable polymer composites, and their mechanical properties like stiffness tensile strength, compressional strength, flexural strength, and impact strength have been evaluated. Sisal fiber obtained from the sisal plant (known formally as Agave sisalana) is one of the most widely used natural fibers in various applications and can be easily cultivated in many parts of the world. The sisal plant grows about

100–200 leaves during its lifetime, and each leaf contains long, straight fibers which can be extracted using specialized processes.

The mechanical and chemical properties of sisal vary depending on source location, age of the fiber, and method of extraction utilized. The principal components of sisal plant fiber are cellulose, hemicelluloses, waxes, pectins, mineral matter, and water. The sisal fiber is primarily made up of cellulose. The cellulose chains are firmly ordered and directed, which enables the sisal plant cellulose a high degree of crystallinity and results in good resistance to chemical and physical agents. Cellulose and lignin are the main chemical properties that are easily affected by environmental and manufacturing processes (Betelie et al., 2019).

(a) (b)

Figure 2.10 Photographic view of, (a) Sisal plant and (b) sisal fiber

2.8.2.3 Availability of sisal fiber in Ethiopia

Sisal fiber obtained from the sisal plant (known formally as Agave sisalana) is one of the most widely used natural fibers in various applications and can be easily cultivated in many parts of the world. The sisal plant grows about 100–200 leaves during its lifetime, and each leaf contains long, straight fibers which can be extracted using specialized processes. Among the various natural fiber composites, sisal fiber-reinforced composites produce superior impact strength with moderate tensile and flexural properties, making them potential alternatives for applications that require good impact strength. Currently, sisal fiber has been used as a reinforcement in a variety of thermoset, thermoplastic, and bio-degradable polymer composites, and their mechanical properties like stiffness tensile strength, compressional strength, flexural strength, and impact strength have been evaluated. Sisal is wide abundance in Ethiopia as well as it has a lower cost compared to synthetic fibers (Betelie et al., 2019).

2.8.2.4 Fiber degradation and treatment

The issue of biodegradability can be overcome by suitable fiber treatment methods. These modification techniques can make natural fibers on par with or even superior to synthetic fibers (Torio-kaimo et al., 2020). Although fibers comprise many desirable engineering properties, degradation due to microorganisms, moisture, and alkali attack remains a major challenge in geotechnical applications of fiber soil reinforcement technique. Such biodegradation of fibers leads to depletion of strength because of the breakdown of cell wall polymers such as cellulose, hemicellulose, and lignin. Moisture absorption effect and biodegradation are interconnected, as moisture absorption resulting from Hemi cellulosic content provides favorable conditions for microorganisms to live and spread on the fiber material, and the presence of moisture on the particle interfaces roles as a lubricant layer that induces slipping and rupture effect which results in the reduction of friction and cohesion in fiber-reinforced soil. The lignin which exists as the outer layer of the fiber matrix protects the fibers up to a certain extent by resisting the intrusion of bacterium (Wei & Meyer, 2015).

Bethel (2021) conducted a test to determine the effect of kerosene on the water absorption capacity of Katcha fiber the effect of Kerosene soaking duration on the water absorption capacity of Katcha fiber is observed for 2 and 3 days-soaked fiber. 2 days of soaking reduces the WAC by 55.43%- and 3-days soaking reduced by 58.039%. It is also observed that the tensile strength of kerosene-coated Katcha fiber is greater than that of uncoated Katcha fiber. Water absorption tests were also conducted on uncoated and kerosene-coated Enset by Keftaw (2021). The authors concluded that the water absorption capacity of kerosene-coated Enset fiber is reduced compared to that of uncoated Enset fiber.

Torio-kaimo et al (2020) Water absorption capacity tests were carried out to determine if a physical coating can help defer the degradation of coir by reducing moisture intake. the effect of kerosene coating on the water absorption behavior of coir. The author concluded that kerosene-coated coir fibers significantly lower water absorption levels than uncoated fibers. There is also a steep increase in water absorption at the beginning of the test. As immersion time increased, water absorption become constant.

2.9 Review of Previous Work on Soil Stabilization Using Bagasse Ash

Worku (2015) has done the Stabilization of Lateritic Soil with Sugarcane Bagasse Ash Using 2%, 4%, 6%, 8%, and 16% bagasse ash by weight of dry soil. The effects of the ash on the geotechnical properties of the soil were investigated by conducting Atterberg limit, free swell, linear shrinkage, compaction, and CBR tests. The test result showed a slight decrease in the maximum dry density and soaked CBR values. The free swell also showed a slight decrement up to 4% of ash then showed an increase and A slight increase in plasticity index, shrinkage limit, optimum moisture content, and unsoaked CBR values. She concluded that sugarcane bagasse ash is not an effective stabilizer for the improvement of some of the geotechnical properties of the soil on its own.

Miresa (2019) used sugar cane bagasse ash which is found to be rich in SiO_2 to partially replace the quartz/silica sand in wall tiles to produce wall tiles of better quality and low cost. The results show that the replacement of quartz with 35% SCBA and at 17MPa pressing pressure was found to be the best for ceramic wall tile production. Hence, it is proved that SCBA has a silica content that could replace the natural quartz. For the test, a partial replacement of 20, 35, and 50% by weight were used.

Bekele (2022) studied the Dynamic Property of Expansive Soil Treated with Sugarcane Bagasse ash. The analysis results showed that SCBA considerably reduces the plasticity characteristics of the soil and increases the unconfined compressive strength (UCS) up to 9% addition by dry mass. The addition of SCBA not only improves the plasticity and UCS but also increases the dynamic shear modulus and the damping ratio.

Surjandari et al. (2017) studied Enhancing the engineering properties of expansive soil using bagasse ash. The soil was treated with (0%, 5%, 10%, 15%, and 20%) bagasse ash based on dry mass. They evaluate the performance of bagasse ash stabilized soil using physical and strength performance tests, namely the plasticity index, standard Proctor compaction, and percentage swelling. X-ray diffraction (XRD) test was conducted to evaluate the clay mineral, whereas an X-ray fluorescence (XRF) was to the chemical composition of bagasse ash. From the results, it was observed that the basic tests carried out proved some soil properties after the addition of bagasse ash. Furthermore, the plasticity index decreased from 53.18 to 47.70%. The maximum dry density of the specimen increased from 1.13 to 1.24 g/cm^3. The percentage of swelling decreased from 5.48 to 3.29% at the optimum of 15% addition of bagasse ash.

Kharade et al. (2014) studied bagasse ash with partial replacement in black cotton soil in various proportions like 3%, 6%, 9%, and 12%. They establish that the optimum proportion of bagasse ash was 6%. The results at this proportion were like MDD increased by 5.8%, CBR increased by 41.52% and UCS increased by 43.58% which showed that by adding bagasse ash CBR and compressive strength increased about 40%, whereas density showed considerable change only.

Khan et al. (2019) studied on engineering properties of soil using bagasse ash and sisal fiber by using Bagasse Ash (2%, 4%, 6%, and 8%) and Sisal Fibers in different lengths (2mm, 4mm, 6mm) with percentages (1%, 1.5%, 2%) by weight of dry soil. They concluded that there is an increase in OMC and a decrease in MDD with the addition of bagasse Ash. There is an increase in the percentage of UCS by 4.70% using 4% BA. and a decrease in the percentage of UCS when samples were prepared with 6%, 8% bagasse ash by 1.01%, 5.70% as compared to raw soil. From the combined effect of BA and sisal fiber, they investigated that the maximum value of UCS is obtained at 4cm length with 1.5% by weight, which is found to be 3.73 kg/cm^2. The percentage increase as compared to the raw soil is 25.16%. There is an increase in soaked CBR by 43.10% using 5% BA and the soaked CBR value of combined soil sample with 4% BA, 1.5% of Sisal Fiber of 4cm length is found to be 3.09%, the increase in CBR value as compared to raw soil is 70.16%.

Dinke (2015) Studied on Effect of Sugarcane Bagasse Ash and Cement on Swelling Characteristics of Expansive Soil around Mojo using clay with high plasticity (CH) by adding 5%, 10%, 15%, and 20% bagasse ash and 2%, 4%, 6% and 8% cement with fixed addition of 10% BA the respective combinations of the additives by dry weight of the soil. He found that 10% BA is optimum based on the Unconfined Compressive Strength (UCS) test result. He showed that the increase in bagasse ash content increases the OMC but decreases the MDD. Also, the value of CBR and UCS of soil increase considerably improved with the BA and cement content. The optimum amount was found to be in the proportion of 88% ES plus10%BA and 2% CE. He concluded that the stabilized material is suitable for pavement.

Singh (2016) Studied on evaluation of black cotton soil stabilized with sugarcane bagasse ash and randomly distributed core fibers on soil that was highly compressible in nature mixed with the varying percentages of Sugarcane bagasse ash from 10 % to 40 % by weight of black cotton soil. The combination of soil and optimum percentage of SCBA mixed soil was added with varying percentages of core fiber of 0.40 mm diameter. The percentage of fiber content varied from 0.25 % to 1.50 % on different aspect ratios of 20, 40, 60, and 80. The author found at an aspect ratio of 40 with 0.75 % fiber content in 20 % SCBA mixed soil, the maximum value of CBR achieved was 4.24 times greater than the CBR value of black cotton soil.

2.10 Review of Previous Work on Soil Reinforcement Using Sisal Fiber

Sandyarani et al. (2018) worked on the Stabilization of black cotton soil by using sisal fiber. By varying percentages of sisal fiber with 0.2%, 0.5%, 0.9% and 1.2% with varying lengths of sisal fiber are 3cm, 3.2cm, and 3.4cm in length at the interval of 0. 2cm. The addition of sisal fiber decreases OMC, and maximum dry density is increased by 0.5%. Unconfined compressive strength and California bearing ratio (Un soaked) are also increased at 0.5% sisal fiber.

Haimanot (2020) studied the application of sisal fiber as a subgrade soil reinforcement by Taking a sample from Alem Tena along Modjo-Meki expressway. Having A-6 classes of soil according to AASHTO soil classification and CL by USCS. In percentages of 0.5%, 1%, 1.5%, and 2% by dry weight of soil and length of 10mm, 15mm, and 20mm. It is observed that MDD is decreased and OMC is increased with an increase in fiber content and length. It is also shown that increasing the length and content of sisal fiber further increases the CBR and UCS of reinforced soil. The optimum CBR and UCS value is obtained at 1.5% fiber content for 15mm fiber length.

Dubey and Tegar (2018) studied the impact of sisal fiber as a reinforcement on the behavior of expansive soil. They used (1%, 2%, 3%, 4%, 5%, and so on) sisal fiber by dry weight of soil. A reduction in the maximum dry density and the optimum moisture content of the soil after the addition of sisal fiber was observed. The CBR value was improved after the addition of sisal fiber. The optimum CBR value is obtained for 1cm length of fiber with 4% fiber content.

Narayana & Praveen (2019) performed an experimental study on the stabilization of loose soil by using sisal fiber. They prepared soil samples with the addition of sisal fibers by 0.25%, 0.5%, 0.75%, and 1% by using the average length of sisal fiber 10- 15mm approximately. They observed that Un soaked and soaked conditions and maximum values of CBR and UCS were obtained when 0.75% sisal fiber was added.

Ellappan et. al (2020) worked on the influence of natural fibers in the strengthening of black cotton soil. They carried out the tests using sisal, banana, and jute fibers with the ratio of 0.2%, 0.4%, and 0.6% by the dry weight of the soil fraction and having 2 cm length. They investigated that the addition of fibers increases the strength in the reasonable value for CBR up to 21.55% in 0.4% of banana, 0.6% of sisal, and 0.6% of jute fiber combination. Optimum Moisture Content (OMC) increased up to 20% for the same combination.

Mathew and Raneesh (2016) Performed attest by randomly mixing soil with varying percentages of sisal fiber (0.3%, 0.6%, 0.9%, and 1.2%), bagasse ash (3.5%,7%, 10.5%, and 14%), and glass powder (7%, 14%, 21%, and 28%) by dry weight of soil. They observed that the unconfined compressive strength and California bearing ratio values increased with the addition of an optimum percentage of sisal fiber, bagasse ash, and glass powder waste to the mixture of black cotton soil. by the optimum dosage of 0.9% of sisal fiber,7% bagasse ash, and 14% glass powder waste.

Sridharan & Prakash (2000) used randomly distributed sisal fiber as reinforcement in black cotton soil at four different percentages of fiber, i.e., 0.25, 0.5, 0.75, and 1% by weight of dry soil, and four different lengths of fiber, i.e., 10, 15, 20 and 25 mm and found significant improvement in the shear strength parameters (c and ϕ) of the soil and concluded that the increase in fiber length and fiber content in soil causes reduction in the OMC and dry density. The cohesion improved linearly with fiber content up to 0.75% and shear strength increased with the increasing length of fiber up to 20 mm.

Panwar et al., (2018) conducted a study on fly ash and sisal fiber for improvement in CBR of clayey soil. They conduct tests like Maximum Dry Density (MDD), Optimum Moisture Content (OMC) and California Bearing Ratio (CBR for different percentage of fly ash (10%, 20%, 30% & 40%) along with Sisal fiber (composition 0.25%, 0.5%, 0.75% & 1%) at the length of 1cm. The optimum combination recommended for clay soil is 30% Fly ash with 0.75% Sisal fiber

1cm in length. The CBR value of clay soil treated with 30% Fly ash, and 0.75% Sisal fiber, having a fiber of 1cm length is increased by 68.97% and 137.95% respectively.

Table 2.13 Summary of related works on bagasse ash and sisal fiber stabilization

Authors	Type of additive	% Of additive (by weight of dry soil)	Soil type	Major finding
Worku (2015)	Bagasse ash	2%, 4%, 6%, 8%, and 16% bagasse ash	Lateritic soil	Slight increase in plasticity index, shrinkage limit, OMC, and unsoaked CBR values.
Bekele (2022)	Bagasse ash	0%,6%,9%,12% of BA	Expansive soil	Plasticity characteristics reduced and unconfined compressive strength (UCS) increased up to 9% addition of BA.
Surjandari et al. (2017)	Bagasse ash	(0, 5, 10, 15, and 20%) of bagasse ash	Expansive soil	The plasticity index decreased MDD increased. The percentage of swelling decreased from 5.48 to 3.29% at the optimum of 15% bagasse ash.
Kharade et al. (2014)	Bagasse ash	3%, 6%, 9%, and 12%. BA	Black cotton	MDD increased by 5.8%, CBR increased by 41.52% and UCS increased by 43.58% by the addition of bagasse ash.
Khan et al. (2019)	Bagasse ash and Sisal fiber	(2%, 4%, 6%, and 8%) BA and (2mm,4mm,6mm) length with 1%,1.5%, 2% SF	Black cotton	An increase in soaked CBR by 43.10% at 5% BA and the soaked CBR value of combined soil sample with 4% BA, 1.5% of Sisal Fiber of 4cm length is found to be 3.09%, The CBR increased by 70.16%.
Dinke (2015)	Bagasse ash and cement	5%, 10%, 15%, and 20% BA with 2%, 4%, 6% and 8% cement	Expansive soil	CBR and UCS of soil increase at the optimum of 88% soil plus 10%BA and 2% Cement.
Singh (2016)	Bagasse ash and Coir fiber	Bagasse ash 10 % to 40 %, and 0.25 % to 1.50 % on different aspect ratios of 20, 40, 60, and 80 of fiber	Black cotton	With an aspect ratio of 40 with 0.75 % fiber content in 20 %, SCBA mixed soil, the maximum value of CBR achieved was 4.24 times greater than the CBR value of black cotton soil

Authors	Type of additive	% Of additive (by weight of dry soil)	Soil type	Major finding
Sandyarani et al. (2018)	Sisal fiber	0.2%, 0.5%, 0.9% and 1.2% at 3cm, 3.2cm, and 3.4cm	Black cotton	0.5% and 3.4cm sisal fiber gave the highest value of UCS and unsoaked CBR.
Haimanot (2020)	Sisal fiber	0.5%, 1%, 1.5%, and 2% by 10 mm, 15 mm, and 20 mm length	Low plastic soil	1.5% fiber content for 15mm fiber length gives maximum CBR and UCS
Dubey and Tegar (2018)	Sisal fiber	(1%, 2%, 3%, 4%, 5%, and	Expansive soil	Maximum CBR value obtained for 1cm length of fiber with 4% fiber content.
Narayana & Praveen (2019)	Sisal fiber	0.25%, 0.5%, 0.75%, and 1% by 10- 15mm length	Loose soil	Maximum values of CBR and UCS were obtained when 0.75% sisal fiber was added.
Ellappan et. al (2020)	sisal, banana, and jute fibers	0.2%, 0.4%, and 0.6% of fibers, having 2 cm length	Black cotton	Maximum CBR was obtained at 0.4% of banana, 0.6% of sisal, and 0.6% of jute fiber combination.
Mathew and Raneesh (2016)	Sisal fiber, Bagasse ash, and glass powder	Sisal fiber (0.3%, 0.6%, 0.9%, and 1.2%), bagasse ash (3.5%,7%, 10.5%, and 14%), and glass powder (7%, 14%, 21%, and 28%)	Black cotton	They observed that the unconfined compressive strength and California bearing ratio values increased at the optimum dosage of 0.9% of sisal fiber,7% bagasse ash, and 14% glass powder waste
Sridharan & Prakash (2000)	Sisal fiber	Sisal fiber (0.25, 0.5, 0.75, and 1%) and four lengths 10, 15, 20 and 25 mm	Black cotton	The cohesion and shear strength increased with the increasing length of fiber up to 20 mm and 0.75% Sisal fiber
Panwar et al., (2018)	Fly ash and sisal fiber	Fly ash (10%, 20%, 30% & 40%) SF (0.25%, 0.5%, 0.75% & 1%) having 1cm length	clayey	The maximum CBR value observed at 30% Fly ash, and 0.75% Sisal fiber, 1 cm length

2.11 Research Gaps

From the reviewed literature, the following summary and conclusion were made. Expansive soils have been reported all over the world and considerable areas of Ethiopia are also covered by these soils. The engineering and physical properties of expansive soil can be improved by the addition of different industrial wastes like fly ash, bagasse ash, and fiber reinforcement. The previous investigations conducted in Ethiopia are mainly focused on chemical stabilization alone or fiber reinforcement to improve the properties of expansive soils. Limited studies have been done on the combination of chemical stabilization and fiber reinforcement. The study on the combined effect of bagasse ash and sisal fiber on the strength properties of expansive soil is limited in the literature. Investigation of bagasse ash stabilized soil was done by considering the effect on Atterberg limit, compaction, UCS, and CBR value but the effect of the bagasse ash on the consolidation properties was not studied. Therefore, it is necessary to conduct an experimental study to investigate the effects of bagasse ash and sisal fiber on the strength properties of expansive soils and consolidation properties of bagasse ash and sisal fiber stabilized soil to mitigate the problems that come from expansive soil.

3 MATERIALS AND METHODS

In this chapter, a description of the study area, soil sampling technique, the materials used, the methods adopted, and laboratory experiments carried out to achieve the objectives of the study are presented.

3.1 Description of The Study Area

Dukem is located along with the Addis Ababa -Adama express way 37 km south east of Addis Ababa along with Adama, Dire Dawa - Djibouti transport axis and its geographical location is 8° 47’ 40 “north,38 ^{0} 54’ 1’’’ east and its elevation is 1959 meter. It is a station on the Ethio-Djibouti railway.it is also the location of an industrial park covering 40 hectares owned and developed by East African Group (Ethiopia). The population is rapidly growing since Dukem is near to the capital city (Addis Ababa) and has economic importance. The town is planned to be one of the largest industrial areas in Ethiopia. In the town, different huge factories- East Africa Bottling, Elsewedy cable factory, marble factory, etc. have been constructed and many more are planned.

The soil profile of the town can be divided into Expansive and non-Expansive soils. The Expansive soil covers a wider area of the town. Expansive soil is clay soil which may be black or gray in color Approximately 80% of the town is covered by black clay soil. 15% of the area is covered by mountains which mainly consist of cinder and gravel. the remaining 5% is covered by red clay soil. Around 50% of the existing structures constructed on black clay soil show the appearance of cracking. during the dry season 0.01-1.08 m open fissures have been observed. Around 60% of the area is used for cash crop production. The remaining part of the town is used for residential and industrial areas (Tamrat, 2013).In this town, most lightweight residential houses show uplifting and cracking. There was also a crack shown on the ground surface around the study area.

Adugna (2021) studied on Effect of Maize Cob Ash and Waste Ceramic Powder on the Geotechnical Properties of Expansive Soil: In Case of Dukem town. He collected soil samples from two stations below a depth of 1.75m from ground level at Tadecha kebele around china's eastern industrial zone. he found that. The soil is grayish-black in color and highly plastic clay. He also conducted a one-dimensional consolidation test on remolded soil samples. He concluded that the soil under this area possesses medium to high settlement and compressibility properties (Adugna, 2021).

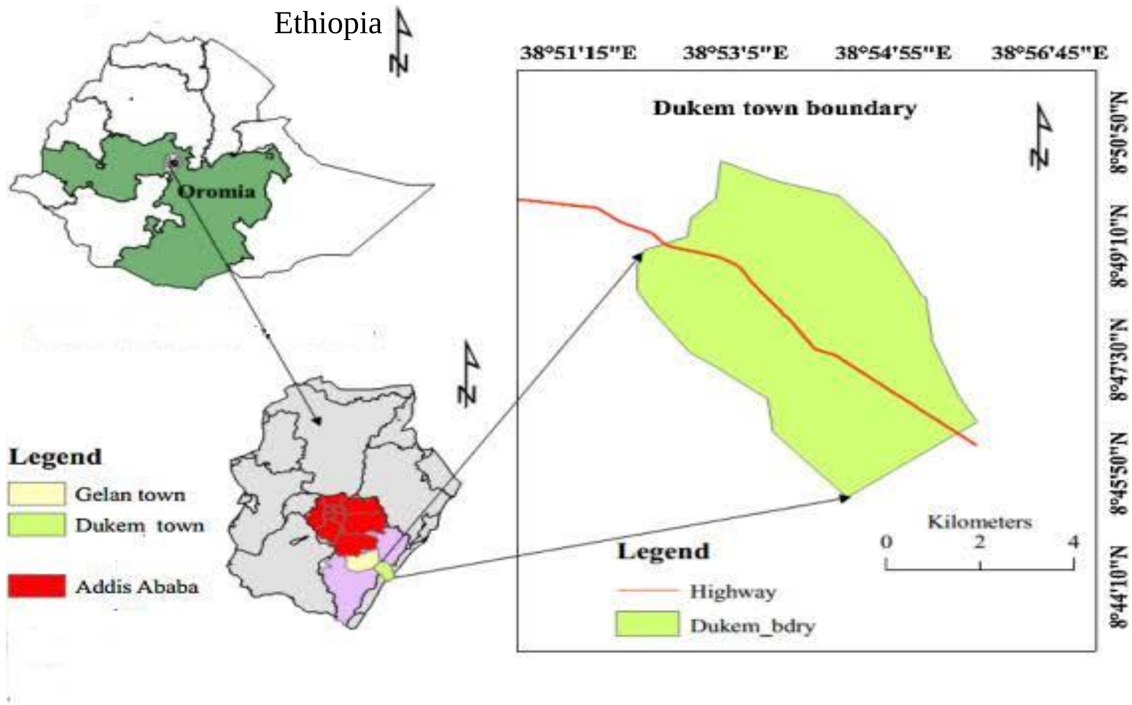

Figure 3.1 Map of the study area

3.2 Materials

Three materials were used for this study was expansive soil from three test pits and the materials involved in the stabilization process which are bagasse ash and kerosene-coated sisal fiber.

3.2.1 Soil

The soil samples used in this investigation were collected from Dukem town by excavating three pits at 1.5m from the natural ground surface for each location to avoid the inclusion of organic matter. After pit excavations, the soil samples were transported in plastic bags to the Adama science and technology university geotechnical laboratory. The location of expansive soil was selected from the previous laboratory results which were investigated before. Laboratory tests such as natural moisture content, specific gravity, Atterberg limits, free swell test, wet sieve, hydrometer analysis, compaction, and UCS tests were performed on disturbed soil samples to characterize the properties of soil in the study area and to select the weaker soil for stabilization work.

Figure 3.2 Test pits location

3.2.2 Bagasse ash

Bagasse ash was collected from Oromia region in Wonji Shewa sugar factory, which is located along the road Adama to Assela. Then it was sieved through a sieve of 150µm to get very fine ash. The properties of bagasse ash used are shown below.

Table 3.1 The properties of bagasse ash used in the study

Characteristics	Specific gravity	Plastic limit	Free swell	Color
Value	2.23	NP	17%	Black

Table 3.2 Chemical composition of bagasse ash (Miresa,2019)

Sr.No	1	2	3	4	5	6	7	8	9	10	11	12
Constituents	SiO_2	Al_2O_3	Fe_2O_3	CaO	MgO	SO_3	K_2O	MnO	P_2O_5	TiO_2	H_2O	LOI
%	72	7.2	4.16	1.44	1.28	2.16	3.5	0.16	0.07	0.09	1.29	0.16
LOI means Loss of Ignition												

3.2.3 Sisal fiber

Sisal fiber is one of the available natural fibers found in Ethiopia. It has white in color. Its length is around 1m-1.2m and taken from Dera sub-city along Adama to Assela road. It is locally available, cheap, and biodegradable hence it does not create disposal problems in the environment. Its inclusion significantly increases the engineering properties of soil. According to available literature, it has good tensile strength in comparison with other natural fibers.

3.2.3.1 Sisal fiber preparation

Sisal fibers are extracted from the sisal plant leaves by using a knife. Extracted manually and then sun-dried and cut to a required length. Before starting mixing sisal fiber with soil fiber treatment with kerosene gas was done to reduce the water absorption capacity and reduce the rate of degradation and the microbial attack caused by water absorption capacity of the Sisal fiber. To investigate the water absorption capacity of the sisal fiber first the dried sisal fiber was soaked in Kerosene for 0, 2,4, and 6 days to determine the effect of kerosene on water absorption capacity of Sisal fiber. After soaking the sisal fiber was removed from the soaking dish after each day of soaking and it was dried. Then the water absorption capacity was measured.

3.2.4 Kerosene

Kerosene gas was used as a physical coating liquid to treat the sisal fiber. 4 Liters of Kerosene were purchased from the TAF gas station in Adama city around Tkur Abay for fiber treatment. It was selected from another type of fiber treatment chemicals since it is easily and widely available in Ethiopia from other fiber treatment methods.

Figure 3.3 Typical photograph of test pit(a) and materials used in the study(b)

3.3 Methods

To achieve the objective of the thesis reviewing the literature, academic journals, research articles, and any previous works that are related to the study topic have done before conducting the tests. The soil samples were collected from three test pits at depth of 1.5 m. Then a series of laboratory tests such as natural moisture content, grain size analysis, specific gravity, free swell, free swell index, free swell ratio Atterberg limits, standard compaction, and unconfined compressive strength (UCS) test was conducted. Based on the test results the weakest soil was selected for stabilization work. Then the soil was mixed with bagasse ash in percentages ranging from 3 % up to 9% of the dry weight of soil and the samples were subjected to Atterberg limit, specific gravity, free swell, free swell index, free swell ratio, standard compaction, and unconfined compressive strength (UCS) tests. The optimum content of bagasse ash was chosen based on the UCS values. the bagasse ash stabilized soil was then reinforced with different percentages and lengths of sisal fiber (10 mm,20 mm,30 mm with 0.5%,1%,1. 5% by dry mass of soil). For expansive soil treated with bagasse ash and reinforced with sisal fiber compaction and UCS, tests were conducted. all sisal fibers used on stabilization were kerosene coated. Then the optimum proportion of bagasse ash and sisal fiber was chosen based on UCS values. Finally, the effect of bagasse ash and sisal fiber on consolidation characteristics of expansive soil was discussed. by conducting a one-dimensional consolidation test for untreated soil and mixing with different percentages of bagasse ash and bagasse ash stabilized soil reinforced with sisal fiber on optimum sisal fiber length with different percentages (0.5%, 1%, and 1.5%).

Table 3.3 Mixed proportion of material used

Soil (%)	100	97	94	91	93.5	93	92.5	93.5	93	92.5	93.5	93	92.5
Bagasse ash (%)	0	3	6	9	6	6	6	6	6	6	6	6	6
Sisal fiber (%)	-	-	-	-	0.5	1	1.5	0.5	1	1.5	0.5	1	1.5
Sisal fiber length (mm)	-	-	-	-	10	10	10	20	20	20	30	30	30

3.3.1 Sample preparation

The sample preparation was made following the method described in AASHTO T87-86. The soil samples taken from three test pits are dried and the larger particles of the soils are crushed and then properly prepared for the laboratory tests. The laboratory tests were done either by air drying of samples or oven drying. Bagasse ash was sieved 150 µm and mixed with the soil by varying the percentages of 0 %,3%,6%, and 9 % then conducting laboratory tests. The kerosene-coated sisal fiber was taken at 0.5 %, 1 %, and 1.5 % by dry weight of the soil, and it was cut in 10 mm, 20 mm, and 30 mm lengths were taken for each fiber percent.

3.3.2 Natural moisture content

This test was performed to determine the moisture content of soil samples. The water content is a percentage, of the mass of “pore” or “free” water in a given mass of soil to the mass of the dry soil solids. Equipment used for this test were Drying oven, Balance, Moisture can, Gloves and Spatula. This test was conducted following ASTM D2216 standard test methods for laboratory determination of water (moisture) content of the soil. The water absorption for sisal fiber was conducted following ASTM-D2495.

3.3.3 Specific gravity

The specific gravity of a given material is defined as the ratio of the weight of a given volume of the material to the weight of an equal volume of distilled water. The specific gravity of the soil sample was determined using ASTM D 854 procedures. It is used to calculate parameters such as void ratio, porosity, particle size distribution using a hydrometer, and degree of saturation. The test was conducted for pure soil, bagasse ash, bagasse ash –soil mix, and sisal fiber.

3.3.4 Particle size distribution

This test is conducted to determine the percentage of different grain sizes contained within a soil. Wet sieve and hydrometer analysis was conducted in this study according to ASTM D422-63. The wet sieve analysis was used to determine the distribution of the course, larger-sized particles, and the hydrometer method is used to determine the distribution of finer soil particles which were passed sieve size 0.075mm (N0.200) to measure the amount of silt and clay size particles. a hydrometer reading was conducted by using hydrometer 151H.

3.3.5 Atterberg limit

Atterberg limit tests are conducted on fine-grained soils to determine the amount of water required to attain different behavioral states. For AASHTO and USCS, soil classification systems value of Atterberg tests is required. The Atterberg limit test that was done in this study includes the determination of the liquid limits, plastic limits, and the plasticity index for the natural soil and soil-bagasse ash mixtures. The tests were conducted following ASTM-D4318. Air-dried samples passing the No.40 (0.425mm) sieve was used to conduct the test.

Liquid limit (LL): The liquid limit is defined as the moisture content at the boundary between the liquid and plastic state. To accomplish the test first, the soil or soil-bagasse ash sample was thoroughly mixed with water by repeatedly stirring, kneading, and chopping with the spatula and placed in the Casagrande cup. The cup containing the sample was lifted and dropped at a rate of 2 drops/sec until the two sides of the sample come in contact at the bottom of the groove along with a distance of about 13mm. The number of blows required to close the grove to this distance was recorded and its moisture content was determined. The relationship between the water content and the number blow is plotted. The water content corresponding to the intersection of the line with the 25-blow abscissa is the liquid limit of the soil.

Plastic limit (PL) Plastic limit of soil is defined as the water content at which the soil changes from a plastic state to a semi-solid state. A portion of the natural soil or the soil-bagasse ash mixture used for the liquid limit test was taken for the determination of the plastic limit. Then the soil or soil-bagasse ash sample was rolled into a diameter of 3mm thread until it begins to crumble.

The plasticity index (PI) is the difference between the liquid limit and the plastic limit of soil, the plasticity index is important in classifying fine-grained soils. It is fundamental to the Casagrande plasticity chart, which is currently the basis for the Unified Soil Classification System.

3.3.6 Free swell, free swell index, and free swell ratio

The free swell test is the simplest test conducted to study the swelling property of the soil and soil bagasse ash mixture. This test has not yet been standardized by AASHTO and ASTM. The method was suggested by Holtz and Gibbs (1956) to measure the expansive potential of cohesive soils. This test was performed by adding 10ml of oven-dry soil that passed No.40 (0.425mm) sieve into 100 ml graduated cylinder then filled with distilled water and letting the content for approximately 24 hours until all the soil completely settles on the bottom of the graduated cylinder. Then the final volume of the soil or soil mixture was noted. measuring the volume after the sample was soaked and settled down in water and kerosene for 24 hr.

The free swell index test was conducted following IS 2720 (Part 40) 1985 testing procedure. First Two oven-dried soil or soil-bagasse ash samples passing through 425μm sieve was taken and 10ml of each sample were placed separately in two 100ml graduated cylinder. One cylinder is filled with kerosene and the other is filled with distilled water. After 24 hours' final volumes are noted. The free swell index value was determined.

3.3.7 Linear shrinkage

Linear shrinkage is the change in length of a soil sample as it dries to the shrinkage limit, SL, expressed as a percentage of the original length. The test is conducted following ASTM D4943-89 for untreated soil, and soil-bagasse ash samples. The apparatus used was a mold of brass 140 mm long and 25 mm diameter, a flat glass plate (as for the liquid limit test), spatula, oil, an oven, and the ruler were used. First, the soil was mixed which has approximately falls on 25 blows. The internal length of the mold was measured, then the mixed sample was placed in the mold, and thoroughly removed all air bubbles from the specimen were by lightly tapping the base of the mold. The mold was slightly filled and leveled off the excess material using a spatula. The sample was allowed to dry in air at room temperature for 24 hours. Linear shrinkage is calculated as $\Delta L/L_o$, where L_o is the original length, L is the length at a given 24 hours, and $\Delta L = L - L_o$.

3.3.8 Compaction

Compaction is the densification of soil by the removal of air, which requires mechanical energy. The degree of compaction of soil is measured in terms of its dry unit weight. When water is added to the soil during compaction, it acts as a softening agent on soil particles. The soil particles slip over each other and move into a densely packed position. The dry unit weight after compaction first increases as the moisture content increases beyond a certain moisture content any increase in the moisture content tends to reduce the dry unit weight. This phenomenon occurs because the water takes up the spaces that would have been occupied by the solid particles. The moisture content at which the maximum dry unit weight is attained is generally referred to as the optimum moisture content. In this study, compaction was done by the standard proctor test according to ASTM D698. Air-dried soil passing no 4 sieve was used to determine the moisture-density relation of the soil mix. Compaction was done for three pits untreated soil samples and soil treated with bagasse with different percentages (i.e., 3%, 6%, and 9% by dry weight of soil).

Figure 3.4 Photographic view of dry mix of soil, BA, and SF (a), Compacted mix(b)

It was also done for kerosene coated sisal fiber-reinforced sample with the optimum of the soil-bagasse ash content by different percentages and different lengths of sisal fiber 0.5 %, 1 %, and 1.5 % by dry weight of soil) and 10mm,20mm and 30mm fiber length. Moisture content versus dry density curve was plotted. The optimum moisture content (OMC) and maximum dry density (MDD) were obtained from the graph.

3.3.9 Unconfined compressive strength (UCS)test

The unconfined compression test is a special type of unconsolidated-undrained test that is commonly used for clay specimens. In this test, an axial load is rapidly applied to the specimen to cause failure. The unconfined compressive strength UCS value of compacted soil is the most common and adaptable method of evaluating the strength of stabilized soil. I this study, The UCS test was conducted according to the ASTM D-2166 standard. UCS test includes soil, soil with varying percentages of Bagasse ash (3%, 6%, 9%, and soil - bagasse ash and sisal fiber mix by varying percentage and length (0.5 %, 1 %, and 1.5 %) with 10mm,20mm and 30mm). To conduct the test, the sample was mixed with its optimum moisture content and dry density and then compacted in a sample tube having 38mm diameter and 76 mm height. Then the sample was removed from the sample tube using a soil extruder and trimmed to make the ends smooth.

The prepared sample was conducted for un-cured and for 7 days curing. Curing was done by putting the samples in the desiccator. The sample was placed in a loading frame and an axial load was applied to the sample. The force applied to the sample and deformation was recorded. Finally, the stress versus percent strain graph was plotted. Unconfined compression strength (UCS) was taken as the maximum load attained per unit area during loading. The undrained shear strength was calculated as half of the compressive stress at failure.

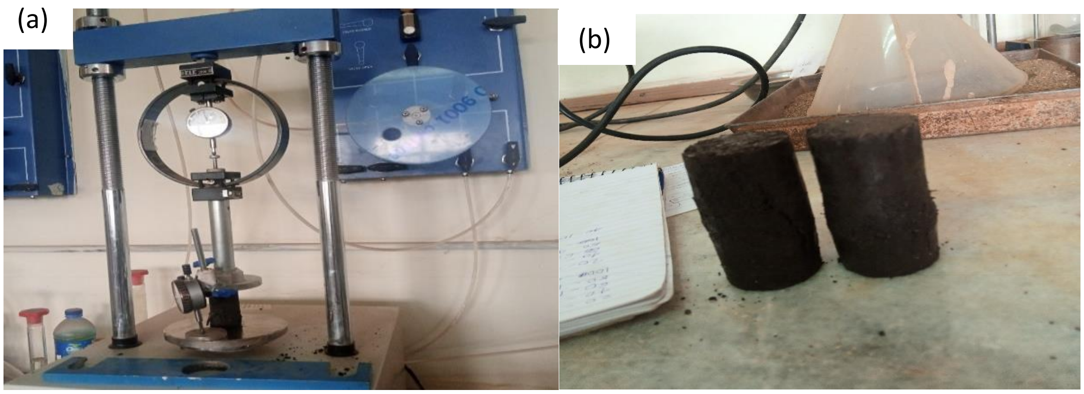

Figure 3.5 Photographic view of UCS test (a) when axial loading (b)samples after load applied

3.3.10 One-dimensional consolidation test

The one-dimensional consolidation test was performed according to the procedure given by ASTM D2435. The samples for the consolidation test were prepared by mixing the soil with the respective optimum moisture content that was obtained from standard compaction test and then compacted with standard compaction mold. The odometer specimen ring of 75 mm diameter and 20mm height was then carefully inserted into the compacted soil. Then soil was extruded by using soil extruders. The samples were placed in the consolidation ring height of 20mm. Then consolidation test was conducted by applying incremental loads starting with 160 kPa and ending with 2560 kPa. During the loading process, water was provided into the cell so that the specimen remains fully saturated. At each loading stage, the deformation at 0, 15, and 30 seconds, then at 1, 2, 4, 8, 15, 30 min, and 1, 2, 4, 8, and 24 hours, was measured. When the maximum load was reached, unloading stages were conducted by reducing the load. The test was conducted for untreated soil, soil with bagasse ash, and soil-bagasse ash - sisal fiber treated samples. The consolidation properties of soils which are the coefficient of consolidation, compression index, coefficient of the volume of compressibility, and void ratio versus pressure were determined. A curve of void ratio versus pressure was derived from the deformation at the end of primary consolidation for each load increment. The void ratio vs log pressure curve was plotted to calculate the compression index, C_c, and the recompression index, C_r from the slopes of the portion of the void ratio versus the log pressure curve.

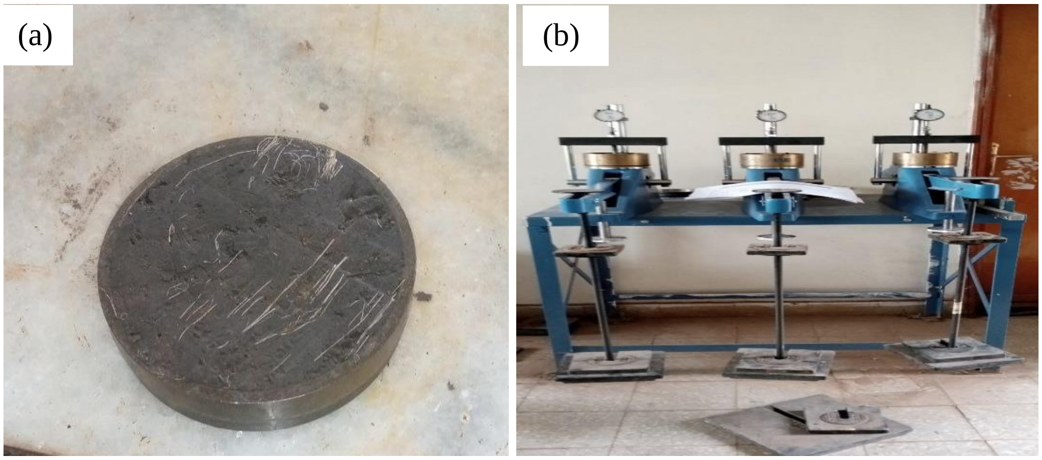

Figure 3.6 Photographic view sample preparation (a)One-dimensional consolidation test (b)

3.3.11 Water absorption capacity test for sisal fiber

A water absorption test is used to determine the amount of water absorbed by sisal fiber. To perform the test first, the dry sisal fiber was immersed in kerosene for 0, 2, 4, and 6 days and on each day the initial mass was taken. Then the kerosene immersed fiber was dried and immersed in the water again for 24 hours and removed the excess water and the final wet mass of the sample was determined. The test is generally used to find out the effects of kerosene on the water absorption of sisal fiber and to identify that a physical coating with kerosene can help to minimize of degradation of sisal fiber by reducing moisture absorption capacity.

Figure 3.7 Photographic view of kerosene immersed (a) and water immersed sisal fiber (b)

4 RESULT AND DISCUSSION

The laboratory test results that are used to identify the effect of bagasse ash and sisal fiber on the properties of the given expansive soil are discussed in this chapter. Tests such as specific gravity, Atterberg limit, particle size analysis, free swell, free swell index, free swell ratio, compaction, uncured and 7 days cured unconfined compressive strength (UCS) test, and one-dimensional consolidation test was conducted for natural soil samples, soil-bagasse ash, and soil-bagasse ash-fiber samples. Then the comparison between untreated expansive soil and after stabilized with bagasse ash and reinforced with sisal fiber was done.

4.1 Properties of Natural soil

The laboratory test results obtained from three test pits of natural soil samples collected from the study are presented in Table 4.1. The soils are black and black-gray in color with a natural moisture content of 23.33%, 25.6 and 24.69 % for TP1, TP2, and TP3 respectively. The specific gravity of soils in the study area is 2.74,2.75, and 2.73 for TP1, TP2, and TP3 respectively. The proportion of fines passing no 200 sieve is 85.30 %,93.30%, and 94.10% for TP1, TP2, and TP3 respectively as shown in Figure 4.1. The Atterberg limit results are, liquid limits 67% ,81% and 78%, the plastic limits 31% ,37%, and 35.5 and plasticity index are 36%, 44 % and 42.5 for TP1, TP2, and TP3 respectively. The values indicate that the soil of the study area is highly plastic clay. Soil falls under A-7-5 soil class based on the AASHTO soil classification system, and CH (Inorganic clays of high plasticity) based on the USCS soil classification system for all samples (TP1, TP2, and TP3) as shown in Figure 4.2 and 4.3. The results obtained are similar to the previous studies in Dukem town.

The soil samples have a free swell of 100%,115, and 110%, free swell index of 71%, 105%, and 91%, and the free swell ratio of 1.71, 2.05, and 1.91 for TP1, TP2, and TP3 respectively. These values indicate that the soils under this area are expansive clay. The soils have a maximum dry density of 1.36 g/cm^3,1.34 g/cm^3 and 1.35 g/cm^3, optimum moisture content of 21 %, 23.8%, and 24.3%.

According to (Alemayehu Teferra and Mesfin, 1999) the liquid limit and plastic index of the study area also showed that the soil in the study area has a higher degree of expansion. Since the liquid limit from 60-70 and plastic index greater than 35 are categorized as a higher degree of expansion soil. The UCS value of the study area also shows that the soil has a lower shear strength value having 53.2 kPa ,48 kPa, and 50.1 kPa for TP1, TP2, and TP3 respectively. The soil generally fell below the standard recommendations for most geotechnical construction works. Therefore, the soil needs improvement in its strength and engineering properties before the construction of a lightly loaded structure on it.

Table 4.1 Properties of the natural soils

Type of tests		Test Methods	Test Results		
			TP 1	TP 2	TP 3
Depth of Sampling, (m)			1.5 m	1.5 m	1.5 m
Natural moisture content, (%)		ASTM D2216	23.33%	25.66%	24.69%
Grain Size Analysis	Clay, %	ASTM D422	55.4	62	60.5
	Silt, %		29.9	31.3	33.6
	Sand, %		14.4	6.5	5.7
	Gravel, %		0.3	0.2	0.2
Specific Gravity		ASTM D854	2.74	2.75	2.73
Atterberg limits, (%)	Liquid Limit, %	ASTM D4318	67	81	78
	Plastic Limit, %		31	37	35.5
	Plastic Index, %		36	44	42.5
Linear shrinkage (%)		ASTM D4943	12	21.7	16.7
Free swell, (%)		IS 2720	100	115	110
Free swell index, (%)			71	105	91
Free swell ratio			1.71	2.05	1.91
AASHTO Classification			A-7-5	A-7-5	A-7-5
USCS Classification			CH	CH	CH
Standard compaction test	MDD, (g/cm^3)	ASTM D698	1.36	1.34	1.35
	OMC, (%)		21	23.8	24.3
UCS test	Un cured (kPa)	ASTM D2166	106.4	96	100.2
Color			Black gray	Black	Black

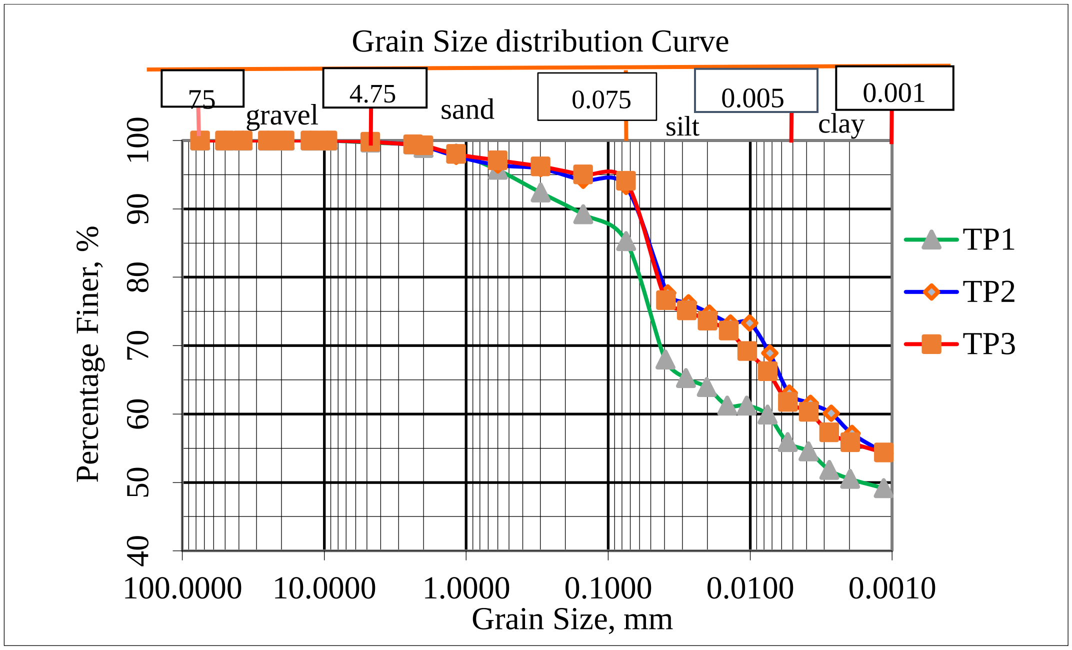

Figure 4.1 Grain size distribution curve for (TP1, TP2, and TP3)

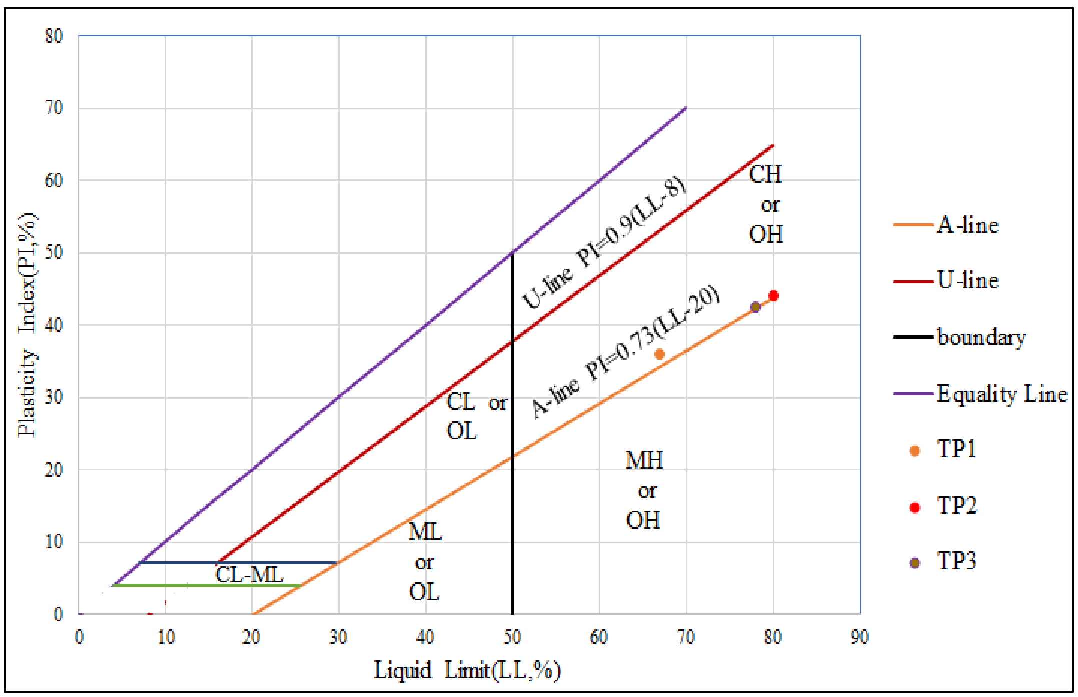

Figure 4.2 USCS Plasticity chart of natural soil samples (TP1, TP2, and TP3)

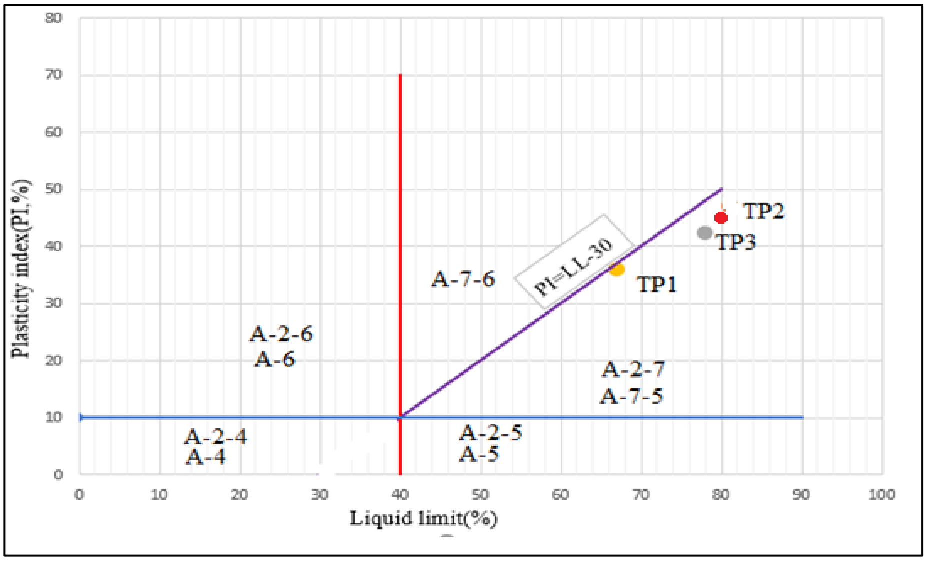

Figure 4.3 AASHTO Plasticity chart of natural soil samples (TP1, TP2, and TP3)

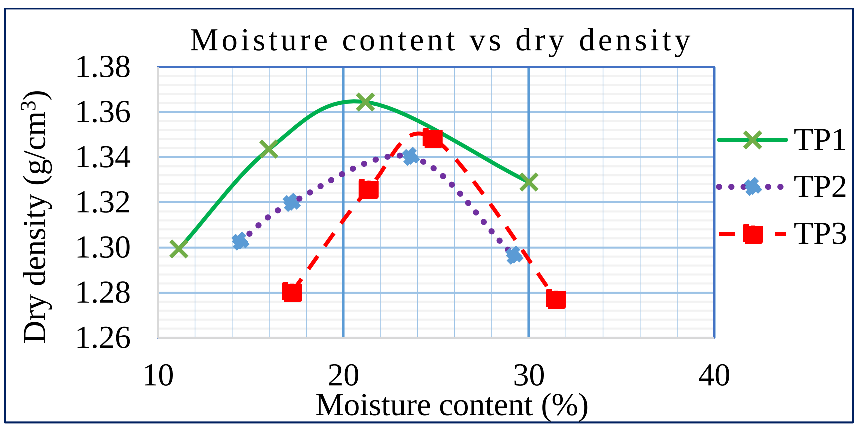

Figure 4.4 Moisture-density relationship for (TP1, TP2, and TP3)

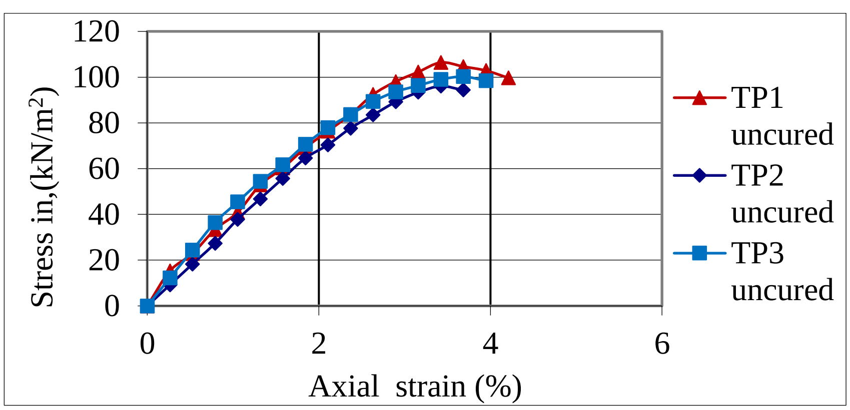

Figure 4.5 UCS stress-strain curve for (TP1, TP2, and TP3)

4.2 Properties of Sisal fiber

The specific gravity and the water absorption capacity of kerosene treated and untreated fiber were done. The test results showed that the individual fibers have a specific gravity of 1.07. The result of the water absorption capacity of un-treated and kerosene-treated sisal fiber showed that at the beginning the water absorption capacity of sisal fiber was decreased when immersion time increased, and the rate of decrease in water absorption capacity was small.

The maximum reduction is observed at 4 and 6 days as shown in Figure 4.6. When further increasing the immersion time the reduction of water absorption capacity become at equilibrium. A similar trend was observed in the effect of kerosene in natural fibers in previous studies (Torio-kaimo et al., 2020).

Table 4.2 Water absorption capacity determination for un-treated and kerosene-treated SF

Days of kerosene immersion	0 day	2 days	4 days	6 days
Moisture content (%)	296.35	162.58	113.84	108.33
% Reduction in water absorption capacity	-	45.1404	61.587	63.444

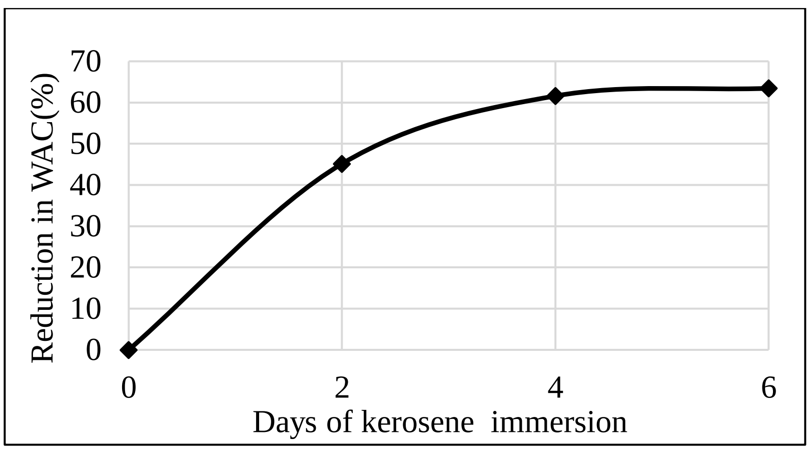

Figure 4.6 Effect of kerosene soaking on water absorption capacity of sisal fiber

4.3 Effect of Bagasse Ash on Properties of Expansive Soil

For studying the effect of stabilizing materials on expansive soil, the TP2 soil was selected. Since it has less strength value compared to other pits TP1 and TP3 the other properties are almost similar.

4.3.1 Effect of bagasse ash on the specific gravity of expansive soil

When different percentages of bagasse ash (0%,3%,6%, and 9%) are added to the natural soil sample the specific gravity is decreased from 2.73 to 2.64 as shown in Table 4.3. This decrease in specific gravity is due to the partial replacement of higher specific gravity soil with bagasse ash which has lower specific gravity. It can be seen that the more the amount of stabilizer lesser would be the specific gravity. It is due to the replacement of soil with the tiny particles of stabilizers, which are lighter in weight than soil particles. The effect of bagasse ash on the specific gravity of the soil is shown in Figure 4.7.

Table 4.3 Specific gravity of natural soil with various percentage of bagasse ash

Bagasse ash (%)	0	3	6	9
Specific gravity (Gs)	2.75	2.68	2.65	2.64
% Decrease in Gs	0	2.6	3.77	4

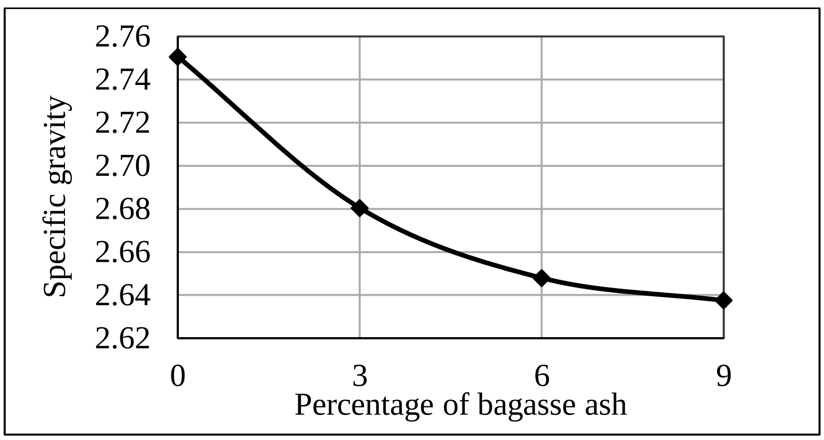

Figure 4.7 Effect of bagasse ash on the specific gravity of expansive soil

4.3.2 Effect of bagasse ash on Atterberg limit

When the addition of bagasse ash to soil the liquid limit was decreased and the plastic limit increased with the increasing bagasse ash content. It also decreased the plasticity index of soil. It is due to the partial replacement of plastic soil particles with non-plastic particles of bagasse ash. Which led to flocculation and agglomeration of clay particles. When there is a reduction in plasticity index significant decrease in swell potential will come. The summary of the effect of bagasse ash on the Atterberg limit is shown in Table 4.4.

Table 4.4 Effect of bagasse ash on Atterberg limits

% Bagasse ash	Liquid limit (LL)	Plastic limit (PL)	Plasticity index (PI)
0	81	37	44
3	68	36	32
6	60	34	26
9	55	33	22

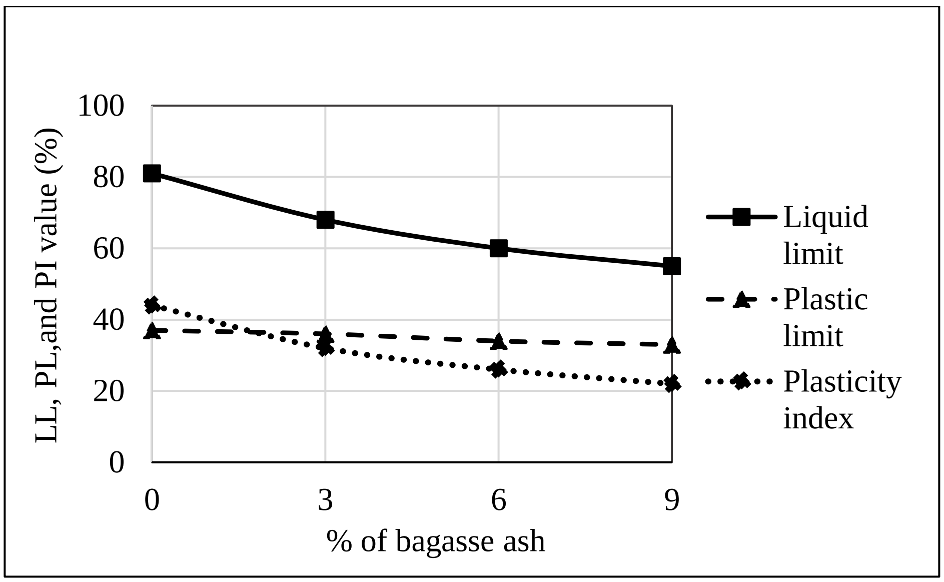

Figure 4.8 Atterberg limit test result for different percentages of bagasse ash

The decrease in the plasticity index is due to the partial replacement of plastic soil particles with non-plastic bagasse ash materials and may be due to a reduction in clay fraction (which is responsible for the plasticity of the soil). It is also due to the cation exchange and flocculation of clay particles. A reduction in plasticity index causes a significant decrease in swell potential and removal of some water that can be absorbed by clay minerals The higher the plasticity index, there will be the greater engineering problems associated with using the soil as an engineering material, such as road subgrade and foundation support for a light building.

4.3.3 Effect of bagasse ash on the free swell, free swell index, and free swell ratio

The addition of bagasse ash to expansive soil slightly decreases the free swell, free swell index, and free swell ratios. The highest decrease is obtained when the soil is treated with 9% bagasse ash. The free swell index value decreased from 115% to 90 % with an increased amount of bagasse ash percentages from 0% to 9%. According to swell classification based on a free swell, the treated soil still has a high degree of expansion as discussed by (Chen, 1975). The decrease in free swell values is mainly due to the replacement of expansive clay minerals with bagasse ash which have less affinity for absorbing water as compared to expansive soil. The summary of the free swell, free swell index, and the free swell ratio is discussed in Table 4.5 and Figures 4.9 and 4.10.

Table 4.5 The summary of the free swell, free swell index, and free swell ratio

Bagasse ash content	Free swell (%)	Free Swell Index (%)	Free swell ratio	%Decrease in free swell	%Decrease in free swell index	%Decrease in free swell ratio
0% BA	115	105	2.05	-	-	-
3% BA	110	91	1.91	4.54	13.33	6.83
6% BA	105	86	1.86	8.7	18.095	10.22
9% BA	90	81	1.81	27.74	22.857	13.26

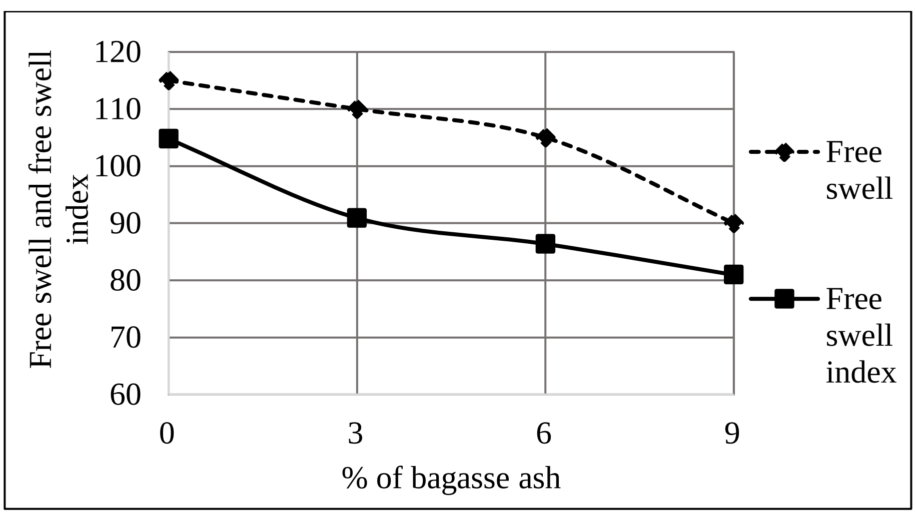

Figure 4.9 Results of the free swell index and free swell

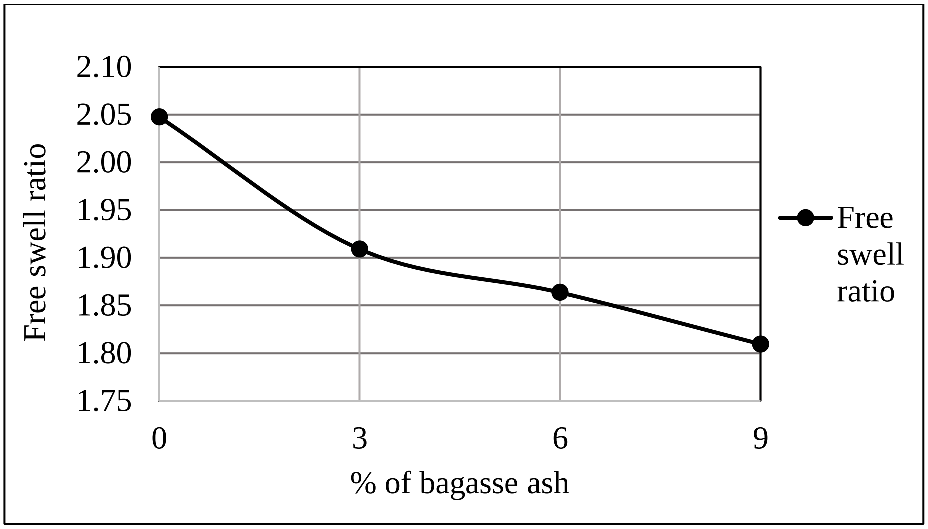

Figure 4.10 Results of free swell ratio

4.3.4 Effect of bagasse ash on linear shrinkage of expansive soil

The effect of different percentages of bagasse ash on linear shrinkage of expansive soil is Summarized in Table 4.6. The addition of bagasse ash decreases the linear shrinkage value. From 14.75 to 8.53. The soil is changed from critical stage to moderate shrinkage behavior of expansive soil. The increase in bagasse ash resulted in a decrease in linear shrinkage of soil. These could be due to the flocculation and aggregation phenomena of clay particles induced by the presence of bagasse ash contributing to the formation of coarser particles and enhancing the strength of the treated soil.

Table 4.6 Effect of bagasse ash on linear shrinkage of expansive soil

Bagasse ash	Initial length(cm)	Final(cm)	Linear shrinkage (%)
0% BA	14	12.2	14.75
3% BA	14	12.5	12.00
6% BA	14	12.7	10.23
9% BA	14	12.9	8.53

Figure 4.11 Linear shrinkage of expansive soil mixed with various bagasse ash contents

4.3.5 Effect of bagasse ash on compaction characteristics

Maximum dry density decreases from 1.34g/cm^3 to 1.27g/cm^3 of soil samples with increased bagasse ash content from 0% to 9%. It shows the addition of bagasse ash on the expansive soil sample reduced the maximum dry density compared to that of natural soil. Thus, the decrease in the maximum dry density is mainly due to the partial replacement of comparatively heavy soils with lightweight bagasse ash. And also, the decrease is due to the flocculation and agglomeration of clay particles in the presence of sufficient water, resulting in an increase in voids and a corresponding decrease in dry density.

The optimum moisture content of the soil samples increased from 23.8% to 28.25% with increases in bagasse ash content of 3% to 9% as shown in Figure 4.12. The reason for the increasing OMC may be due to the affinity of the soil-bagasse ash mixed samples for more water to complete the cation exchange reaction. Thus, the increase in OMC may be due to more water absorption by bagasse ash. This implies that more water is needed to compact the soil with bagasse ash the optimum moisture content of the soil increases with increases in bagasse ash because it is finer than the soil. The more fines the more surface area, so more water is required to provide well lubrication. The increase in water content was also attributed to the pozzolanic reaction of the mixes with the soil.

Table 4.7 Compaction test results of soil with different bagasse ash percentage

Bagasse ash (%)	MDD(g/cm^3)	OMC (%)	% Decrease (MDD)	%Increase (OMC)
0	1.34	23.8	_	_
3	1.32	25.4	1.52	6.723
6	1.29	26.6	3.88	11.765
9	1.27	28.25	5.51	18.697

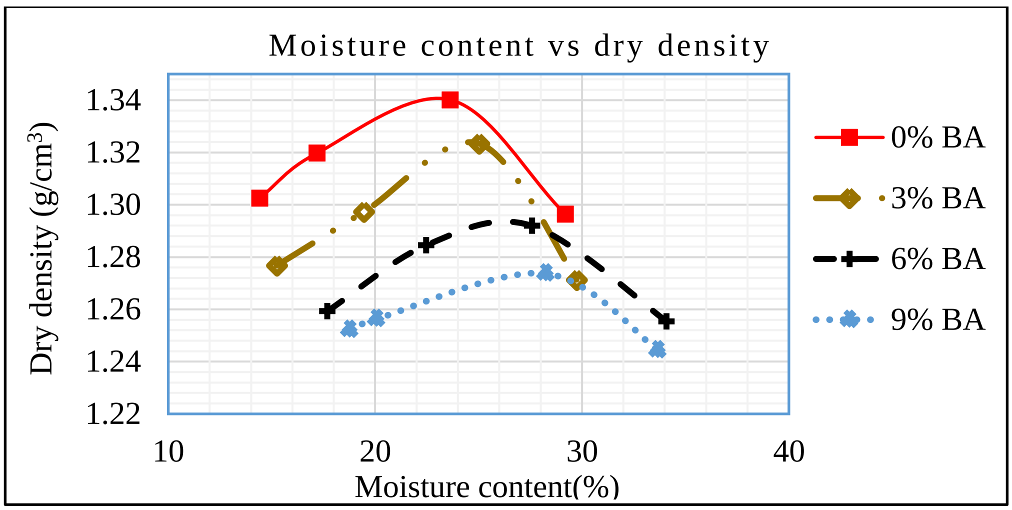

Figure 4.12 The effect of bagasse ash on compaction

4.3.6 Effect of bagasse ash on unconfined compressive strength (UCS) of expansive soil

UCS value of soil sample increases with the addition of bagasse ash content up to 6 % and beyond this limit, the value decreases with the increase in bagasse ash content. The maximum value of UCS is 141.5 kPa and 159.2kPa observed at 6% bagasse ash content for uncured and 7 days cured conditions respectively. The summary of the UCS test result for different percentages of bagasse ash is tabulated in Appendix I from Table I-5 to I-10 for uncured and 7 days cured samples. Generally, it can be expressed that the additions of bagasse ash expansive soils result in chemical reactions in the forms of cation exchange, pozzolanic reaction, and cementation. During cation exchange, flocculation of clay particles occurs giving rise to agglomeration into coarser particles helping resist the compressive stresses much more effectively in comparison with those of natural soil. In addition, the cementation process plays a key role in binding the clay particles together and consequently increasing the compressive stress.

Table 4.8 UCS test results of soil with different bagasse ash percentage

% Bagasse ash	UCS (kPa) (uncured)	Cu(kPa) (uncured)	UCS (kPa) (7 days cured)	Cu (kPa) (7 days cured)	% Increase in uncured(cu)	% Increase 7 days cured(cu)
0	96	48	102.9	51.45	-	-
3	100.8	50.4	110.2	55.1	5	7.09
6	141.5	70.75	159.2	79.6	47.4	54.7
9	116.1	58.05	131.9	65.95	20.93	28.18

The substantial improvement in compressive strength could be attributed to cation exchange and pozzolanic reactions due to a high amount of alumina and silica available in bagasse ash. it is also seen that the unconfined compressive strength of treated expansive soil increased with increasing curing time as illustrated in Table 4.8. The compressive strength of treated soil increases significantly with curing time, which reveals the higher increase in additive content stabilized expansive soil produced a larger impact on the compressive strength of treated soils. As shown in Figure 4.13 the curing time has a significant impact on the strength gain of stabilized soil.

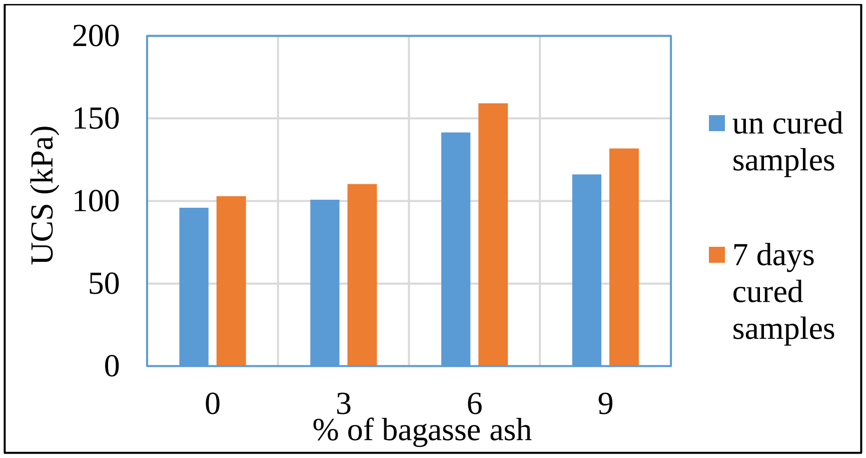

Figure 4.13 Effect of curing time on stress-strain behavior of soil with different % of BA

The unconfined compressive strength of treated expansive soil samples was significantly higher than that of untreated soil samples. An increase in UCS value. this is due to the adhesion between the soil sample and the bagasse ash, which contribute to increased resistance to an axially applied force. But, with further, increments in bagasse ash content beyond the optimum content, the strength of treated soil decreased. This is because the addition of more cohesion less material to the expansive soil reduces the cohesion property of natural soil particles. The stress-strain curves of UCS tests for various percentage of bagasse ash for uncured and 7 days cured samples is shown in Figure 4.14 and 4.15 respectively.

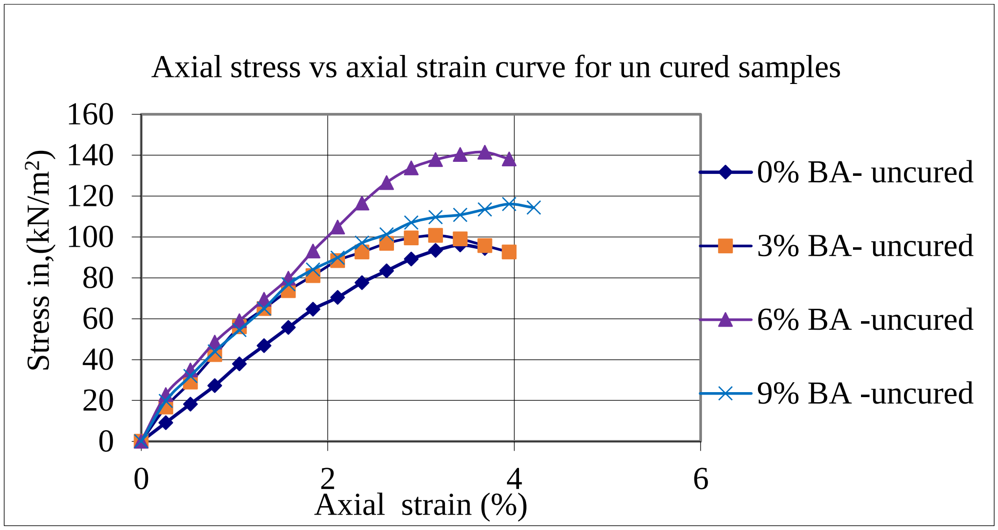

Figure 4.14 Axial stress vs Axial strain for uncured samples with the variation of BA

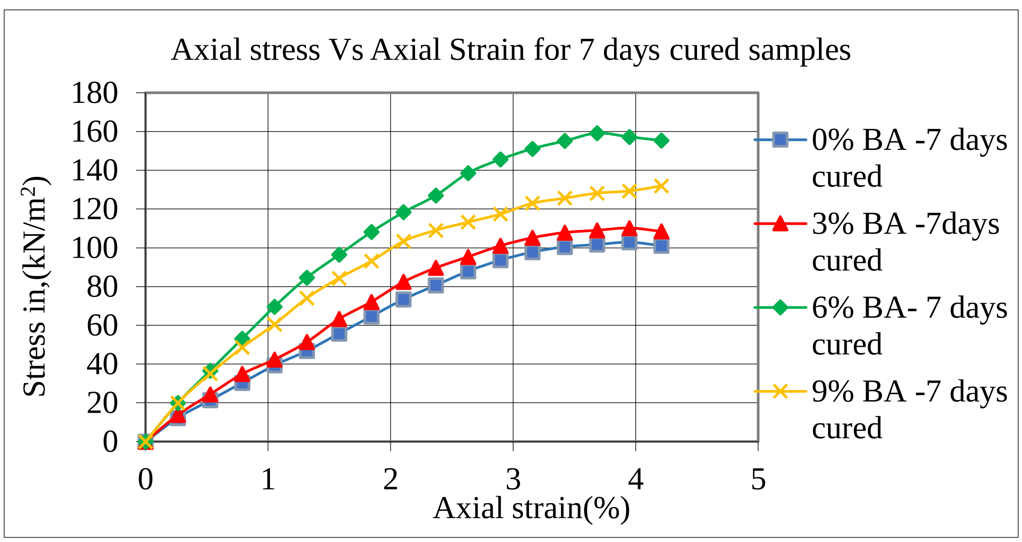

Figure 4.15 Axial stress vs Axial strain for 7-day curing with the variation of BA

4.4 Effect of Sisal Fiber on Bagasse Ash Stabilized Expansive Soil

The optimum bagasse ash content (6%) and different percentages of sisal fiber with different lengths were used for further investigation of the effect of sisal fiber on bagasse ash stabilized expansive soil. A compaction test and unconfined compressive strength (UCS) test were done.

4.4.1 Effect of bagasse ash and sisal fiber on compaction characteristics

The maximum dry density decreases from 1.34g/cm^3 to 1.28g/cm^3 of soil samples with increased bagasse ash and sisal fiber content and length of sisal fiber to that of natural soil. Thus, the decrease in the maximum dry density is mainly due to the partial replacement of dense soils with the light weight bagasse ash and sisal fiber or it is due to the partial replacement of higher specific gravity soil with low specific gravity bagasse ash and sisal fiber. And also, the decrease is due to the flocculation and agglomeration of clay particles in the presence of sufficient water, resulting in an increase in voids and a corresponding decrease in dry density.

Table 4.9 Compaction test results of 6% bagasse ash stabilized soil with different % of SF

Length of SF (mm)	Sisal fiber (%)	MDD (g/cm^3)	OMC (%)	% Decrease in MDD (%)	% Decrease in MDD(BA)	% Increase in OMC (natural soil)	% Increase in OMC (BA)
-		1.34	23.8	-	-	-	-
0		1.32	25.4	1.52	-	6.72	-
10	0.5	1.27	28.5	5.51	3.94	19.75	12.20
10	1	1.25	30	7.20	5.60	26.05	18.11
10	1.5	1.23	31.5	8.94	7.32	32.35	24.02
20	0.5	1.26	29.5	6.35	4.76	23.95	16.14
20	1	1.23	32	8.94	7.32	34.45	25.98
20	1.5	1.22	33	9.84	8.20	38.66	29.92
30	0.5	1.25	31	7.20	5.60	30.25	22.05
30	1	1.22	32.5	9.84	8.20	36.55	27.95
30	1.5	1.21	34	10.74	9.09	42.86	33.86

The optimum moisture content of the soil samples increased from 22.5% to 26.3% with increases in bagasse ash and sisal fiber content and length increased. The reason for the increasing OMC may be attributable to the affinity of the soil-bagasse ash and sisal fiber mixed samples for more water to complete the cation exchange reaction. Thus, the increase in OMC may be due to more water absorption by bagasse ash and sisal fiber. This implies that more water is needed to compact the soil with bagasse ash and sisal fiber mixture. Figure 4.16, 4.17, and 4.18 illustrates the variation of OMC and MDD with different lengths of sisal fiber. It is observed that as fiber length increases the OMC increases and dry density decreased.

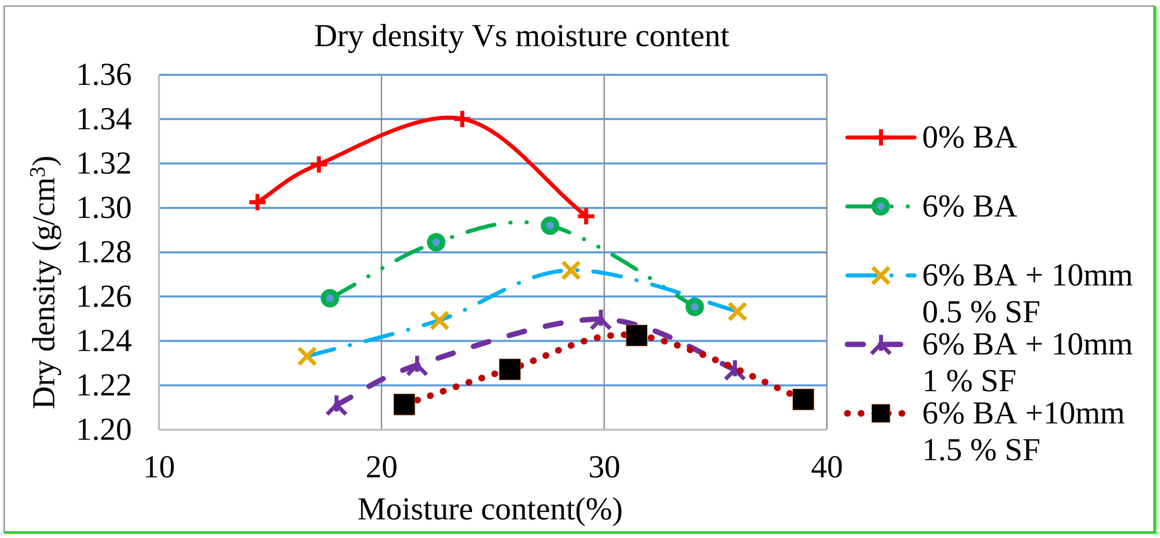

Figure 4.16 Variation of OMC and MDD 10 mm SF with different percentages of SF

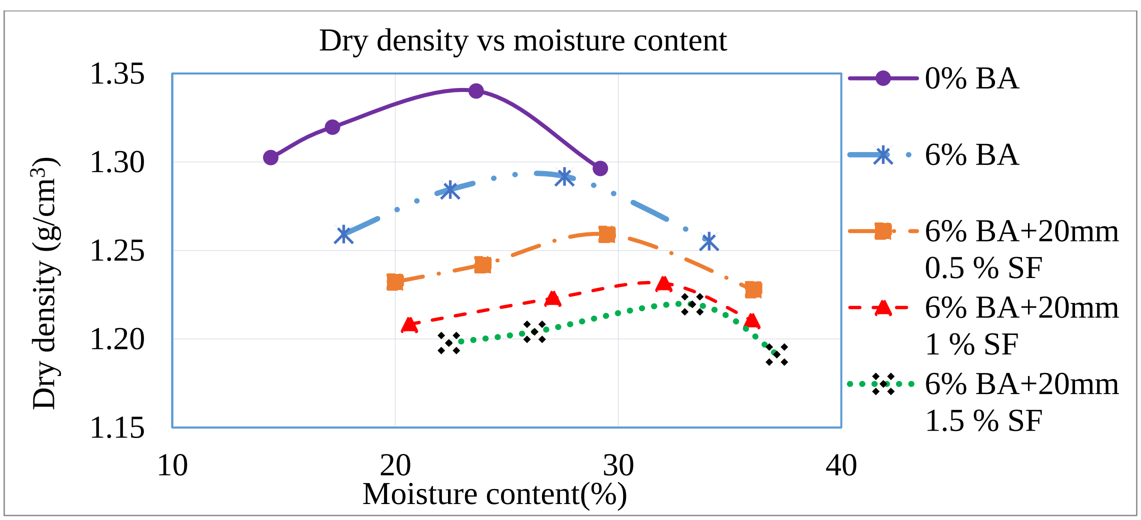

Figure 4.17 Variation of OMC and MDD 20 mm length SF with different percentages of SF

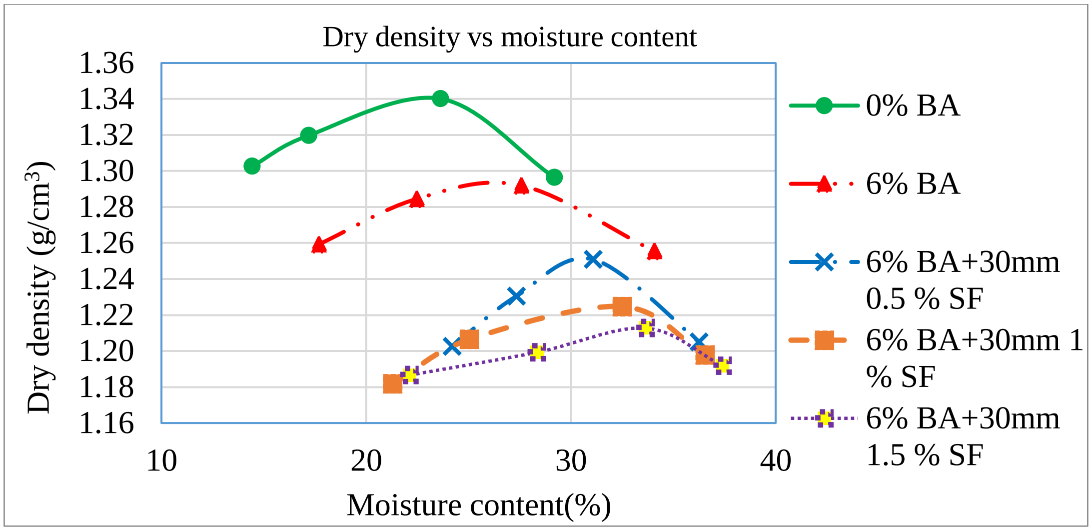

Figure 4.18 Variation of OMC and MDD 30 mm length SF with different percentages of SF

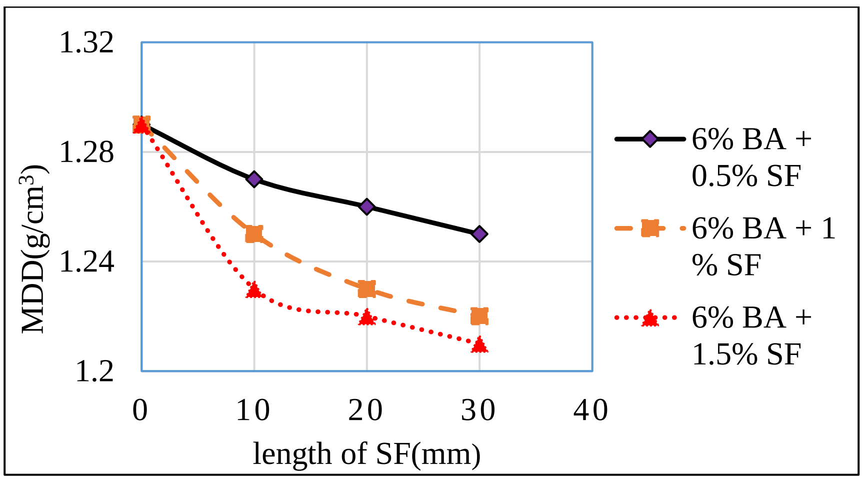

(a)

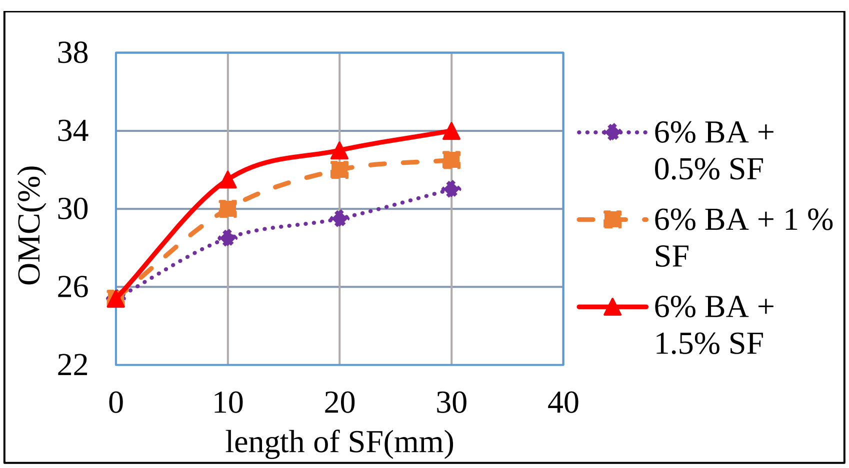

(b)

Figure 4.19 Variation of MDD(a) and OMC(b) BA stabilized soil with increasing SF length

4.4.2 Effect of sisal fiber on unconfined compressive strength of BA stabilized soil

UCS value of soil sample increases with the addition of 6 % BA and different percentages of sisal fiber with length up to the optimum percentages and length of sisal fiber, beyond that it will decrease. The maximum value of UCS obtained is 187.6 kPa and 212.5 kPa for cured and uncured soil samples that were observed at expansive soil with 6% bagasse ash and reinforced with having 20mm length 1% sisal fiber for uncured and 7 days cured samples respectively. These experimental results reveal that the addition of bagasse ash and reinforcement with sisal fiber gives more strength value than using bagasse ash alone. The increase in unconfined compressive of bagasse ash stabilized expansive soil when reinforcing with sisal fiber is due to the fibers' good tensile strength to resist the applied load and gives shear strength. The variation of UCS when uncured and cured conditions with a 20 mm length of sisal fiber are shown in Figure 4.20 and 4.21. The stress vs axial strain curve for 10mm and 30mm length of SF is shown in Appendix I, Figures I-1 to I-4. All UCS test data and results are tabulated in Appendix I.

Table 4.10 Summary of UCS and Cu for 6% bagasse ash stabilized soil and reinforced with different lengths and percent of SF

length of SF, mm	SF (%)	UCS (kPa) - uncured)	Cu (kPa) - uncured)	UCS (kPa) - 7 days cured)	Cu (kPa) - 7 days cured	% Increase in UCS - Uncured natural soil	% Increase in UCS - cured natural soil	% Increase in UCS Uncured -BA stabilized soil	% Increase UCS cured - BA stabilized soil
-	-	96	48	102.9	51.45	-	-	-	-
-	-	141.5	70.8	159.2	79.6	47.4	54.71	-	-
10	0.5	169	84.5	184.6	92.3	76	79.4	19.43	15.95
10	1	175.4	87.7	199.5	99.75	82.7	93.88	23.96	25.31
10	1.5	164.9	82.5	177.3	88.65	71.8	72.3	16.54	11.37
20	0.5	173.4	86.7	186.1	93.05	80.6	80.86	22.54	16.9
20	1	187.6	93.8	212.5	106.25	95.4	106.51	32.58	33.5
20	1.5	169	84.5	183.1	91.55	76	77.94	19.43	15.01
30	0.5	155.2	77.6	171.5	85.75	58.5	66.67	9.7	7.73
30	1	160.2	80.1	182.7	91.35	66.9	77.55	13.22	14.76
30	1.5	150.7	75.35	169.5	84.75	57	64.72	6.5	6.47

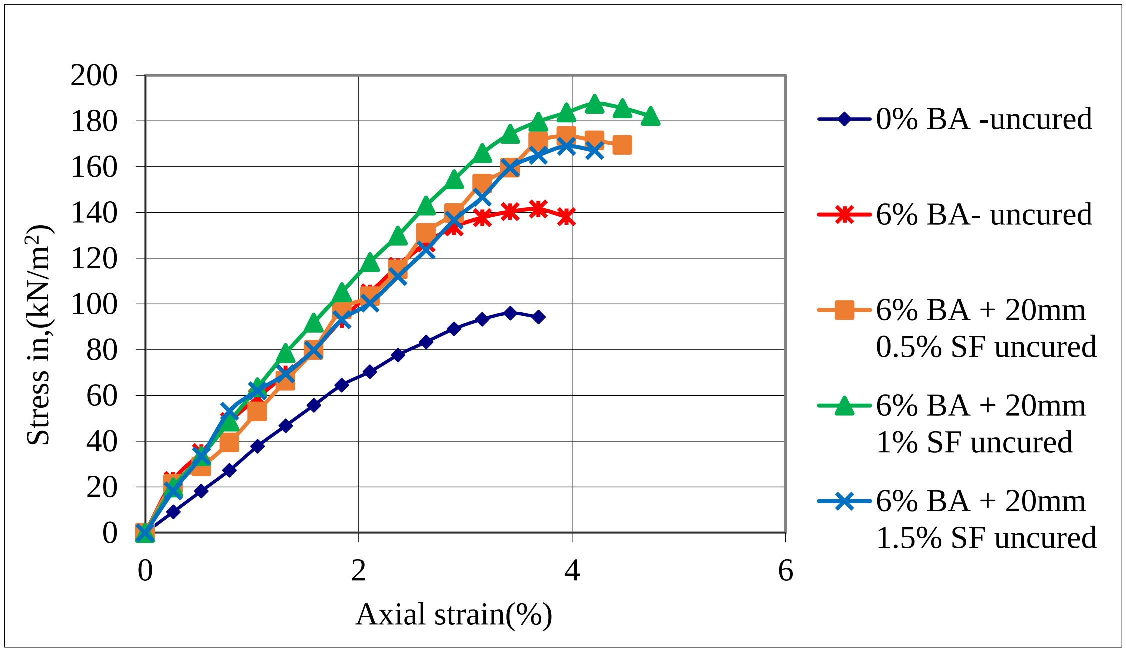

Figure 4.20 Stress vs axial strain curve(uncured) for BA stabilized soil and reinforced with 20mm length and different percent of SF

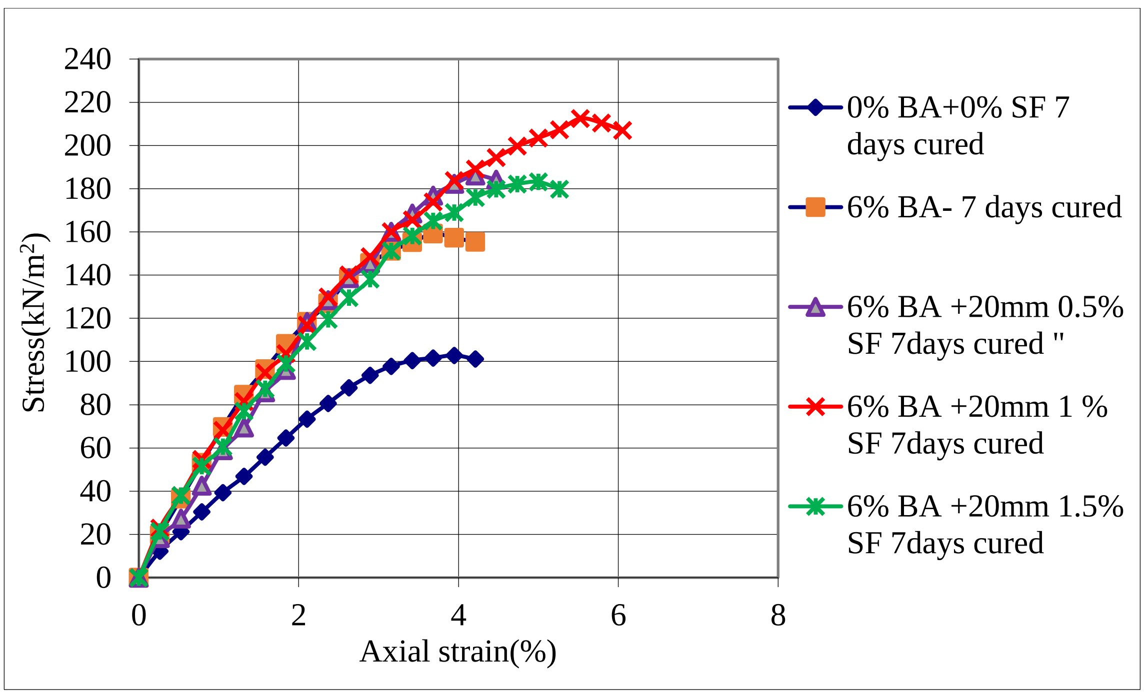

Figure 4.21 Stress vs axial strain (7 days cured) for BA stabilized soil and reinforced with 20mm length and different percent of SF

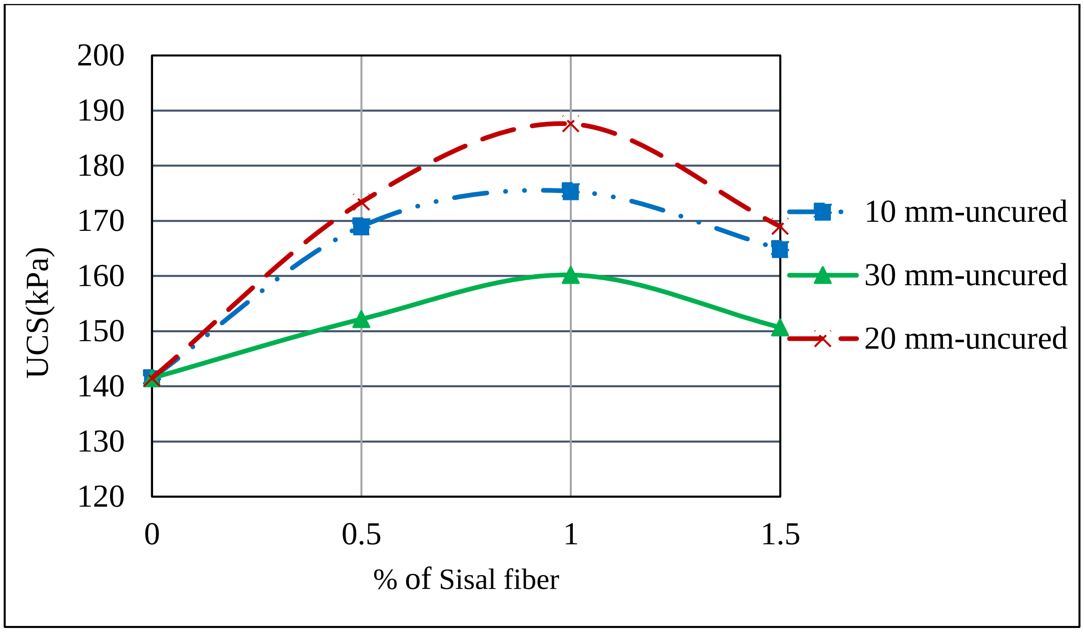

Figure 4.22 Variation of UCS on bagasse ash stabilized soil with different length and % of Sisal fiber (uncured)

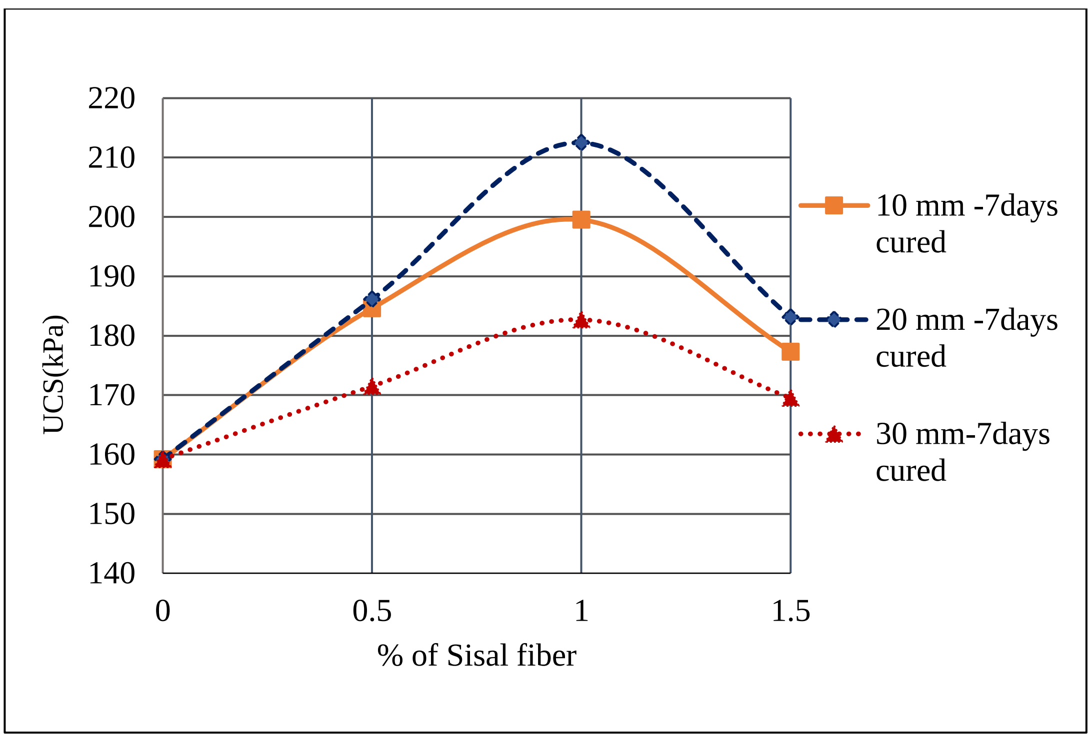

Figure 4.23 Variation of UCS of bagasse ash stabilized soil with different length and % of sisal fiber (7 days cured)

4.5 The Effect of Bagasse Ash and Sisal Fiber on Consolidation Properties of Expansive Soil

One dimensional consolidation test was conducted for natural soil, soil with different percentages of bagasse ash and bagasse ash stabilized soil reinforced with different percentages of sisal fiber with optimum length selected based on UCS value, (20mm). The effect of bagasse ash and sisal fiber on the coefficient of consolidation, volume compressibility, void ratio, compression index, and recompression index is discussed in this section.

4.5.1 The effect of bagasse ash and sisal fiber on coefficient of consolidation of soil

The coefficient of consolidation C_v is revealed the amount of settlement in each loading period. The coefficient of consolidation was determined by using Taylor's square root of time fitting method. The result of the one-dimensional consolidation test shows that the coefficient of consolidation (C_v) increases with an increase in bagasse ash content by up to 6% of bagasse ash content. The addition beyond the optimum content the coefficient of consolidation shows a slight decrement as shown in Figure 4.24. It also increased when bagasse ash stabilized soil reinforced with sisal fiber. The increasing coefficient of consolidation with the addition of bagasse ash and sisal fiber is due to aggregation particles of soil by cation exchange and flocculation process and the soil has less affinity with water when it is mixed with bagasse ash and reinforced with sisal fiber. It can be seen that from Figure 4.25 application of bagasse ash and sisal fiber mix gives better improvement than using bagasse ash alone. It is known that the soils having a higher coefficient of consolidation have good engineering properties and improve the stability of the soil.

The time required to achieve primary consolidation decreases for bagasse ash stabilized soil and bagasse ash stabilized soil with fiber reinforcement. For a given degree of consolidation and a given drainage path and leads to an improvement in the stability and bearing capacity of the soil. It indicates that the combination of bagasse ash with sisal fiber reinforcement is important to improve the stability and bearing capacity of expansive soil.

When proceeding the effect of the stabilizers on the 90% primary consolidation (t_{90}) also decreased with the addition of bagasse ash alone and a combination of the optimum percentages of bagasse ash with sisal fiber as shown in Figures 4.26 and 4.27. The decreasing of t_{90} can leads to an improvement in the rate of consolidation.

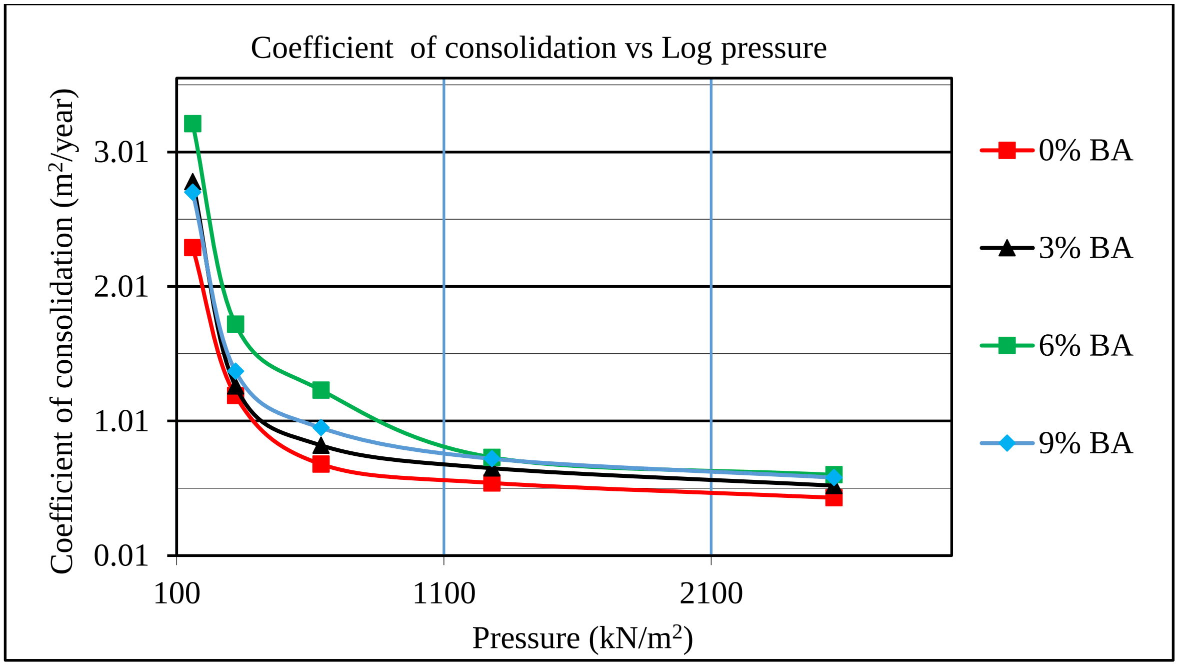

Figure 4.24 Coefficient of consolidation versus pressure for different percentages of bagasse ash

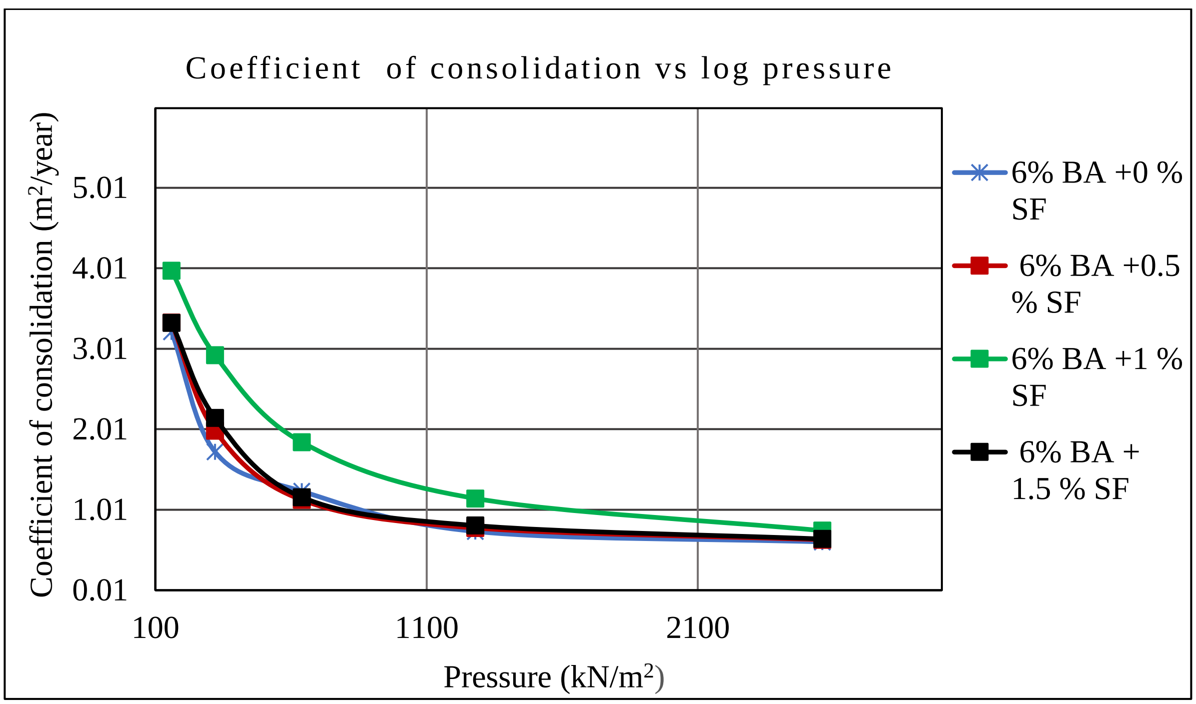

Figure 4.25 Coefficient of consolidation of bagasse ash stabilized soil with different % of SF

Table 4.11 Summary of t_{90} for soil+ different percentages of BA and soil+BA+SF

Pressure (kPa)	% Of Bagasse ash				% Of Sisal fiber		
	0 %	3 %	6 %	9 %	0.5 %	1 %	1.5 %
160	144	117	100	121	96	81	95
320	256	237	169	219	145	100	130
640	400	324	223.16	282.24	230	144	216
1280	441	361	317	327.61	301	210	280
2560	481	400	342.25	361	334	296	320

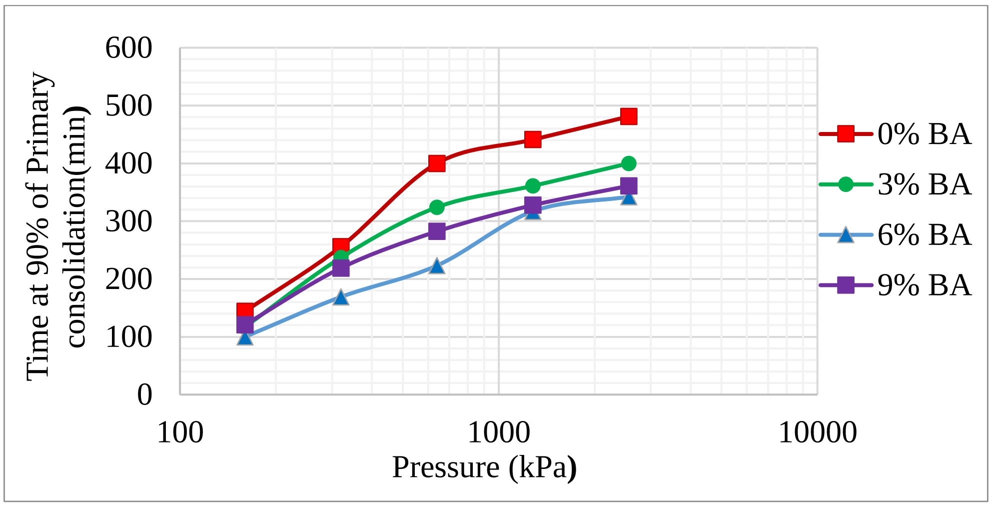

Figure 4.26 The effect of bagasse ash on t_{90} of expansive soil

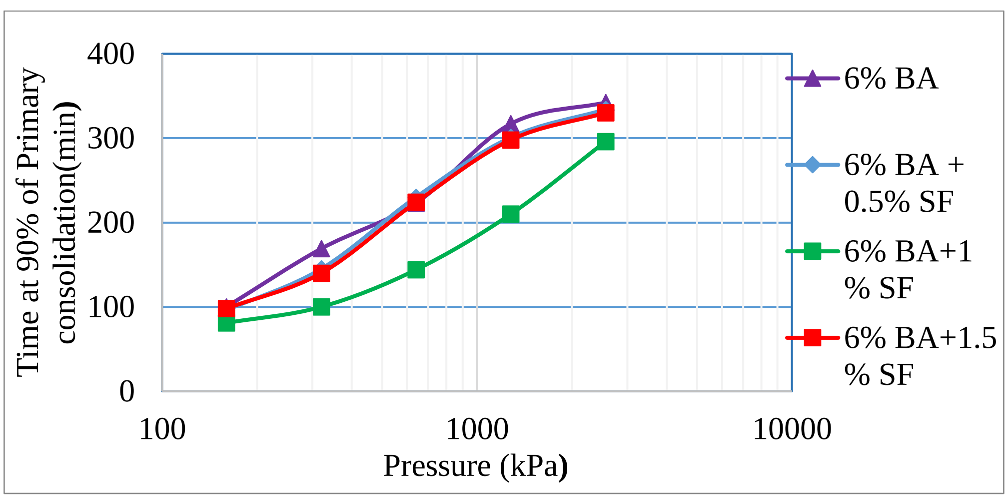

Figure 4.27 The effect of sisal fiber on t_{90} of soil bagasse ash stabilized expansive soil

4.5.2 The Effect of bagasse ash and sisal fiber on Coefficient of Volume Compressibility

The coefficient of volume compressibility, m_v, is defined as the volume change per unit increase in effective stress for a unit volume of soil. The volume change may be expressed in terms of void ratio or specimen thickness. This parameter is useful to estimate the primary consolidation settlement. The coefficient of volume compressibility of each sample was determined from the plot of void ratio versus pressure. the variation of results of coefficient of volume compressibility is shown in Figure 4.28. It can be noticed that the average coefficient of volume compressibility decreases with increasing bagasse ash alone and reinforcing with sisal fiber on the expansive soil. This could probably be due to a pozzolanic reaction taking place within the soil which in turn changes the soil matrix. The addition, of bagasse ash and sisal fiber amount, also led to a reduction in the initial void ratio of stabilized samples.

Table 4.12 Summary of coefficient of volume compressibility for different percentage of BA

	Percentages of Bagasse ash			
Pressure(kPa)	0%	3%	6%	9%
160	0.292	0.291	0.284	0.288
320	0.202	0.199	0.178	0.195
640	0.090	0.085	0.083	0.083
1280	0.047	0.045	0.044	0.045

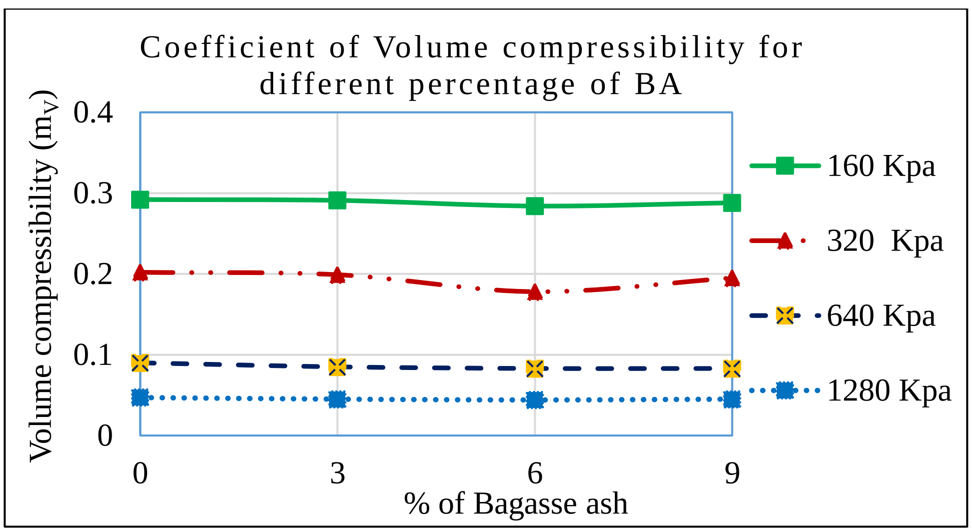

Figure 4.28 Coefficient of volume compressibility different percentage of bagasse ash

Table 4.13 Summary of coefficient of volume compressibility of BA stabilized soil with different % of SF

	Percentages of sisal fiber			
Pressure(kPa)	0	0.5	1	1.5
160	0.284	0.294	0.276	0.328
320	0.178	0.170	0.157	0.155
640	0.083	0.068	0.065	0.075
1280	0.044	0.043	0.030	0.037

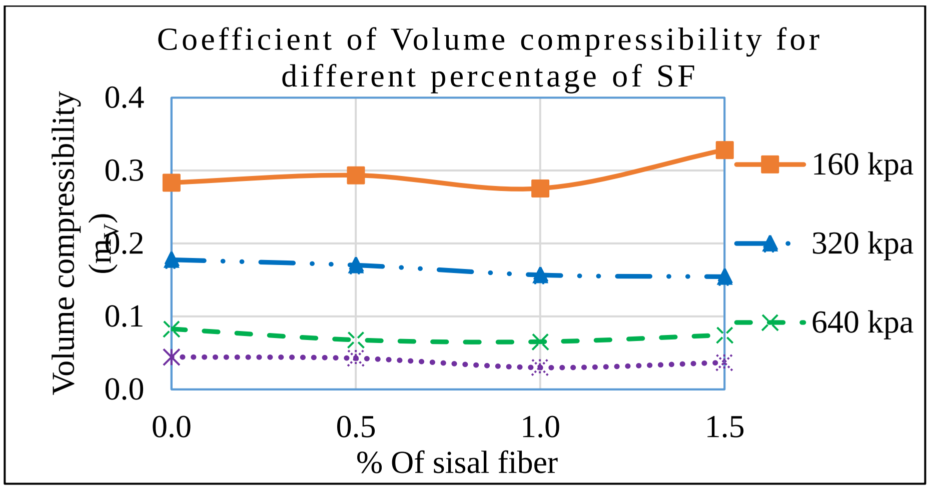

Figure 4.29 The coefficient of volume compressibility with different percentages of SF

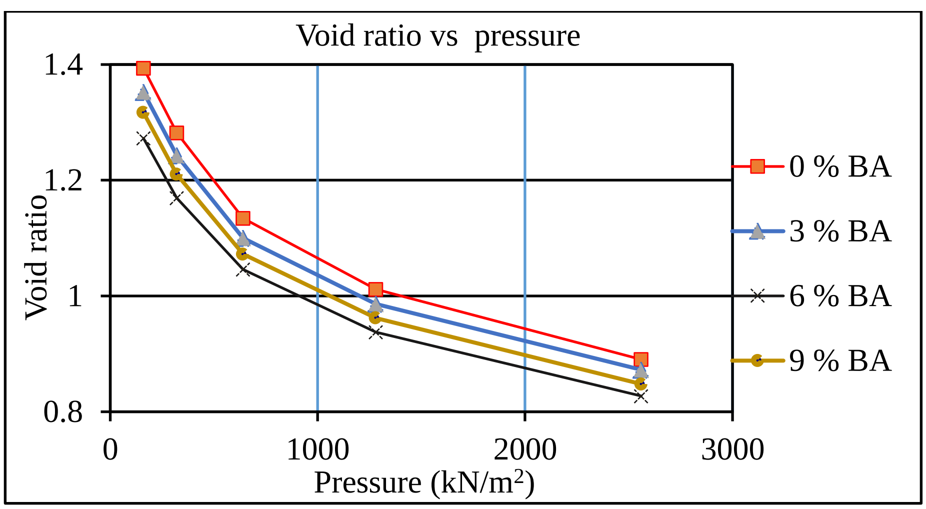

Figure 4.30 Void ratio vs pressure for different percentages of bagasse ash

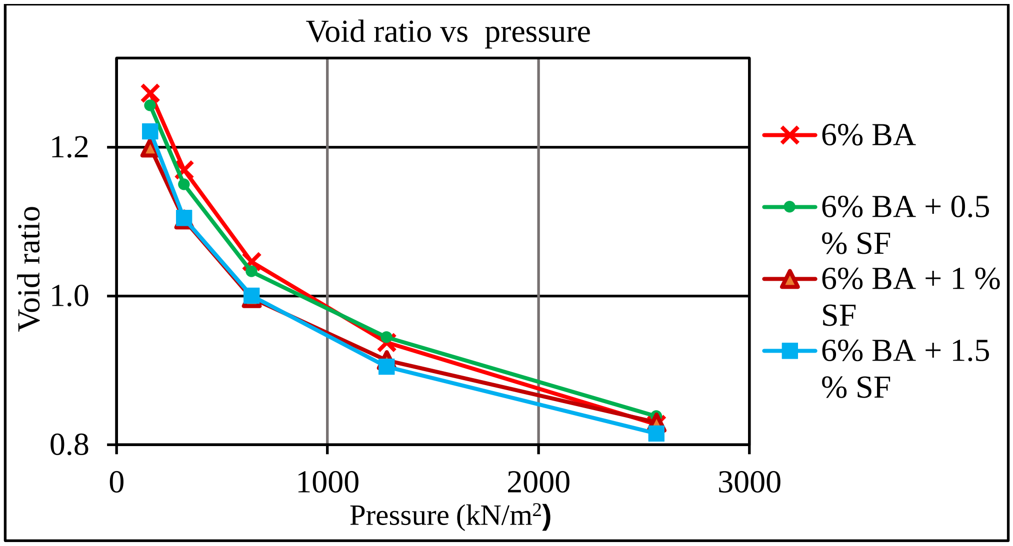

Figure 4.31 Variation of void ratio vs pressure of bagasse ash stabilized soil with different percentages of sisal fiber

4.5.3 The Effect of BA and sisal fiber on Compression and Re-Compression Index

The compression index (C_c) is a key parameter to predict the settlement of an engineering foundation. The higher the value of the compression index, high will be the settlement. A decrease in compression index is an indication of less settlement. The compression (C_c) and recompression index (C_r) is determined by the curve of void ratio versus the effective vertical stress. As shown in Figures 4.32 and 4.33 The compressibility of soils at a given pressure level, the void ratio of samples decreases, the compression index, and re-compression index decrease when soil is stabilized with bagasse ash only and sisal fiber and bagasse ash mix up to the addition of 6% BA and 1% SF. The reduction of compression index and re compression index is due to bonds developed between soil particles during cation exchange, flocculation reaction, and pozzolanic action increase in the flocculation and aggregation because of cation exchange reactions between calcium cations and other exchangeable cations including sodium, magnesium and so forth, which are responsible for the improvement on the compressibility characteristics of stabilized expansive and it prevents the swelling potential of expansive soil and due to the binding of soil particles due to the inclusion of fibers. C_c has decreased with increasing bagasse ash only and stabilized with bagasse ash and reinforced with sisal up to optimum content of the stabilizers. This could be due to the filling-up of voids with a stabilizer, which results in a decrease in void ratio with the same applied load.

Table 4.14 Summary for compression index, re-compression index, and initial void ratio of soil bagasse ash and soil bagasse ash -sisal fiber mix samples

Sample Name	Compression Index, C_c	Re Compression Index, C_r	e_o
Expansive soil	0.418	0.123	1.455
Expansive soil+3% BA	0.398	0.118	1.421
Expansive soil+6% BA	0.37	0.092	1.392
Expansive soil+9% BA	0.39	0.119	1.4
Expansive soil+6% BA+ 20mm 0.5 % SF	0.347	0.087	1.387
Expansive soil+6% BA+20mm 1 % SF	0.291	0.086	1.25
Expansive soil+6% BA+20mm 1.5 % SF	0.337	0.088	1.382

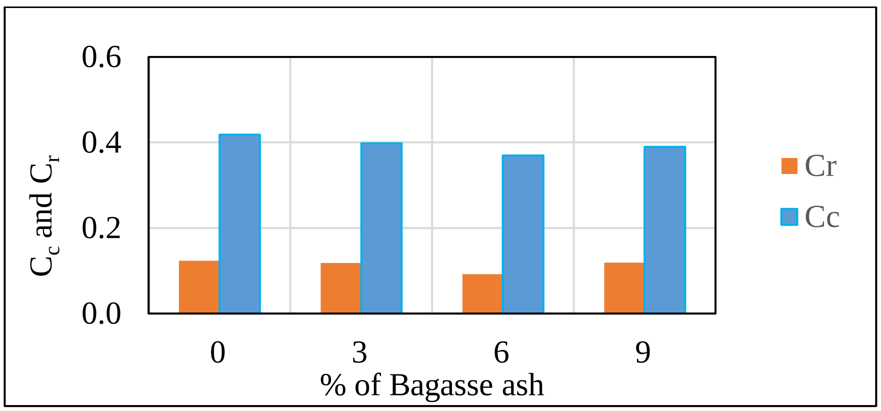

Figure 4.32 Variation of C_c and C_r with bagasse ash content

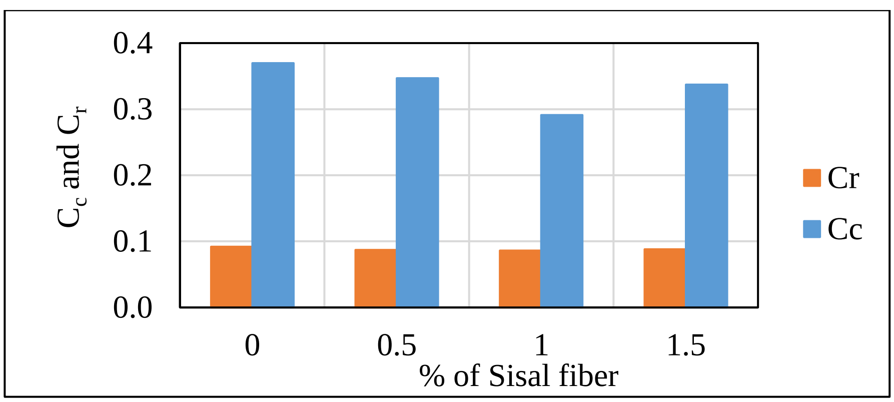

Figure 4.33 Variation of C_c and C_r of bagasse ash stabilized soil with the addition of SF

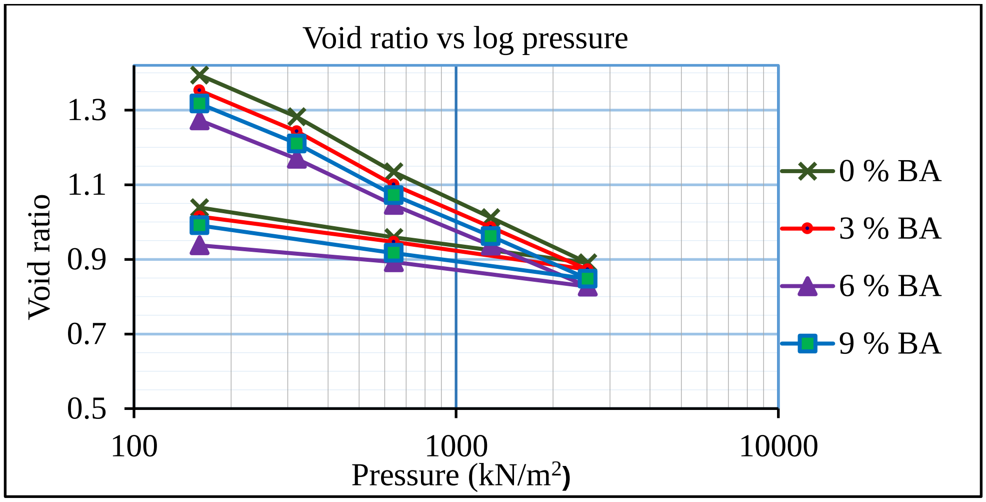

Figure 4.34 Variation of void ratio vs log pressure with different percentages of BA

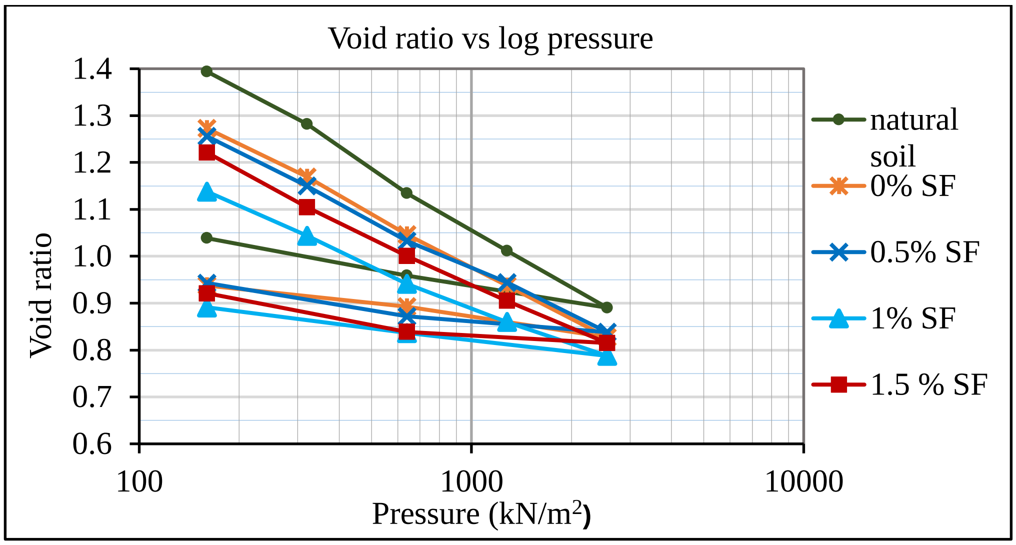

Figure 4.35 Variation of void ratio vs log pressure on bagasse ash stabilized soil with different percentages of sisal fiber

By varying the percentages of bagasse ash (0%, 3%, 6% and 9%) the compression index shows slight decrement. It was decreased from 0.418 to 0.370 with the addition of 6% Bagasse ash. The compression index varies from 0.418 to 0.291 for 6 % bagasse ash content and reinforced with 1% of sisal fiber having 20 mm. The recompression index also decreases by the addition of bagasse ash from 0.123 to 0.086. It also shows decrement by reinforcing bagasse ash stabilized soil. The addition of bagasse ash and sisal fiber showed little improvement in the consolidation properties of the expansive soil.

5 CONCLUSION AND RECOMMENDATION

5.1 Conclusions.

- ✓ The addition of bagasse ash showed a decrease in the plasticity index of expansive soil. Free swell, free swell index, and free swell ratio also showed little decrement with an increasing amount of bagasse ash and OMC increased and MDD decreased and the specific gravity shows a decrease.
- ✓ The UCS also increased when the soil was mixed with bagasse ash. From the trial mixes addition of 6% bagasse ash gave a better result. When compared to the natural soil. the UCS at 6% bagasse ash stabilized soil increased by 47.4 % and 55 % for uncured and 7 days cured conditions respectively
- ✓ The combined effect of sisal fiber and bagasse ash gives good strength than the strength given by stabilizing bagasse ash alone. The addition of 1 % sisal fiber having 20mm length into bagasse ash stabilized soil gives a higher strength value. The UCS is increased by 33% and 33.5% for un-cured and 7 days cured samples when compared with bagasse ash stabilized soils. The increasing the fiber length and fiber content the MDD decreases and the OMC increases.
- ✓ The addition of bagasse ash increases the coefficient of consolidation of the expansive soil up to 6% addition by dry mass of soil. and the compression index and re-compression index decreased when soil is stabilized with bagasse ash only and reinforced with sisal fiber up to the addition of 6% BA and 20 mm 1% SF.
- ✓ The coefficient of volume compressibility also decreases with increasing of bagasse ash alone and reinforcing with sisal fiber on the expansive soil.
- ✓ The combination of Bagasse ash and sisal fiber is more effective than the addition of Bagasse ash alone for the strength improvement of expansive soil and for controlling the consolidation characteristics. The combination of 6% bagasse ash and 1% sisal fiber having 20 mm gave a better result.
- ✓ By considering the improvement of some geotechnical properties of expansive soil. these two stabilizing materials can be used for ground improvement.

5.2 Recommendations

- ✓ In this thesis the curing time of samples for UCS test was limited to 7 days so, Further study is recommended on the effect of curing time on bagasse ash stabilized soil.
- ✓ Cutting of sisal fiber in different lengths and mixing by hand was done in this study, finding other means of cutting is recommended in the future.
- ✓ The improvement in the durability of natural fibers should be further studied.
- ✓ The effect of kerosene coating on the strength properties of natural fiber reinforced soil, the biochemical composition of fiber, and its effect on the environment should be studied.

REFERENCES

Adimas, D. (2015). *Effect of Sugarcane Bagasse Ash and Cement on Swelling Characteristics of Expansive Soil around Mojo*. MSc. Thesis, Adama Science &Technology University, Adama.

Adugna. (2021). *Effect of maize cob ash and waste ceramic powder on geotechnical properties of expansive soil: in the case of Dukem town*. MSc. Thesis, Adama Science &Technology University, Adama.

Afewerk, S. (2004). *Assessment of damage of buildings constructed in expansive soil areas of Addis ababa.* MSc. Thesis, Addis Ababa University, Addis Ababa.

Alemayehu Teferra and Mesfin, L. (1999). *Soil Mechanics* Faculty of Technology. Addis Ababa University, Addis Ababa.

Alemayehu Teferra and solomon, Y. (1986). *Investigations on the expansive soils of Addis Ababa*. Civil Engineering Department Addis Ababa University,Addis Ababa.

Ali, N., Kumar, A., Kumar, M., & Ash, F. (2022). Compaction and consolidation characteristics of chemically treated expansive soil of Jamshoro. *Mehran University Research Journal of Engineering and Technology*. *41*(2), 1–11.

Argaw, A. & Patra, N. R. (2016). Behavior of Expansive Soil Treated with Steel Slag, Rice Husk Ash, and Lime. *J. Mater. Civ. Eng., 28* (7), 06016008

Arulsurya, M., Dhanasri, A., & Hariharan, S. (2019). Experimental Inspection on Black Cotton Soil Stabilization By Using Sisal Fibre and Copper Slag. *International Research Journal of Engineering and Technology (IRJET), 06(12*). 1977–1982.

Aschalew, B. (2021). *Stabilization of expansive soil using biomedical waste incinerator ash.* MSc. Thesis, Addis Ababa University, Addis Ababa.

Asres, E. (2017). *Stabilization of Expansive Clay Soils Using Quarry Waste*. MSc. Thesis, Addis Ababa University, Addis Ababa.

ASTM. (2004). "Special Procedures for Testing Soil and Rock for Civil Engineering Purpose"

U.S.A

ASTM C618-03 (2003). "Specification for fly ash and raw or calcined natural pozzolanas for use as mineral admixture in Portland cement concrete."

Bantayehu, U. U. (2017). Performance , Problems and Remedial Measures for Roads Constructed on Expansive Soil in Ethiopia – A Review. *Civil and Environmental Research 9*(5), 28–37.

Bekele, A. (2022). *A Study on the Dynamic Property of Expansive Soil Treated With Sugarcane Bagasse Ash*. MSc. Thesis, Adama Science and Technology University, Adama.

Benítez-Guerrero, M., Pérez-Maqueda, L. A., Artiaga, R., Sánchez-Jiménez, P. E., & Pascual-Cosp, J. (2017). Structural and Chemical Characteristics of Sisal Fiber and Its Components: Effect of Washing and Grinding. *Journal of Natural Fibers*, *14*(1), 26–39.

Bersisa, A., & Zekaria, A. (2021). Assessment of the Mechanical Properties of Bagasse Ash Concrete.*Engineering science* ,*6*(3), 39–44.

Betelie, A. A., Sinclair, A. N., Kortschot, M., & Li, Y. (2019). Mechanical properties of sisal-epoxy composites as functions of fiber-to-epoxy ratio. *AIMS Materials Science, 6(6),* 985–996.

Bethel. (2021). *Investigation on the application of natural fiber (Katcha) as a weak subgrade soil reinforcement blended with sand in case of Koyefeche project 18 road projects*. MSc. Thesis, Adama Science and Technology University, Adama.

Braja M .Das. (2014). *Principles of geotechnical engineering*.

Chen. (1975). foundations on expansive soil. Elsevier, Amsterdam.

Dang, L. C. (2019). *Enhancing the Engineering Properties of Expansive Soil Using Bagasse Ash, Bagasse Fibre, and Hydrated Lime*. Phd thesis .University of Technology Sydney (UTS)

Dang, L. C., Khabbaz, H., & Fatahi, B. (2017). An experimental study on engineering behaviour of lime and bagasse fibre reinforced expansive soils .*Proceedings of the 19th international* *conference on soil mechanics and geotechnical engineering.*

Das , Arindam .and Roy, S. (2014). Effect of Expansive Soil on Foundation and Its Remedies. *International Journal of Innovative Research in Science, Engineering and Technology*, *3*(6), 92–95.

Fattah, M. Y., & Jaber, M. M. (2014). Consolidation Properties of Compacted Soft Soil Stabilized with Lime-Silica Fume Mix. *International Journal of Science and Engineering research* , *5*(7), 1675–1682.

Fikadu, A. (2015). *Relationship Between Swelling and Consolidation Characteristics of Expansive soil s of Gelan town*. MSc. Thesis, Addis Ababa University, Addis Ababa.

Fuqua, M. A., Huo, S., & Ulven, C. A. (2012). Natural fiber reinforced composites. *Polymer Reviews*, *52*(3–4), 259–320.

Gowthaman, S., Nakashima, K., & Kawasaki, S. (2018). A State-of-the-Art Review on Soil Reinforcement Technology Using Natural Plant Fiber Materials : Past Findings , Present Trends and Future Directions. *Materials, 11* (553), 1-23.

Gupta, P., Wirquin, E., & Bokhoree, C. (2021). Case Studies in Construction Materials Sustainable concrete : Potency of sugarcane bagasse ash as a cementitious material in the construction industry. *Case Studies in Construction Materials*, *14*, e00545.

Haimanot, Z. (2020). *Application of sisal fiber as a subgrade soil reinforcement: in case of alem tena town along modjo-meki express way*. MSc. Thesis, Adama Science and Technology University, Adama.

Hejazi, S. M., Sheikhzadeh, M., Abtahi, S. M., & Zadhoush, A. (2012). A simple review of soil reinforcement by using natural and synthetic fibers. *Construction and Building Materials*, *30*, 100–116.

Holtz, W. G., & Gibbs, H. J. (1956). Engineering Properties of Expansive Clays. *Transactions of the American Society of Civil Engineers*, *121*(1), 641–663.

K. Rupa Narayana Reddy & Praveen Kumar, P. (2019). An Experimental Study on Stabilisation of Loose Soil by Using Sisal Fiber. *International Journal of Trend in Scientific Research* *and Development*, *3*(5), 673–676.

Kassahun, H. (2006). Examining Atterberg Limits for Expansive soil. MSc. Thesis, Addis Ababa University, Addis Ababa.

Keftaw, H. (2021). *A study on strength characteristics of subgrade soil treated with fly ash and enset fiber in case of Tarchachida road section, southern Ethiopia*. MSc. Thesis, Adama Science and Technology University, Adama.

Khan, A., Fahiem Tahir, M., & Goyal, E. T. (2019). Study on engineering properties of soil using bagasse ash and sisal fiber. *International Research Journal of Engineering and Technology*, 1614.

Kharade, AS. Suryavanshi, VV. Gujar, BS. and Deshmukh, RR.2014. Waste product 'bagasse ash' from sugar industry can be used as stabilizing material for expansive soil. *IJRET: International Journal of Research in Engineering and Technology*. **3**(3):506-512

Maja. (2018). *Problematic Sub-Grade Soil Reinforcement Using Local Natural Fibers on Selected Road Section from Wolaita , South Western Ethiopia*. MSc. Thesis, Addis Ababa University, Addis Ababa.

Mathew & Raneesh (2016). Effect on Strength Characteristics of Expansive Soil Using Sisal Fibre and Waste Materials. *International Journal of Science and Research (IJSR)*, *5*(9)

Maya, M. G., George, S. C., Jose, T., Sreekala, M. S., & Thomas, S. (2017). Mechanical Properties of Short Sisal Fibre Reinforced Phenol Formaldehyde Eco-Friendly Composites. *Polymers from Renewable Resources*, *8*(1), 1–16.

Miresa, T. (2019). *Investigation of the Potential of Sugar Cane Bagasse Ash for Production of Ceramic Material (Wall Tiles)*. MSc. Thesis, Addis Ababa University, Addis Ababa.

Molenaar. (2005). Road Materials, Part I: Cohesive and Non-Cohesive Soils and Unbound Granular Materials for Bases and Subbases in Roads. Lecture notes. *University of Stellenbosch and University of Delft, South Africa.*

Naveen, J., Jawaid, M., Amuthakkannan, P., & Chandrasekar, M. (2019).Mechanical and Physical Testing of Biocomposites, Fibre-Reinforced Composites and Hybrid Composites, *Elsevier*,427–440.

Osinubi, K. (2009). Bagasse ash stabilization of lateritic soil. *Appropriate Technologies for Environmental Protection in the Developing World*, 281-290.

Panwar, R. S., Sonthwal, V. K., & Kaswan, S. (2018). Enhancing the engineering properties of soil by using sisal fibre and fly ash. *International Journal of Technical Innovation in Modern Engineering & Science*, *4*(7).

Prabakaran Ellappan, V. A. and N. M. (2020). Influence of Natural Fibres in Strengthening of Black Cotton Soil. *IOP Conf. Series: Materials Science and Engineering (955)*.

Sandyarani et al. (2018). Stabilization of black cotton soil by using Sisal fiber. *International Research Journal of Engineering and Technology (IRJET)*, *05*(08), 694–698.

Singh, V. K. (2016). Performance Evaluation of Block Cotton Soil Stabilized with Sugarcane Bagasse Ash and Randomly Distributed Core fiber. *International Journal for Innovative Research in Science,and Technology ,2(11).*

Sissay, D. (2011). *Computation of soil compressibility using tangent modulus approach*. MSc. Thesis, Addis Ababa University, Addis Ababa.

Sridharan, A., & Prakash, K. (2000). *Classification procedures for expansive soils*. 235–240.

Srinivasan, R. (2010). Experimental Study on Bagasse Ash in Concrete. *International journal for service learning in engineering*, *5(2)*, 60–66.

Sumi, & Unnikrishnan, N. (2015). Natural Fibres in Engineering Applications: An Overview. *International Jornal of Scientific and Engineering Research*, *5*(7), 260–265.

Surjandari, N. S., Djarwanti, N., & Ukoi, N. U. (2017). Enhancing the engineering properties of expansive soil using bagasse ash. *Journal of Physics: Conference Series*, *909*(1).

Tamilvendan D, Prabu G, M., S, S., & Ravikumar, D. A. R. (2020). Mechanical Behaviour of Hybrid Composites Prepared using Sisal-Pineapple-Kenaf Fibre. *International Journal of Recent Technology and Engineering (IJRTE)*, *8*(5), 3210–3214.

Tamrat, A. (2013). *Study on index properties and swelling pressure of expansive soils found in*

Dukem. MSc. Thesis, Addis Ababa University, Addis Ababa.

Teklu. (2003). *Examining the swelling pressure of Addis Ababa*. MSc. Thesis, Addis Ababa University, Addis Ababa.

Tibebu, S. (2015). *Assessment of damages caused by expansive soil on buildings constructed in Bahir dar*. MSc. Thesis, Addis Ababa University, Addis Ababa.

Torio-kaimo, L. V, Diego, A. M. S., & Alcantara, M. T. M. (2020). Unconfined compressive strength of clay reinforced with kerosene-treated coir fiber. I*nternational journal of GEOMATE .18*(69), 97–103.

Vikrant Dubey and Dr. J.P.Tegar. (2018). Impact of sisal fiber as a reinforcement on the behavior of expansive soil .*International Research Journal of Engineering and Technology (IRJET), 05*(09).

Wang, Y., Guo, P., Ren, W., Yuan, B., Yuan, H., & Zhao, Y. (2018). Laboratory Investigation on Strength Characteristics of Expansive Soil Treated with Jute Fiber Reinforcement. *American Society of Civil Engineers. 17*(11).

Worku, B. (2015). *Stabilization of Lateritic Soil with Sugarcane bagasse ash.* MSc. Thesis, Addis Ababa University, Addis Ababa.

Wubshet, M., & Tadesse, S. (2014). Stabilization of expansive soil using bagasse ash & lime. In *Journal of EEA* (Vol. 32).

Research Fund Acknowledgement

This research project is funded by Adama Science and Technology University under the grant number:

ASTU/SM-R/528/22

Adama, Ethiopia

APPENDICES

Appendix : A Natural moisture content test result

Table A-1 Natural moisture content for TP1, TP2, and TP3

Sample name	TP1			TP2			TP3		
Trial No	1	2	3	1	2	3	1	2	3
Container No	W1	W2	W3	A3	A4	A5	B5	B6	B7
Mass of container, g	61	62	62	60.96	61.57	60.78	62.42	61.06	61.35
Mass of container + Wet soil, g	81	82	82	80.99	81.78	81.79	83.38	82.81	86.26
Mass of container + Dry soil, g	76	77	78	75.67	76.91	76.26	78.19	77.51	80.05
Mass of water, g	20	20	20	20.03	20.21	21.01	20.96	21.75	24.91
Mass of dry soil, g	5	5	4	5.32	4.87	5.53	5.19	5.3	6.21
Moisture content	25	25	20	26.56	24.10	26.32	24.76	24.37	24.93
Average moisture content (%)	23.33			25.66			24.69		

Appendix : B Specific gravity test result results

Table B-1 Specific gravity test results for TP1, TP2 and TP3

Sample name	TP1		TP2		TP3	
Pycnometer No.	T30	T28	T3	T9	T18	T20
Weight of dry soil, w_s (gm)	10	10	10	10	10	10
Weight of pycnometer + soil + water, W_{pws} (g)	146.13	141.01	146.09	141.01	140.25	146.32
Temperature, T_x(°c)	21	21	22	22	22	22
Weight of pycnometer + water at T_x, W_{pw} (at T_x) (g)	139.78	134.67	139.7	134.67	133.9	140
Conversion factor, K	0.9998	0.9998	0.9996	0.9996	0.9996	0.9996
Specific Gravity of soil at 20=(Kws/(ws+Wpw-Wps)	2.73918	2.73169	2.76898	2.73115	2.73863	2.7163
Average specific gravity of soil.	2.74		2.75		2.73	

Table B-2 Specific gravity test result for different percentages of bagasse ash +soil

Sample name	0%		3%		6%		9%	
Pycnometer No.	T3	T9	T17	T23	T22	T4	T16	T21
Weight of dry soil, ws (gm)	10	10	10	10	10	10	10	10
Weight of pycnometer + soil + water, W_{pws} (g)	146.09	141.01	141.19	146.82	146.7	143.43	148.63	141.67
Temperature, T_x(°c)	22	22	22	22	21	21	21	21
Weight of pycnometer + water at T_x , W_{pw}(atT_x) (g)	139.7	134.67	134.93	140.54	140.48	137.2	142.43	135.45
Conversion factor, K	0.9998	0.9998	0.9998	0.9998	0.9996	0.9996	0.9996	0.9996
Specific Gravity of soil at 20=(Kws/(ws+Wpw-Wpws)	2.76953	2.73169	2.67326	2.68763	2.64444	2.65146	2.63053	2.64444
Average specific gravity of soil.	2.75		2.68		2.65		2.64	

Table B-3 Specific gravity result for BA and sisal fiber

Sample name	Bagasse ash only		Sisal fiber only	
Pycnometer No.	T26	T6	T06	T07
Weight of dry soil, ws (gm)	10	10	10	10
Weight of pycnometer + soil + water, W_{pws} (g)	143.34	139.61	136.84	137.61
Temperature, T_x(°c)	21	21	21	21
Weight of pycnometer + water at T_x, W_{pw}(atT_x) (g)	137.77	134.14	136.3	136.86
Conversion factor, K	0.9998	0.9998	0.9998	0.9998
Specific Gravity of soil at 20=(Kws/(ws+Wpw-Wps)	2.25688	2.20706	1.05687	1.08086
Average specific gravity of soil.	2.23		1.07	

Appendix : C Water absorption capacity determination

Table C-1 WAC result of sisal fiber

Days of kerosene immersion	0 day	2 days	4 days	6 days
Mass of dry sisal fiber + container (gm)	43.9	30.2	29	28
Mass of wet sisal fiber + container (gm)	84.5	73	63	68
Mass of water (gm)	40.6	46.5	44.9	47.2
Mass of container (gm)	30.2	16.3	15.9	19.2
Mass of dry coated sisal fiber (gm)	13.7	26.5	18.1	20.8
Moisture content (%)	296.35	162.58	113.84	108.33

Appendix : D Wet sieve and hydrometer analysis test result

Table D-1 Wet sieve analysis test result for TP 1

Sieve Analysis

Total mass of sample, g =1000

Sieve No	Sieve Opening (mm)	Mass of Sieve (g)	Mass of sieve + Retained soil (g)	Mass of Retained soil (g)	Percentage Retained (%)	Cum. Percentage Retained (%)	Perc. Passing (%)
3"	75.0	0.0	0.0	0.0	0.0	0.0	100.0
2"	50.0	0.0	0.0	0.0	0.0	0.0	100.0
1.5"	37.5	0.0	0.0	0.0	0.0	0.0	100.0
1"	25.0	0.0	0.0	0.0	0.0	0.0	100.0
3/4"	19.0	0.0	0.0	0.0	0.0	0.0	100.0
1/2"	12.5	0.0	0.0	0.0	0.0	0.0	100.0
3.8"	9.5	0.0	0.0	0.0	0.0	0.0	100.0
No 4	4.75	426	429.0	3.0	0.3	0.3	99.7
No 8	2.36	406	409.0	3.0	0.3	0.6	99.4
No 10	2	384	389.0	5.0	0.5	1.1	98.9
No 16	1.18	359	367.0	8.0	0.8	1.9	98.1
No 30	0.6	329	353.0	24.0	2.4	4.3	95.7
No 50	0.3	294	327.0	33.0	3.3	7.6	92.4
No 100	0.15	278	310.0	32.0	3.2	10.8	89.2
No 200	0.075	272	311.0	39.0	3.9	14.7	85.3
pan	pan	253	1106.0	853.0	85.3	100.0	-------

Table D-2 Hydrometer analysis test result for TP1

Specific Gravity of soil= 2.74				Test Temperature, deg.c= 21				
Elapsed Time (min)	Actual Hydrometer Reading	Composite Correction	Corrected Hydrometer Reading	Effective Depth (cm)	Coefficient K	Grain Size (mm)	Perc. Finer (%)	Perc. Finer Combined (%)
3/4	1.0280	-0.0027	1.0253	8.89	0.0133	0.0397	79.68	67.97
1	1.0270	-0.0027	1.0243	9.16	0.0133	0.0285	76.53	65.28
2	1.0265	-0.0027	1.0238	9.29	0.0133	0.0203	74.96	63.94
4	1.0255	-0.0027	1.0228	9.55	0.0133	0.0145	71.81	61.25
8	1.0250	-0.0027	1.0228	9.55	0.0133	0.0106	71.81	61.25
15	1.0240	-0.0027	1.0223	9.69	0.0133	0.0076	70.23	59.91
30	1.0235	-0.0027	1.0213	9.95	0.0133	0.0054	67.08	57.22
60	1.0230	-0.0027	1.0208	10.08	0.0133	0.0055	65.51	55.88
120	1.0220	-0.0027	1.0203	10.22	0.0133	0.0039	63.93	54.54
240	1.0215	-0.0027	1.0193	10.48	0.0133	0.0028	60.78	51.85
480	1.0210	-0.0027	1.0188	10.61	0.0133	0.0020	59.21	50.51
1440	1.0205	-0.0027	1.0183	10.75	0.0133	0.0011	57.63	49.16

Table D-3 Wet sieve analysis result for TP2

Sieve No	Sieve openig (mm)	Mass of Sieve (g)	Mass of sieve +Retained soil(g)	Mass of Retained soil	Percentage Retained(g)	Cum. PercentageRetained(%)	Perc.Passing(%)
3"	75	0	0	0	0	0	100
2"	50	0	0	0	0	0	100
1.5"	37.5	0	0	0	0	0	100
1"	25	0	0	0	0	0	100
3/4"	19	0	0	0	0	0	100
1/2"	12.5	0	0	0	0	0	100
3.8"	9.5	0	0	0	0	0	100
No 4	4.75	426	428	2	0.2	0.2	99.8
No 8	2.36	402	406	4	0.4	0.6	99.4
No 10	2	375	377	2	0.2	0.8	99.2
No 16	1.18	354	369	15	1.5	2.3	97.7
No 30	0.6	328	341	13	1.3	3.6	96.4
No 50	0.3	294	299	5	0.5	4.1	95.9
No 100	0.15	277	294	17	1.7	5.8	94.2
No 200	0.075	272	281	9	0.9	6.7	93.3
Pan	---	253	1186	933	93.3	100	-------

Table D 4 Hydrometer analysis result for TP2

Specific Gravity of soil= 2.75			Test Temperature, deg.c= 21					
Elapsed Time (min)	Actual Hydrometer Reading	Composite Correction	Corrected Hydrometer Reading	Effective Depth (cm)	Coefficient K	Grain Size (mm)	Perc. Finer (%)	Perc. Finer Combined (%)
3/4	1.0290	-0.0025	1.0265	8.63	0.013018	0.0382	83.29	77.71
1	1.0285	-0.0025	1.0260	8.76	0.013018	0.0272	81.71	76.24
2	1.0280	-0.0025	1.0255	8.89	0.013018	0.0194	80.14	74.77
4	1.0275	-0.0025	1.0250	9.03	0.013018	0.0138	78.57	73.31
8	1.0260	-0.0025	1.0250	9.03	0.013018	0.0101	78.57	73.31
15	1.0250	-0.0025	1.0235	9.42	0.013018	0.0073	73.86	68.91
30	1.0240	-0.0025	1.0225	9.69	0.013018	0.0052	70.71	65.98
60	1.0235	-0.0025	1.0215	9.95	0.013018	0.0053	67.57	63.04
120	1.0230	-0.0025	1.0210	10.08	0.013018	0.0038	66.00	61.58
240	1.0220	-0.0025	1.0205	10.22	0.013018	0.0027	64.43	60.11
480	1.0210	-0.0025	1.0195	10.48	0.013018	0.0019	61.29	57.18
1440	1.0210	-0.0025	1.0185	10.75	0.013018	0.0011	58.14	54.25

Table D-5 Wet sieve analysis result for TP3

Sieve No	Sieve openig (mm)	Mass of Sieve (g)	Mass of sieve +Retained soil(g)	Mass of Retained soil	Percentage Retained(g)	Cum.Percentage Retained (%)	Perc.Passing (%)
3"	75	0	0	0	0	0	100
2"	50	0	0	0	0	0	100
1.5"	37.5	0	0	0	0	0	100
1"	25	0	0	0	0	0	100
3/4"	19	0	0	0	0	0	100
1/2"	12.5	0	0	0	0	0	100
3.8"	9.5	0	0	0	0	0	100
No 4	4.75	426	428	2	0.2	0.2	99.8
No 8	2.36	402	406	4	0.4	0.6	99.4
No 10	2	375	376	1	0.1	0.7	99.3
No 16	1.18	354	367	13	1.3	2	98
No 30	0.6	328	337	9	0.9	2.9	97.1
No 50	0.3	294	303	9	0.9	3.8	96.2
No 100	0.15	277	289	12	1.2	5	95
No 200	0.075	272	281	9	0.9	5.9	94.1
Pan	-------	253	1194	941	94.1	100	-------

Table D-6 Hydrometer analysis result for TP3

Specific Gravity of soil= 2.73					Test Temperature, deg.c= 21			
Elapsed Time (min)	Actual Hydrometer Reading	Composite Correction	Corrected Hydrometer Reading	Effective Depth (cm)	Coefficient K	Grain Size (mm)	Perc. Finer (%)	Perc. Finer Combined (%)
3/4	1.0285	-0.0027	1.0258	8.76	0.01325	0.0392	81.43	76.62
1	1.0280	-0.0027	1.0253	8.89	0.01325	0.0279	79.85	75.14
2	1.0275	-0.0027	1.0248	9.03	0.01325	0.0199	78.27	73.65
4	1.0270	-0.0027	1.0243	9.16	0.01325	0.0142	76.69	72.17
8	1.0260	-0.0027	1.0233	9.42	0.01325	0.0105	73.54	69.20
15	1.0250	-0.0027	1.0223	9.69	0.01325	0.0075	70.38	66.23
30	1.0240	-0.0027	1.0213	9.95	0.01325	0.0054	67.22	63.26
60	1.0235	-0.0027	1.0208	10.08	0.01325	0.0054	65.65	61.77
120	1.0230	-0.0027	1.0203	10.22	0.01325	0.0039	64.07	60.29
240	1.0220	-0.0027	1.0193	10.48	0.01325	0.0028	60.91	57.32
480	1.0215	-0.0027	1.0188	10.61	0.01325	0.0020	59.33	55.83
1440	1.0210	-0.0027	1.0183	10.75	0.01325	0.0011	57.76	54.35

Appendix : E Liquid limit and Plastic limit test results

Table E-1 Liquid limit and plastic limit results for TP1

	Liquid Limit			Plastic Limit		
Trial No	1	2	3	1	2	3
Container No	A1	A2	A3	B1	B2	B3
Mass of container, g	17.4	20	17.3	19.55	18.43	19.55
Mass of container + Wet soil, g	36	30	29	24.08	22.1	22.6
Mass of container + Dry soil, g	23.06	23.88	23.77	23.03	21.2	21.9
Mass of water, g	12.94	6.12	5.23	1.05	0.9	0.7
Mass of dry soil, g	18.6	10	11.7	3.48	2.77	2.35
Water content, %	69.57	61.20	44.70	30.17	32.49	29.79
No of blows	24	27	34			

Liquid Limit, % = 67 Plastic Limit, %= 32 PI, %=36

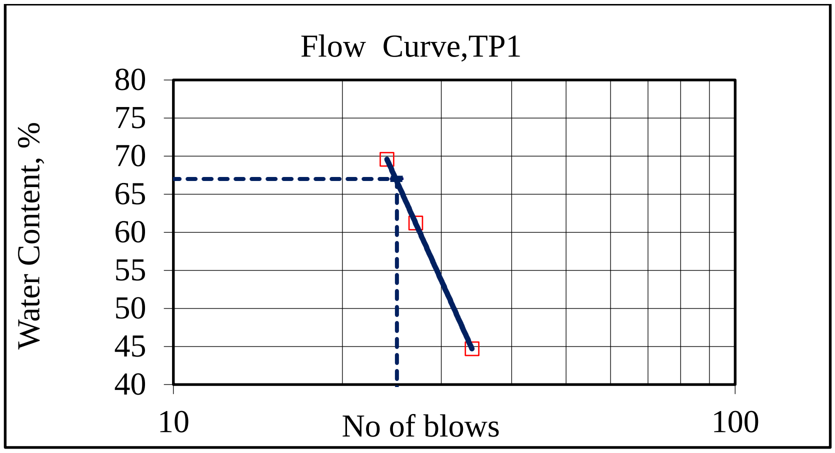

Figure E-1 Liquid limit determination for TP1

Table E-2 Liquid limit and plastic limit results for TP2

	Liquid Limit			Plastic Limit		
Trial No	1	2	3	1	2	3
Container No	C1	C2	C3	D1	D2	D3
Mass of container, g	19.79	19.5	19.54	19.22	19.5	19.56
Mass of container + Wet soil, g	35.12	30.84	29.59	23.16	22.33	22.48
Mass of container + Dry soil, g	28.14	25.79	25.21	22.09	21.58	21.68
Mass of water, g	6.98	5.05	4.38	1.07	0.75	0.8
Mass of dry soil, g	8.35	6.29	5.67	2.87	2.08	2.12
Water content, %	83.59	80.29	77.25	37.28	36.06	37.74
No of blows	19	26	34		37.03	

Liquid Limit, % = 81 Plastic Limit, % = 37 PI, %= 44

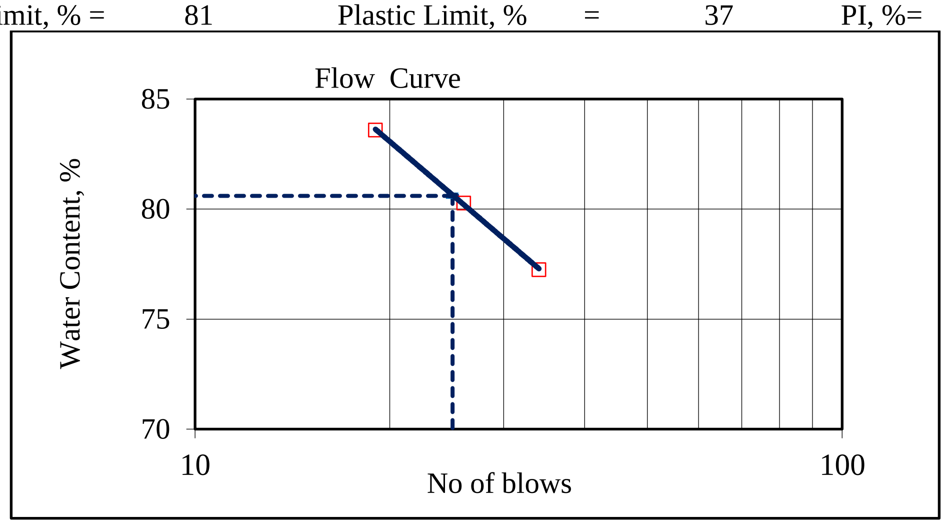

Figure E-2 Liquid limit determination for TP2

Table E-3 Liquid limit and Plastic limit results for TP3

Trial No	Liquid Limit			Plastic Limit		
	1	2	3	1	2	3
Container No	A1	A2	A3	P1	P2	P3
Mass of container, g	19.62	19.16	19.21	19.42	18.86	19.5
Mass of container + Wet soil, g	30.96	31.25	30.69	22.34	22.63	25.27
Mass of container + Dry soil, g	25.91	25.92	25.75	21.57	21.64	23.77
Mass of water, g	5.05	5.33	4.94	0.77	0.99	1.5
Mass of dry soil, g	6.29	6.76	6.54	2.15	2.78	4.27
Water content, %	80.29	78.85	75.54	35.81	35.61	35.13
No of blows	19	24	34		35.52	

Liquid Limit, % = 78 Plastic Limit, % 35.5 PI, %= 42.5

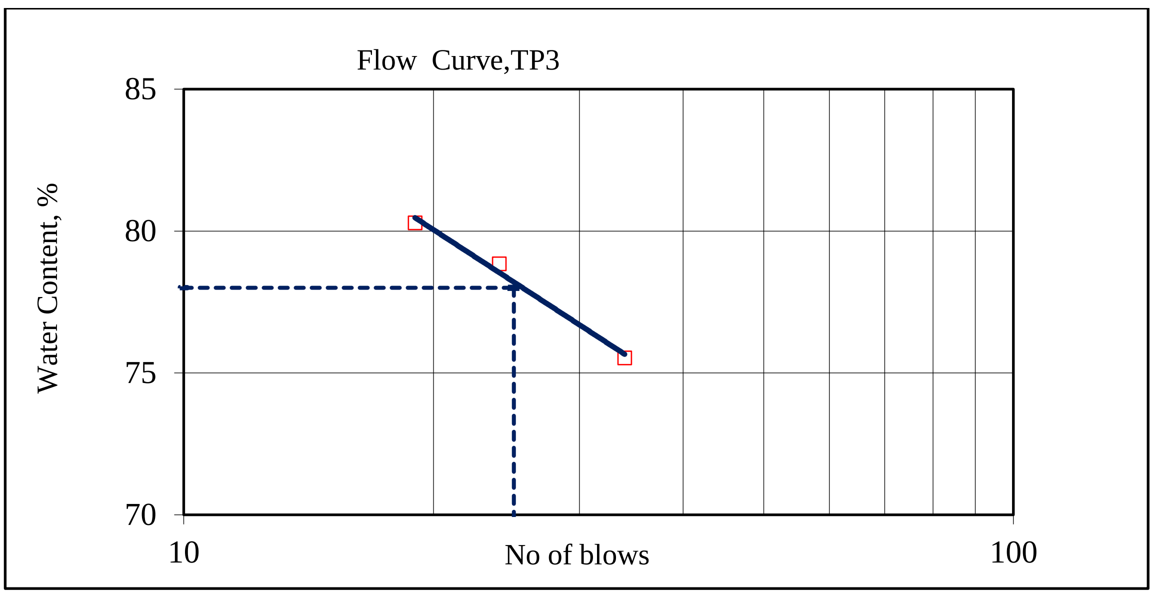

Figure E-3 liquid limit determination for TP3

Table E-4 Liquid limit and Plastic limit test results for soil + 3% BA

	Liquid Limit			Plastic Limit		
Trial No	1	2	3	1	2	3
Container No	C1	C2	C3	D1	D2	D3
Mass of container, g	19.05	19.58	19.5	19.44	19.42	19.64
Mass of container + Wet soil, g	26.86	28.64	29.26	23.49	24.69	24.83
Mass of container + Dry soil, g	20.84	22	23.39	22.41	23.29	23.45
Mass of water, g	6.02	6.64	5.87	1.08	1.4	1.38
Mass of dry soil, g	7.81	9.06	9.76	2.97	3.87	3.81
Water content, %	77.08	73.29	60.14	36.36	36.18	36.22
No of blows	16	21	34		36.25	

Liquid Limit, % = 68 Plastic Limit, % = 36 PI, %= 32

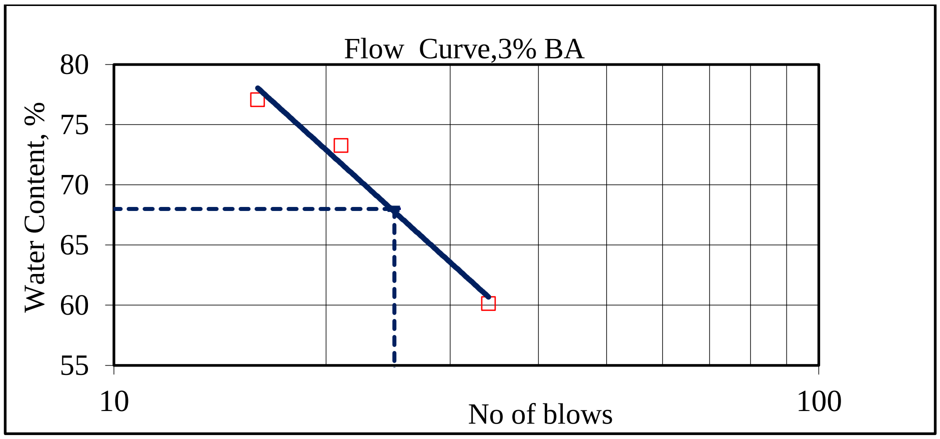

Figure E-4 Liquid limit determination for soil +3% BA

Table E-5 Liquid limit and Plastic limit test results for soil + 6% BA

	Liquid Limit			Plastic Limit		
Trial No	1	2	3	1	2	3
Container No	C1	C2	C3	D1	D2	D3
Mass of container, g	19.31	19.47	19.41	19.46	19.39	19.52
Mass of container + Wet soil, g	29.16	30.19	27.17	24.8	25.17	26.14
Mass of container + Dry soil, g	24.99	26.17	24.98	23.47	23.71	24.4
Mass of water, g	4.17	4.02	2.19	1.33	1.46	1.74
Mass of dry soil, g	5.68	6.7	5.57	4.01	4.32	4.88
Water content, %	73.42	60.00	39.32	33.17	33.80	35.66
No of blows	19	26	35		34.21	

Liquid Limit, % = 60 Plastic Limit, % = 34 PI, %= 26

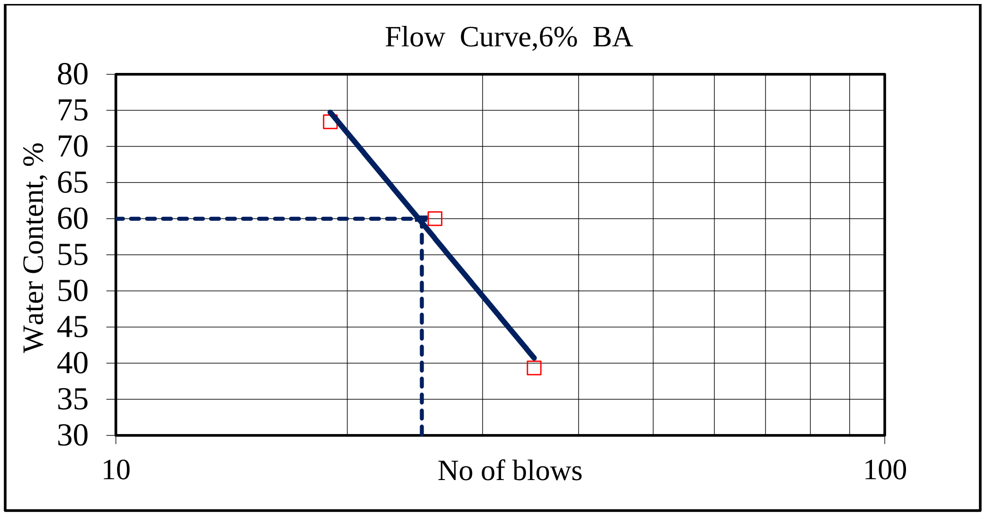

Figure E-4 Liquid limit determination for soil +6% BA

Table E-6 Liquid limit and Plastic limit test results for soil + 9 % BA

	Liquid Limit			Plastic Limit		
Trial No	1	2	3	1	2	3
Container No	C1	C2	C3	D1	D2	D3
Mass of container,g	19.55	19.43	30.26	19.12	19.36	19.4
Mass of container + Wet soil, g	31.92	30.69	45.09	26.44	25.11	25.7
Mass of container + Dry soil, g	28.59	26.79	39.24	24.68	23.69	24.12
Mass of water, g	3.33	3.9	5.85	1.76	1.42	1.58
Mass of dry soil, g	9.04	7.36	8.98	5.56	4.33	4.72
Water content, %	36.84	52.99	65.14	31.65	32.79	33.47
No of blows	34	26	21		32.64	

Liquid Limit, % = 55 Plastic Limit, % = 33 PI, %= 22

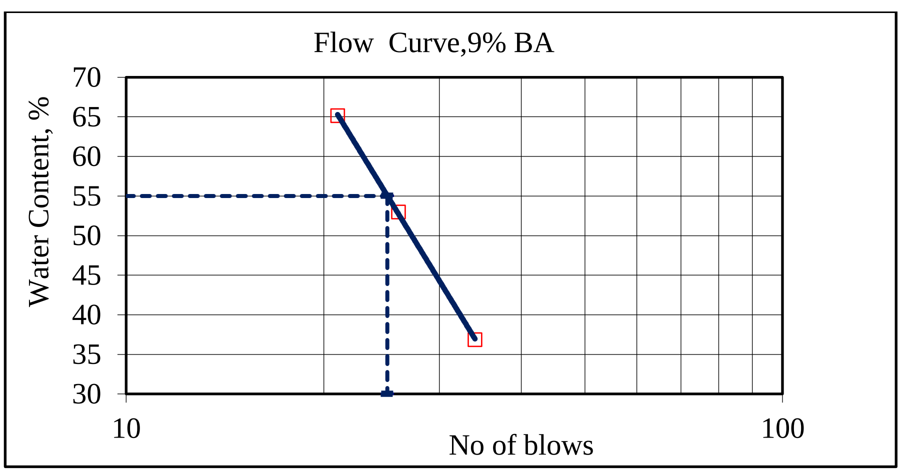

Figure E-6 Liquid limit determination for soil +9% BA

Appendix : F Free swell, free swell index, and free swell ratio test result

Table F-1 Free swell, free swell index, and free swell ratio test results for TP1, TP2, and TP3

Test pits	Initial volume of sample (ml)	Final volume in kerosene(ml)	Final volume in water(ml)	Free Swell Index (%)	Free swell	Free swell ratio
TP1	10	10.5	20	90	100	1.90
TP2	10	10.5	21.5	105	115	2.05
TP3	10	11	21	91	110	1.91

Table F-2 Free swell, free swell index and free swell ratio test results for different percentages of BA

% Of BA	Initial volume of sample (ml)	Final volume in kerosene(ml)	Final volume in water(ml)	Free Swell Index (%)	Free swell	Free swell ratio
0	10	10.5	21.5	105	115	2.05
3	10	11	21	91	110	1.91
6	10	11	19.5	77	95	1.77
9	10	10.5	18	71	80	1.71

Appendix : G Linear shrinkage results for different percentages of BA

Table G-1 For different percentages of bagasse ash

% BA	Initial length(cm)	Final length(cm)	Shrinkage limit
0%	14	12.2	14.75
3%	14	12.4	12.90
6%	14	12.6	11.11
9%	14	12.7	10.24

Appendix : H Compaction Test Results

Table H-1 Compaction test result for TP1

Trial number	1	2	3	4
Mass of mold	3756	3756	3756	3756
Mass of mold+ Compacted Soil, g	5119	5227	5317	5387
Mass of Compacted soil, g	1363	1471	1561	1631
Volume of Mold, cm^3	944	944	944	944
Bulk density, g/cm^3	1.44	1.56	1.65	1.73
mass of container	30.42	30.9	30.29	30.34
mass of container +wet soil	148.64	113.83	114.69	185.03
Mass of container dry soil, g	136.8	102.4	99.93	149.32
mass of wet soil	11.84	11.43	14.76	35.71
Mass of dry soil, g	106.38	71.5	69.64	118.98
Mass of water, g	11.840	11.430	14.760	35.710
Water Content, %	11.13	15.99	21.19	30.01
Dry density, g/cm^3	1.30	1.34	1.36	1.33

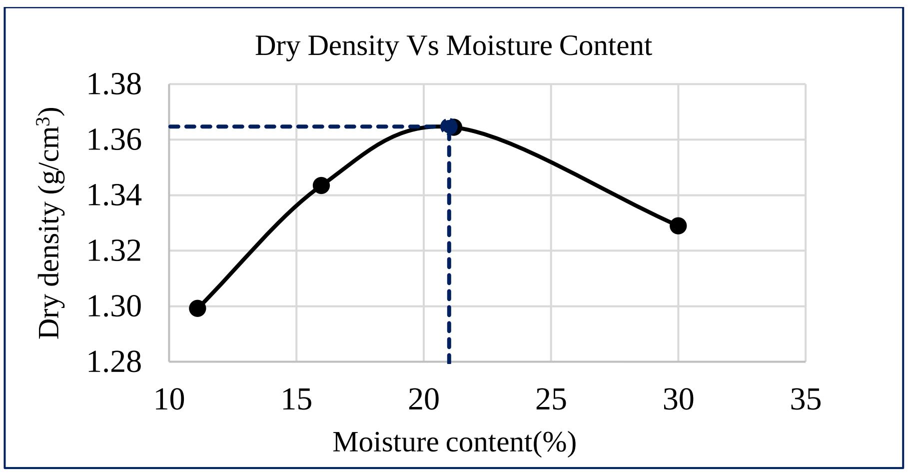

Figure H-1 Compaction curve for TP1

Table H-2 Compaction test result for TP2

Trial number	1	2	3	4
Mass of mold	3756	3756	3756	3756
Mass of mold+ Compacted Soil, g	5163	5215	5321	5339
Mass of Compacted soil, g	1407	1459	1565	1583
Volume of Mold, cm^3	944	944	944	944
Bulk density, g/cm^3	1.49	1.55	1.66	1.68
Water Content, %	14.42	17.19	23.74	29.19
Dry density, g/cm^3	1.30	1.32	1.34	1.30

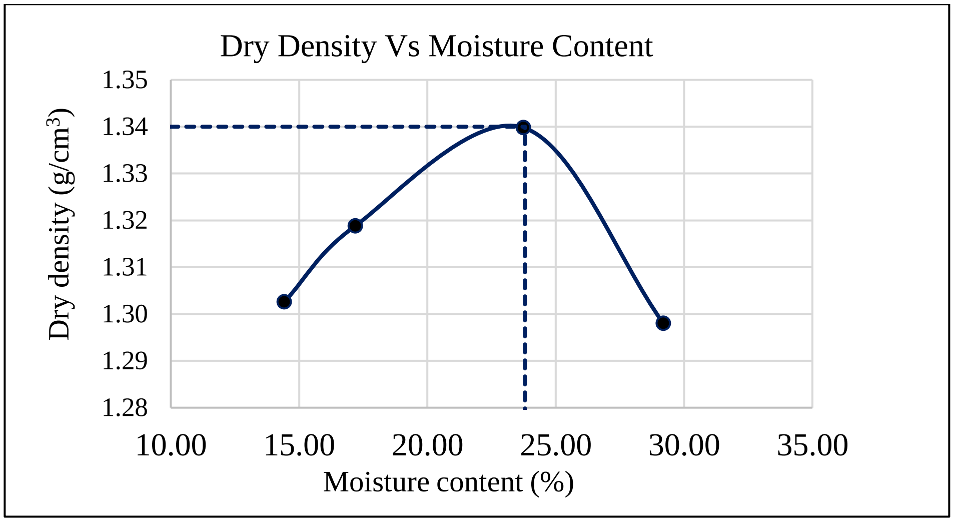

Figure H-2 Compaction curve for TP2

Table H-3 Compaction test result for TP3

Trial number	1	2	3	4
Mass of mold	3756	3756	3756	3756
Mass of mold+ Compacted Soil, g	5173	5275	5345	5341
Mass of Compacted soil, g	1417	1519	1589	1585
Volume of Mold, cm^3	944	944	944	944
Bulk density, g/cm^3	1.50	1.61	1.68	1.68
Water Content, %	17.24	21.36	24.82	31.46
Dry density, g/cm^3	1.28	1.33	1.35	1.28

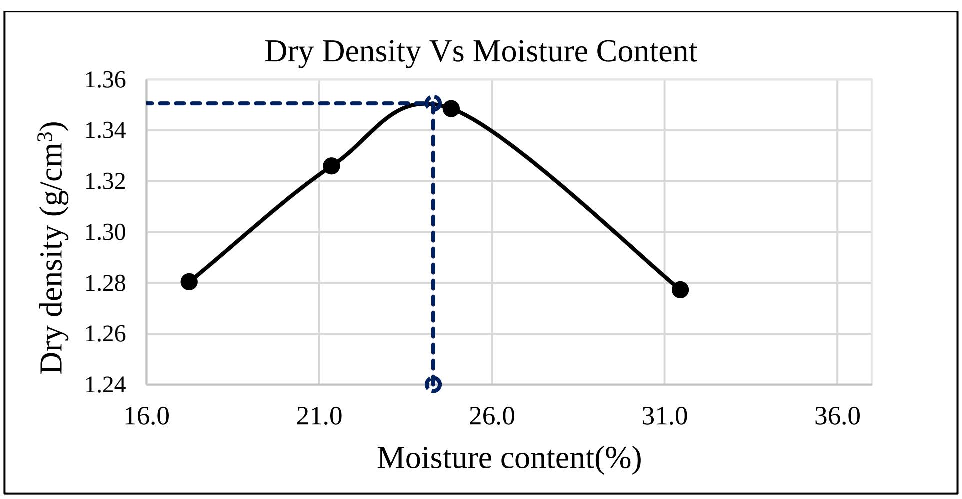

Figure H-3 Compaction curve for TP3

Table H-4 Compaction data result for (Soil + 3% bagasse ash)

Trial number	1	2	3	4
Mass of mold	3756	3756	3756	3756
Mass of mold+ Compacted Soil, g	5145	5219	5318	5313
Mass of Compacted soil, g	1389	1463	1562	1557
Volume of Mold, cm^3	944.00	944.00	944.00	944.00
Bulk density, g/cm^3	1.47	1.55	1.65	1.65
Water Content, %	15.246	19.461	25.032	29.744
Dry density, g/cm^3	1.28	1.30	1.32	1.271

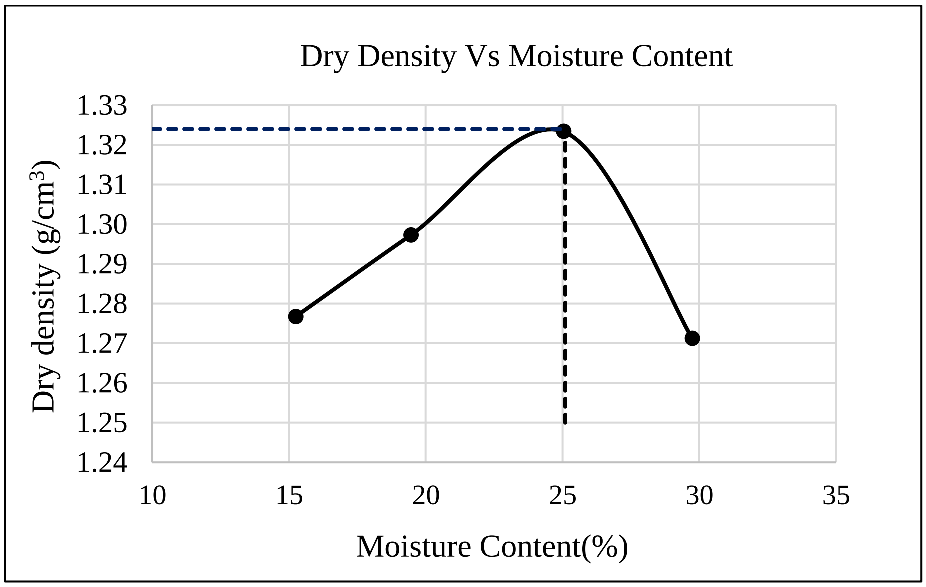

Figure H-4 Compaction curve for (Soil + 3% Bagasse ash)

Table H-5 Compaction data sheet for (Soil + 6% bagasse ash)

Trial number	1	2	3	4
Mass of mold	3756	3756	3756	3756
Mass of mold+ Compacted Soil, g	5155	5241	5312	5345
Mass of Compacted soil, g	1399	1485	1556	1589
Volume of Mold, cm^3	944	944.00	944.00	944.00
Bulk density, g/cm^3	1.48	1.57	1.65	1.68
Water Content, %	17.69	22.47	27.58	34.08
Dry density, g/cm^3	1.259	1.284	1.292	1.255

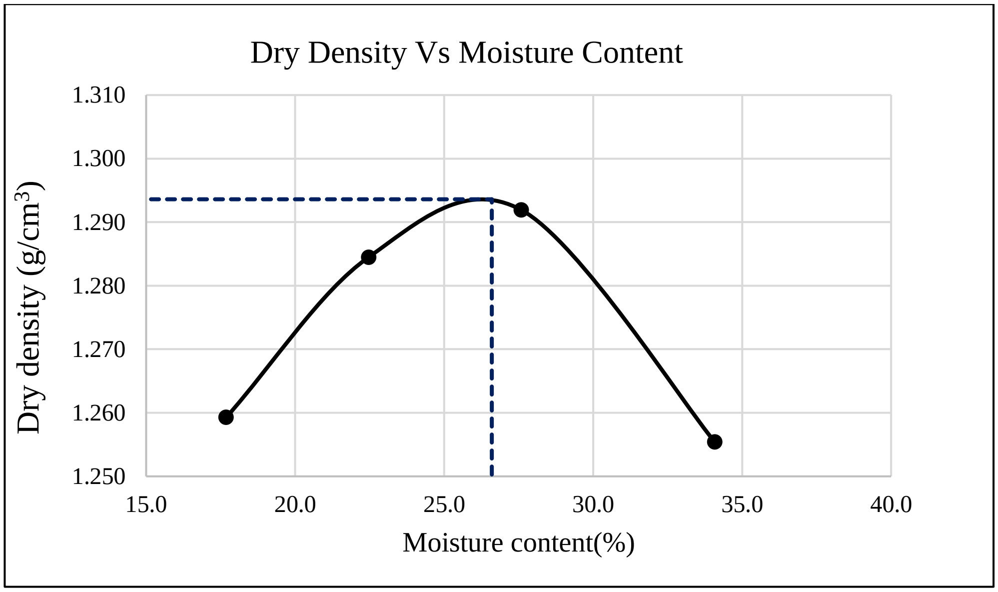

Figure H-5 Compaction curve for (Soil + 6% bagasse ash)

Table H-6 Compaction data sheet for (Soil + 9% bagasse ash)

Trial number	1	2	3	4
Mass of mold	3756	3756	3756	3756
Mass of mold+ Compacted Soil, g	5160	5180	5298	5326
Mass of Compacted soil, g	1404	1424	1542	1570
Volume of Mold, cm^3	944	944	944	944
Bulk density, g/cm^3	1.49	1.51	1.63	1.66
Water Content, %	18.77	20.07	28.25	33.65
Dry density, g/cm3	1.25	1.26	1.27	1.24

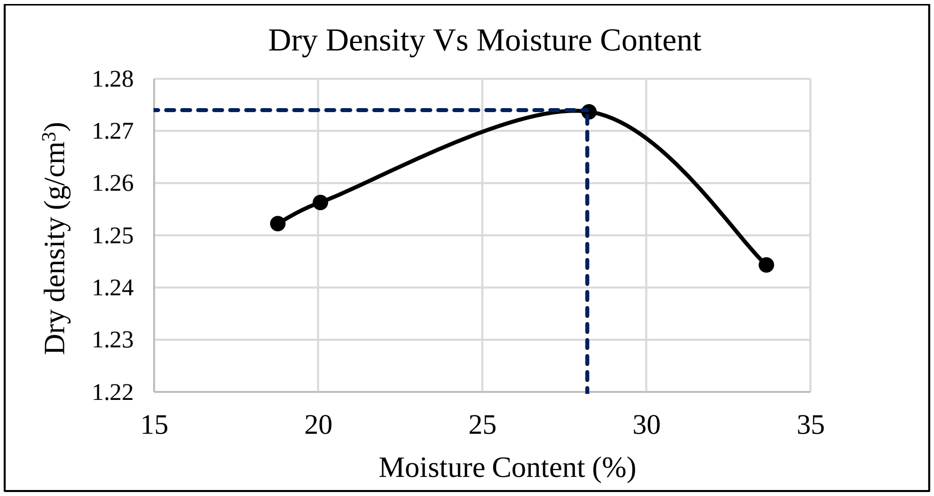

Figure H-6 Compaction curve for (Soil + 9% bagasse ash)

Table H-7 Compaction result for soil+6BA+10mm 0.5% SF

Mass of mold	3756	3756	3756	3756
Mass of mold+ Compacted Soil, g	5114	5202	5299	5365
Mass of Compacted soil, g	1358	1446	1543	1609
Volume of Mold, cm^3	944	944	944	944
Bulk density, g/cm^3	1.44	1.53	1.63	1.70
Water Content, %	16.66	22.60	28.51	35.98
Dry density, g/cm^3	1.23	1.25	1.272	1.25

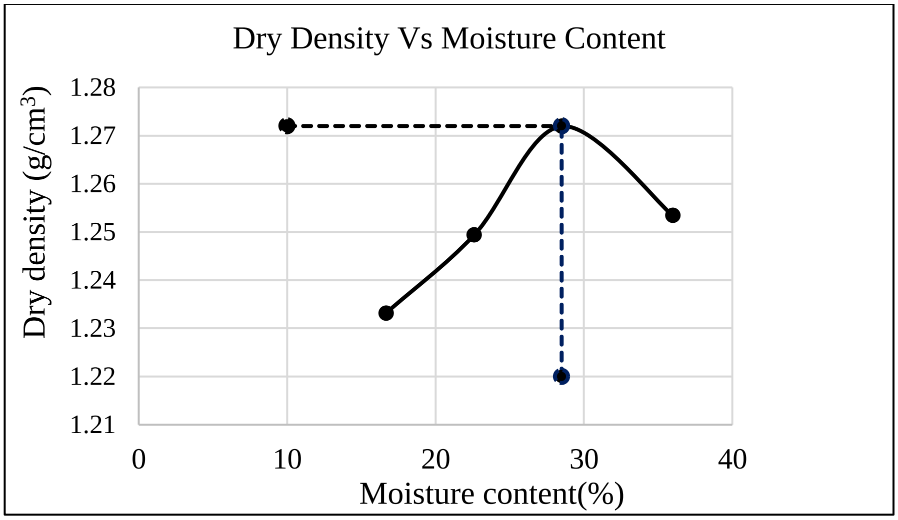

Figure H-7 Compaction curve for soil+6BA+10mm 0.5% SF

Table H-8 Compaction result for soil+6BA+10mm 1% SF

Mass of mold	3756	3756	3756	3756
Mass of mold+ Compacted Soil, g	5105	5167	5288	5330
Mass of Compacted soil, g	1349	1411	1532	1574
Volume of Mold, cm^3	944	944	944	944
Bulk density, g/cm^3	1.43	1.49	1.62	1.67
Water Content, %	17.98	21.61	29.85	35.88
Dry density, g/cm^3	1.21	1.23	1.25	1.23

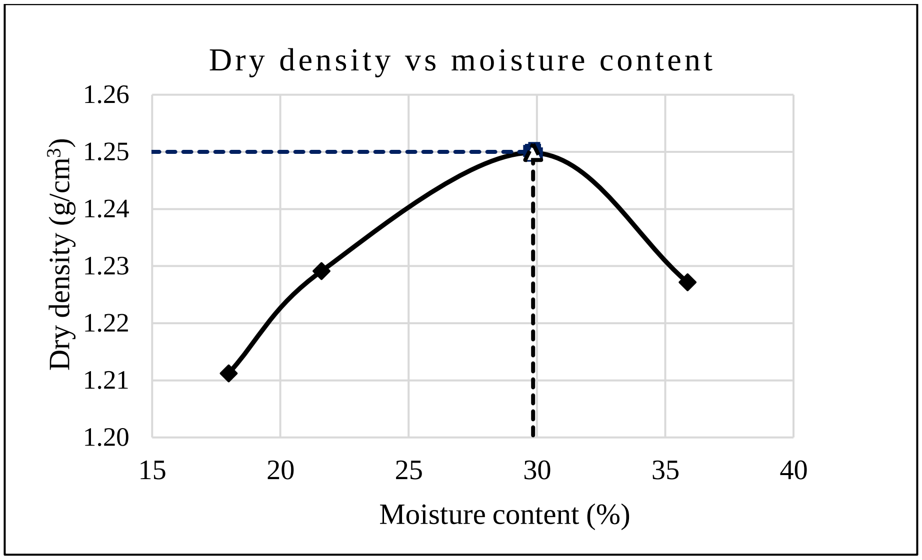

Figure H-8 Compaction curve for soil+6BA+10mm 1 % SF

Table H-9 Compaction result for soil+6BA+10mm 1.5% SF

Mass of mold	3756	3756	3756	3756
Mass of mold+ Compacted Soil, g	5140	5213	5298	5348
Mass of Compacted soil, g	1384	1457	1542	1592
Volume of Mold, cm^3	944	944	944	944
Bulk density, g/cm^3	1.47	1.54	1.63	1.69
Water Content, %	21.0	25.8	31.5	39.0
Dry density, g/cm^3	1.21	1.23	1.24	1.21

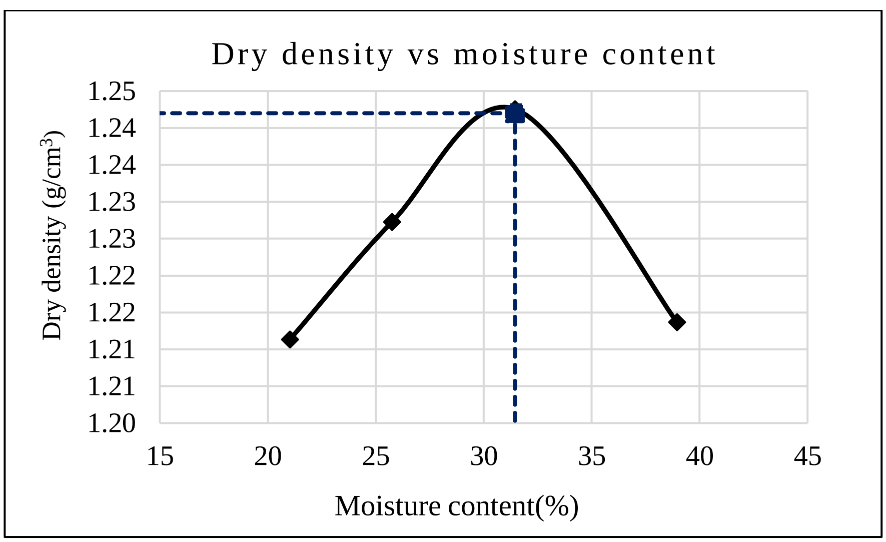

Figure H-9 Compaction curve for soil+6BA+10mm 1.5% SF

Table H-10 Compaction result for soil+6BA+20mm 0.5% SF

Mass of mold	3756	3756	3756	3756
Mass of mold+ Compacted Soil, g	5152	5209	5229	5333
Mass of Compacted soil, g	1396	1453	1473	1577
Volume of Mold, cm^3	944	944	944	944
Bulk density, g/cm^3	1.48	1.54	1.56	1.67
Water Content, %	20.01	23.92	29.50	36.06
Dry density, g/cm^3	1.23	1.24	1.26	1.23

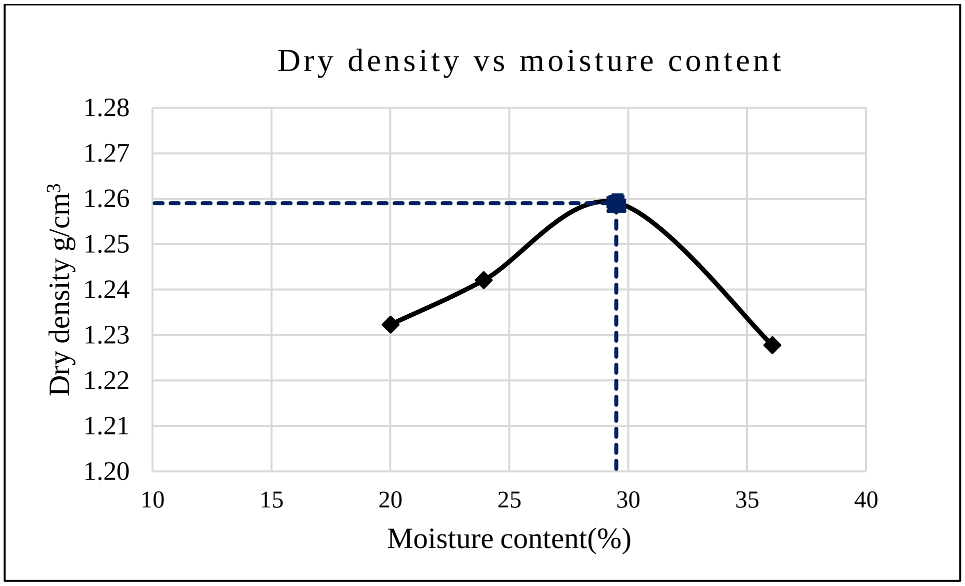

Figure H-9 Compaction curve for soil+6BA+20mm 0.5% SF

Table H-11 Compaction result for soil+6BA+20mm 1% SF

Mass of mold	3756	3756	3756	3756
Mass of mold+ Compacted Soil, g	5132	5223	5291	5310
Mass of Compacted soil, g	1376	1467	1535	1554
Volume of Mold, cm^3	944	944	944	944
Bulk density, g/cm^3	1.46	1.55	1.63	1.65
Water Content, %	20.63	27.07	32.04	35.99
Dry density, g/cm^3	1.21	1.22	1.23	1.21

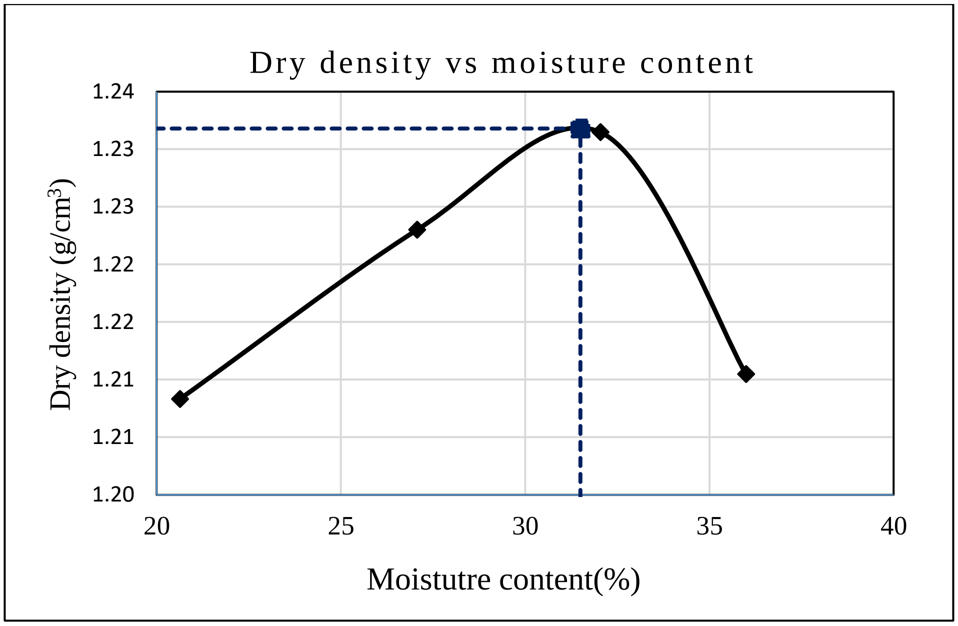

Figure H-9 Compaction curve for soil+6BA+20mm 1 % SF

Table H-12 Compaction result for soil+6BA+20mm 1.5% SF

Mass of mold	3756	3756	3756	3756
Mass of mold+ Compacted Soil, g	5140	5191	5291	5298
Mass of Compacted soil, g	1384	1435	1535	1542
Volume of Mold, cm^3	944	944	944	944
Bulk density, g/cm^3	1.47	1.52	1.63	1.63
Water Content, %	22.40	26.24	33.32	37.11
Dry density, g/cm^3	1.198	1.204	1.220	1.191

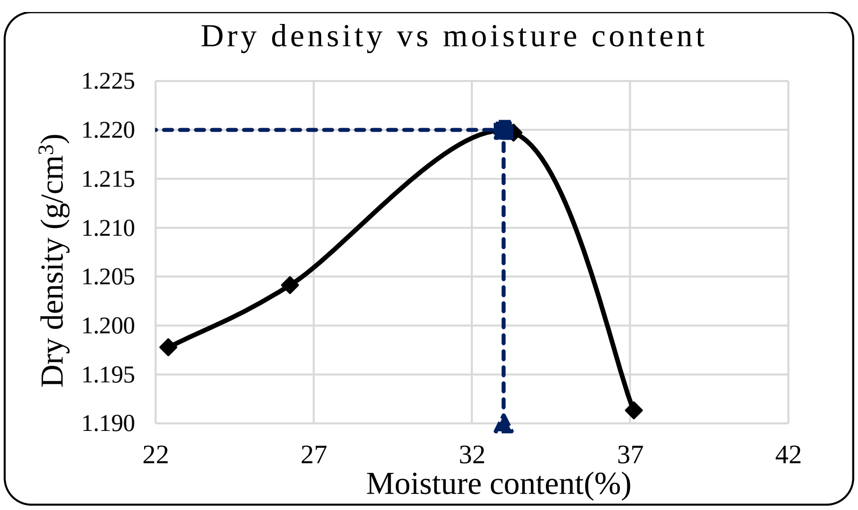

Figure H-12 Compaction curve for soil+6BA+20mm 1.5% SF

Table H-13 Compaction result for soil+6BA+30mm 0.5% SF

Mass of mold	3756	3756	3756	3756
Mass of mold+ Compacted Soil, g	5166	5235	5304	5306
Mass of Compacted soil, g	1410	1479	1548	1550
Volume of Mold, cm^3	944	944	944	944
Bulk density, g/cm^3	1.49	1.57	1.64	1.64
Water Content, %	24.2	27.3	31.1	36.3
Dry density, g/cm^3	1.20	1.23	1.25	1.21

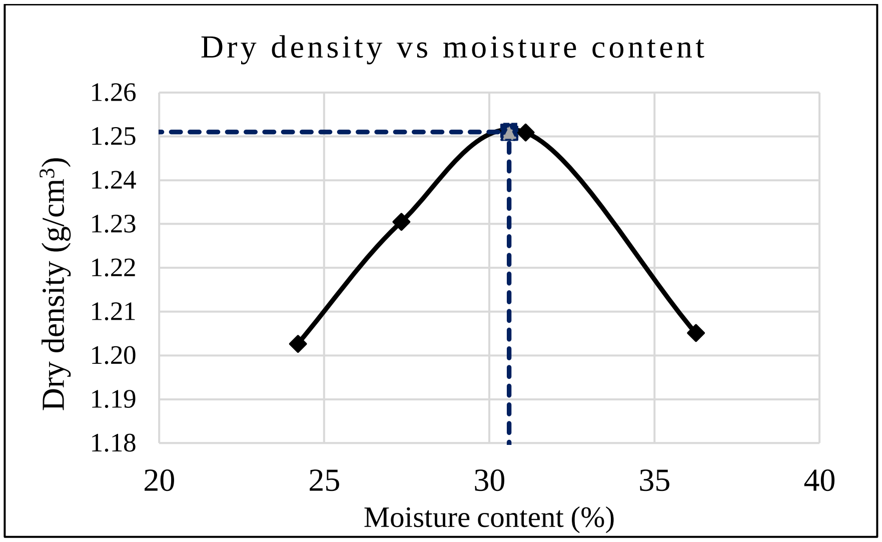

Figure H-13 Compaction curve for soil+6BA+30 mm 0.5% SF

Table H-14 Compaction result for soil+6BA+30 mm 1% SF

Mass of mold	3756	3756	3756	3756
Mass of mold+ Compacted Soil, g	5109	5180	5288	5300
Mass of Compacted soil, g	1353	1424	1532	1544
Volume of Mold, cm^3	944	944	944	944
Bulk density, g/cm^3	1.43	1.51	1.62	1.64
Water Content, %	21.29	25.04	32.51	36.56
Dry density, g/cm^3	1.18	1.21	1.22	1.20

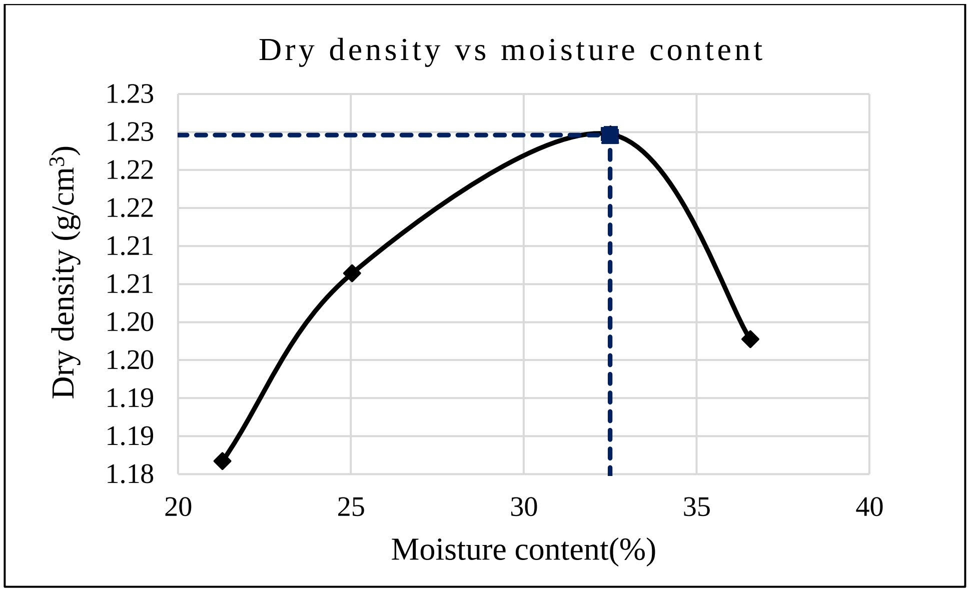

Figure H-14 Compaction curve for soil+6BA+30mm 1 % SF

Table H-15 Compaction result for soil+6BA+30mm 1.5% SF

Mass of mold	3756	3756	3756	3756
Mass of mold+ Compacted Soil, g	5124	5209	5286	5302
Mass of Compacted soil, g	1368	1453	1530	1546
Volume of Mold, cm^3	944	944	944	944
Bulk density, g/cm^3	1.45	1.54	1.62	1.64
Water Content, %	22.12	28.34	33.65	37.42
Dry density, g/cm^3	1.19	1.20	1.21	1.19

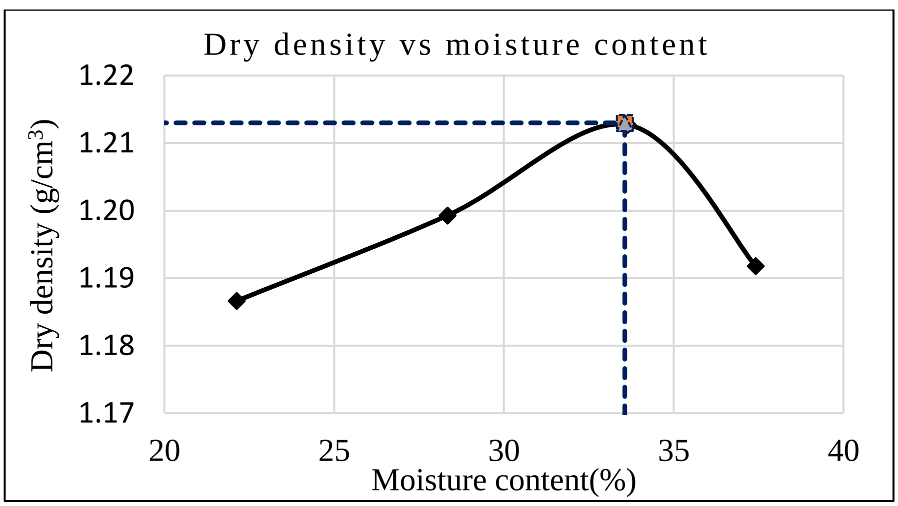

Figure H-15 Compaction curve for soil+6BA+30mm 1.5% SF

Appendix : I Unconfined compressive strength (UCS) test data for uncured and 7 days cured condition

For all UCS test samples the following data are similar

Initial Diameter (mm)	38	Initial Volume (cm^3)	86.2
Initial Height Ho, (mm)	76	P.R. Factor (KN/div)	0.00153
Initial Area Ao (m^2)	0.0010		

Table I-1 UCS test result for TP1(uncured)

Axial deformation (mm)	Unit strain $\epsilon = \Delta H/\Delta Ho$	axial strain (%)	Proving Ring reading	Load in [kN]	Cross - sectional Area $A = A_o/1-\epsilon$	stress in [kN/m^2]
0.00	0.0000	0.0000	0.0	0.0000	0.00100	0.0
0.20	0.0026	0.2632	10	0.0153	0.00100	15.3
0.40	0.0053	0.5263	15	0.0230	0.00101	22.8
0.60	0.0079	0.7895	22	0.0337	0.00101	33.4
0.80	0.0105	1.0526	27	0.0413	0.00101	40.9
1.00	0.0132	1.3158	35	0.0536	0.00101	52.8
1.20	0.0158	1.5789	40	0.0612	0.00102	60.2
1.40	0.0184	1.8421	46	0.0704	0.00102	69.1
1.60	0.0211	2.1053	51	0.0780	0.00102	76.4
1.80	0.0237	2.3684	56	0.0857	0.00102	83.7
2.00	0.0263	2.6316	62	0.0949	0.00103	92.4
2.20	0.0289	2.8947	66	0.1010	0.00103	98.1
2.40	0.0316	3.1579	69	0.1056	0.00103	102.2
2.60	0.0342	3.4211	72	0.1102	0.00104	**106.4**
2.80	0.0368	3.6842	71	0.1086	0.00104	104.6
3.00	0.0395	3.9474	70	0.1071	0.00104	102.9
3.20	0.0421	4.2105	68	0.1040	0.00104	99.7

Table I-2 UCS test result for TP2 (uncured)

Axial deformation (mm)	Unit strain $\epsilon = \Delta H/\Delta Ho$	axial strain (%)	Proving Ring reading	Load in [kN]	Cross - sectional Area $A = Ao/1-\epsilon$	stress in [kN/m^2]
0.00	0.0000	0	0.0	0.0000	0.00100	0.0
0.20	0.0026	0.2631579	6	0.0092	0.00100	9.2
0.40	0.0053	0.5263158	12	0.0184	0.00101	18.3
0.60	0.0079	0.7894737	18	0.0275	0.00101	27.3
0.80	0.0105	1.0526316	25	0.0383	0.00101	37.8

1.00	0.0132	1.3157895	31	0.0474	0.00101	46.8
1.20	0.0158	1.5789474	37	0.0566	0.00102	55.7
1.40	0.0184	1.8421053	43	0.0658	0.00102	64.6
1.60	0.0211	2.1052632	47	0.0719	0.00102	70.4
1.80	0.0237	2.3684211	52	0.0796	0.00102	77.7
2.00	0.0263	2.6315789	56	0.0857	0.00103	83.4
2.20	0.0289	2.8947368	60	0.0918	0.00103	89.1
2.40	0.0316	3.1578947	63	0.0964	0.00103	93.3
2.60	0.0342	3.4210526	65	0.0995	0.00104	**96.0**
2.80	0.0368	3.6842105	64	0.0979	0.00104	94.3

Table I-3 UCS test for TP2-7 days cured

Axial deformation (mm)	Unit strain $\epsilon = \Delta H/\Delta Ho$	axial strain (%)	Proving Ring reading	Load in [kN]	Cross - sectional Area $A = Ao/1-\epsilon$	stress in [kN/m^2]
0.00	0.0000	0.000000	0	0.0000	0.00100	0.0
0.20	0.0026	0.263158	8	0.0122	0.00100	12.2
0.40	0.0053	0.526316	14	0.0214	0.00101	21.3
0.60	0.0079	0.789474	20	0.0306	0.00101	30.4
0.80	0.0105	1.052632	26	0.0398	0.00101	39.4
1.00	0.0132	1.315789	31	0.0474	0.00101	46.8
1.20	0.0158	1.578947	37	0.0566	0.00102	55.7
1.40	0.0184	1.842105	43	0.0658	0.00102	64.6
1.60	0.0211	2.105263	49	0.0750	0.00102	73.4
1.80	0.0237	2.368421	54	0.0826	0.00102	80.7
2.00	0.0263	2.631579	59	0.0903	0.00103	87.9
2.20	0.0289	2.894737	63	0.0964	0.00103	93.6
2.40	0.0316	3.157895	66	0.1010	0.00103	97.8
2.60	0.0342	3.421053	68	0.1040	0.00104	100.5
2.80	0.0368	3.684211	69	0.1056	0.00104	101.7

3.00	0.0395	3.947368	70	0.1071	0.00104	**102.9**
3.20	0.0421	4.210526	69	0.1056	0.00104	101.1

Table I-4 UCS test result for TP 3 (uncured)

Axial deformation (mm)	Unit strain $\epsilon = \Delta H/\Delta Ho$	axial strain (%)	Proving Ring reading	Load in [kN]	Cross - sectional Area $A = Ao/1-\epsilon$	stress in [kN/m^2]
0.00	0.0000	0	0.0	0.0000	0.00100	0.0
0.20	0.0026	0.263158	8	0.0122	0.00100	12.2
0.40	0.0053	0.526316	16	0.0245	0.00101	24.4
0.60	0.0079	0.789474	24	0.0367	0.00101	36.4
0.80	0.0105	1.052632	30	0.0459	0.00101	45.4
1.00	0.0132	1.315789	36	0.0551	0.00101	54.4
1.20	0.0158	1.578947	41	0.0627	0.00102	61.7
1.40	0.0184	1.842105	47	0.0719	0.00102	70.6
1.60	0.0211	2.105263	52	0.0796	0.00102	77.9
1.80	0.0237	2.368421	56	0.0857	0.00102	83.7
2.00	0.0263	2.631579	60	0.0918	0.00103	89.4
2.20	0.0289	2.894737	63	0.0964	0.00103	93.6
2.40	0.0316	3.157895	65	0.0995	0.00103	96.3
2.60	0.0342	3.421053	67	0.1025	0.00104	99.0
2.80	0.0368	3.684211	68	0.1040	0.00104	**100.2**
3.00	0.0395	3.947368	67	0.1025	0.00104	98.5

Table I-5 UCS test result for soil + 3% BA (uncured)

Axial deformation (mm)	Unit strain $\epsilon = \Delta H/\Delta Ho$	axial strain (%)	Proving Ring reading	Load in [kN]	Cross - sectional Area $A = Ao/1-\epsilon$	stress in [kN/m^2]
0.00	0.0000	0	0.0	0.0000	0.00100	0.0
0.20	0.0026	0.263158	11	0.0168	0.00100	16.8
0.40	0.0053	0.526316	19	0.0291	0.00101	28.9
0.60	0.0079	0.789474	28	0.0428	0.00101	42.5
0.80	0.0105	1.052632	37	0.0566	0.00101	56.0
1.00	0.0132	1.315789	43	0.0658	0.00101	64.9
1.20	0.0158	1.578947	49	0.0750	0.00102	73.8
1.40	0.0184	1.842105	54	0.0826	0.00102	81.1

1.60	0.0211	2.105263	59	0.0903	0.00102	88.4
1.80	0.0237	2.368421	62	0.0949	0.00102	92.6
2.00	0.0263	2.631579	63	0.0964	0.00103	93.9
2.20	0.0289	2.894737	64	0.0979	0.00103	95.1
2.40	0.0316	3.157895	66	0.1010	0.00103	**97.8**
2.60	0.0342	3.421053	65	0.0995	0.00104	96.0
2.80	0.0368	3.684211	64	0.0979	0.00104	94.3
3.00	0.0395	3.947368	63	0.0964	0.00104	92.6

Table I-6 UCS test result for soil + 3 % BA 7 days cured

Axial deformation (mm)	Unit strain $\epsilon = \Delta H/\Delta H_o$	axial strain (%)	Proving Ring reading	Load in [kN]	Cross - sectional Area $A = A_o/1\text{-}\epsilon$	stress in [kN/m^2]
0.00	0.0000	0	0	0.0000	0.00100	0.0
0.20	0.0026	0.263158	11	0.0168	0.00100	16.8
0.40	0.0053	0.526316	17	0.0260	0.00101	25.9
0.60	0.0079	0.789474	23	0.0352	0.00101	34.9
0.80	0.0105	1.052632	28	0.0428	0.00101	42.4
1.00	0.0132	1.315789	32	0.0490	0.00101	48.3
1.20	0.0158	1.578947	39	0.0597	0.00102	58.7
1.40	0.0184	1.842105	47	0.0719	0.00102	70.6
1.60	0.0211	2.105263	51	0.0780	0.00102	76.4
1.80	0.0237	2.368421	54	0.0826	0.00102	80.7
2.00	0.0263	2.631579	58	0.0887	0.00103	86.4
2.20	0.0289	2.894737	62	0.0949	0.00103	92.1
2.40	0.0316	3.157895	64	0.0979	0.00103	94.8
2.60	0.0342	3.421053	68	0.1040	0.00104	100.5
2.80	0.0368	3.684211	72	0.1102	0.00104	106.1
3.00	0.0395	3.947368	75	0.1148	0.00104	**110.2**
3.20	0.0421	4.210526	74	0.1132	0.00104	108.5

Table I-7 UCS test result for soil + 6 % BA uncured

Axial deformation (mm)	Unit strain $\epsilon = \Delta H/\Delta H_o$	axial strain (%)	Proving Ring reading	Load in [kN]	Cross - sectional Area $A = A_o/1\text{-}\epsilon$	stress in [kN/m^2]
0.00	0.0000	0	0.0	0.0000	0.00100	0.0
0.20	0.0026	0.263158	15	0.0230	0.00100	22.9
0.40	0.0053	0.526316	23	0.0352	0.00101	35.0
0.60	0.0079	0.789474	32	0.0490	0.00101	48.6

0.80	0.0105	1.052632	39	0.0597	0.00101	59.0
1.00	0.0132	1.315789	46	0.0704	0.00101	69.5
1.20	0.0158	1.578947	53	0.0811	0.00102	79.8
1.40	0.0184	1.842105	62	0.0949	0.00102	93.1
1.60	0.0211	2.105263	70	0.1071	0.00102	104.8
1.80	0.0237	2.368421	78	0.1193	0.00102	116.5
2.00	0.0263	2.631579	85	0.1301	0.00103	126.6
2.20	0.0289	2.894737	90	0.1377	0.00103	133.7
2.40	0.0316	3.157895	93	0.1423	0.00103	137.8
2.60	0.0342	3.421053	95	0.1454	0.00104	140.4
2.80	0.0368	3.684211	96	0.1469	0.00104	**141.5**
3.00	0.0395	3.947368	94	0.1438	0.00104	138.1

Table I-8 UCS data for soil + 6 % BA 7 days cured

Axial deformation (mm)	Unit strain $\epsilon = \Delta H/\Delta H_o$	axial strain (%)	Proving Ring reading	Load in [kN]	Cross - sectional Area $A = A_o/1-\epsilon$	stress in [kN/m^2]
0.00	0.0000	0	0	0.0000	0.00100	0.0
0.20	0.0026	0.263158	13	0.0199	0.00100	19.8
0.40	0.0053	0.526316	24	0.0367	0.00101	36.5
0.60	0.0079	0.789474	35	0.0536	0.00101	53.1
0.80	0.0105	1.052632	46	0.0704	0.00101	69.6
1.00	0.0132	1.315789	56	0.0857	0.00101	84.6
1.20	0.0158	1.578947	64	0.0979	0.00102	96.4
1.40	0.0184	1.842105	72	0.1102	0.00102	108.1
1.60	0.0211	2.105263	79	0.1209	0.00102	118.3
1.80	0.0237	2.368421	85	0.1301	0.00102	127.0
2.00	0.0263	2.631579	93	0.1423	0.00103	138.5
2.20	0.0289	2.894737	98	0.1499	0.00103	145.6
2.40	0.0316	3.157895	102	0.1561	0.00103	151.1
2.60	0.0342	3.421053	105	0.1607	0.00104	155.2
2.80	0.0368	3.684211	108	0.1652	0.00104	**159.2**
3.00	0.0395	3.947368	107	0.1637	0.00104	157.2
3.20	0.0421	4.210526	106	0.1622	0.00104	155.4

Table I-9 UCS data for soil + 9 % BA uncured

Axial deformation (mm)	Unit strain ϵ = ΔH/ΔHo	axial strain (%)	Proving Ring reading	Load in [kN]	Cross - sectional Area A = Ao/1-ϵ	stress in [kN/m^2]
0.00	0.0000	0	0.0	0.0000	0.00100	0.0
0.20	0.0026	0.263158	13	0.0199	0.00100	19.8
0.40	0.0053	0.526316	21	0.0321	0.00101	32.0
0.60	0.0079	0.789474	29	0.0444	0.00101	44.0
0.80	0.0105	1.052632	36	0.0551	0.00101	54.5
1.00	0.0132	1.315789	43	0.0658	0.00101	64.9
1.20	0.0158	1.578947	51	0.0780	0.00102	76.8
1.40	0.0184	1.842105	56	0.0857	0.00102	84.1
1.60	0.0211	2.105263	60	0.0918	0.00102	89.9
1.80	0.0237	2.368421	65	0.0995	0.00102	97.1
2.00	0.0263	2.631579	68	0.1040	0.00103	101.3
2.20	0.0289	2.894737	72	0.1102	0.00103	107.0
2.40	0.0316	3.157895	74	0.1132	0.00103	109.6
2.60	0.0342	3.421053	75	0.1148	0.00104	110.8
2.80	0.0368	3.684211	77	0.1178	0.00104	113.5
3.00	0.0395	3.947368	79	0.1209	0.00104	**116.1**
3.20	0.0421	4.210526	78	0.1193	0.00104	114.3

Table I-10 UCS data for soil + 9 % BA 7 days cured

Axial deformation (mm)	Unit strain ϵ = ΔH/ΔHo	axial strain (%)	Proving Ring reading	Load in [kN]	Cross - sectional Area A = Ao/1-ϵ	stress in [kN/m^2]
0.00	0.0000	0	0	0.0000	0.00100	0.0
0.20	0.0026	0.263158	13	0.0199	0.00100	19.8
0.40	0.0053	0.526316	23	0.0352	0.00101	35.0
0.60	0.0079	0.789474	32	0.0490	0.00101	48.6
0.80	0.0105	1.052632	40	0.0612	0.00101	60.6

1.00	0.0132	1.315789	49	0.0750	0.00101	74.0
1.20	0.0158	1.578947	56	0.0857	0.00102	84.3
1.40	0.0184	1.842105	62	0.0949	0.00102	93.1
1.60	0.0211	2.105263	69	0.1056	0.00102	103.3
1.80	0.0237	2.368421	73	0.1117	0.00102	109.0
2.00	0.0263	2.631579	76	0.1163	0.00103	113.2
2.20	0.0289	2.894737	79	0.1209	0.00103	117.4
2.40	0.0316	3.157895	83	0.1270	0.00103	123.0
2.60	0.0342	3.421053	85	0.1301	0.00104	125.6
2.80	0.0368	3.684211	87	0.1331	0.00104	128.2
3.00	0.0395	3.947368	88	0.1346	0.00104	129.3
3.20	0.0421	4.210526	90	0.1377	0.00104	**131.9**
3.40	0.0447	4.473684	89	0.1362	0.00105	130.1

UCS data for bagasse ash stabilized expansive soil with sisal fiber reinforcement

Table I-11 UCS test result for (soil+0.5 % SF,10mm) uncured

Axial deformation (mm)	Unit strain $\epsilon = \Delta H/\Delta Ho$	axial strain (%)	Proving Ring reading	Load in [kN]	Cross - sectional Area A = Ao/1-ϵ	stress in [kN/m^2]
0.00	0.0000	0	0.0	0.0000	0.00100	0.0
0.20	0.0026	0.263158	19	0.0291	0.00100	29.0
0.40	0.0053	0.526316	25	0.0383	0.00101	38.0
0.60	0.0079	0.789474	32	0.0490	0.00101	48.6
0.80	0.0105	1.052632	40	0.0612	0.00101	60.6
1.00	0.0132	1.315789	48	0.0734	0.00101	72.5
1.20	0.0158	1.578947	55	0.0842	0.00102	82.8
1.40	0.0184	1.842105	63	0.0964	0.00102	94.6
1.60	0.0211	2.105263	70	0.1071	0.00102	104.8
1.80	0.0237	2.368421	78	0.1193	0.00102	116.5
2.00	0.0263	2.631579	84	0.1285	0.00103	125.1
2.20	0.0289	2.894737	90	0.1377	0.00103	133.7
2.40	0.0316	3.157895	100	0.1530	0.00103	148.2
2.60	0.0342	3.421053	105	0.1607	0.00104	155.2
2.80	0.0368	3.684211	109	0.1668	0.00104	160.6
3.00	0.0395	3.947368	115	0.1760	0.00104	**169.0**
3.20	0.0421	4.210526	114	0.1744	0.00104	167.1

Table I-12 UCS test result for (soil+0.5 % SF,10mm) 7 days uncured

Axial deformation (mm)	Unit strain ϵ = ΔH/ΔHo	axial strain (%)	Proving Ring reading	Load in [kN]	Cross - sectional Area A = Ao/1-ϵ	stress in [kN/m^2]
0.00	0.0000	0	0.0	0.0000	0.00100	0.0
0.20	0.0026	0.263158	14	0.0214	0.00100	21.4
0.40	0.0053	0.526316	25	0.0383	0.00101	38.0
0.60	0.0079	0.789474	36	0.0551	0.00101	54.6
0.80	0.0105	1.052632	45	0.0689	0.00101	68.1
1.00	0.0132	1.315789	56	0.0857	0.00101	84.6
1.20	0.0158	1.578947	68	0.1040	0.00102	102.4
1.40	0.0184	1.842105	78	0.1193	0.00102	117.1
1.60	0.0211	2.105263	85	0.1301	0.00102	127.3
1.80	0.0237	2.368421	90	0.1377	0.00102	134.4
2.00	0.0263	2.631579	96	0.1469	0.00103	143.0
2.20	0.0289	2.894737	100	0.1530	0.00103	148.6
2.40	0.0316	3.157895	106	0.1622	0.00103	157.1
2.60	0.0342	3.421053	110	0.1683	0.00104	162.5
2.80	0.0368	3.684211	115	0.1760	0.00104	169.5
3.00	0.0395	3.947368	117	0.1790	0.00104	171.9
3.20	0.0421	4.210526	120	0.1836	0.00104	175.9
3.40	0.0447	4.473684	123	0.1882	0.00105	179.8
3.60	0.0474	4.736842	125	0.1913	0.00105	182.2
3.80	0.0500	5	127	0.1943	0.00105	**184.6**
4.00	0.0526	5.263158	125	0.1913	0.00106	181.2

Table I-13 UCS test result for (soil+ 1% SF,10mm) uncured

Axial deformation (mm)	Unit strain ϵ = ΔH/ΔHo	axial strain (%)	Proving Ring reading	Load in [kN]	Cross - sectional Area A = Ao/1-ϵ	stress in [kN/m^2]
0.00	0.0000	0	0.0	0.0000	0.00100	0.0
0.20	0.0026	0.263158	17	0.0260	0.00100	25.9
0.40	0.0053	0.526316	26	0.0398	0.00101	39.6
0.60	0.0079	0.789474	37	0.0566	0.00101	56.2
0.80	0.0105	1.052632	44	0.0673	0.00101	66.6
1.00	0.0132	1.315789	54	0.0826	0.00101	81.5
1.20	0.0158	1.578947	63	0.0964	0.00102	94.9
1.40	0.0184	1.842105	69	0.1056	0.00102	103.6
1.60	0.0211	2.105263	78	0.1193	0.00102	116.8
1.80	0.0237	2.368421	87	0.1331	0.00102	130.0
2.00	0.0263	2.631579	96	0.1469	0.00103	143.0
2.20	0.0289	2.894737	104	0.1591	0.00103	154.5
2.40	0.0316	3.157895	113	0.1729	0.00103	167.4
2.60	0.0342	3.421053	118	0.1805	0.00104	174.4
2.80	0.0368	3.684211	119	0.1821	0.00104	**175.4**
3.00	0.0395	3.947368	118	0.1805	0.00104	173.4

3.20	0.0421	4.210526	116	0.1775	0.00104	170.0
3.40	0.0447	4.473684	115	0.1760	0.00105	168.1

Table I-14 UCS test result for (soil+1 % SF,10mm) 7 days uncured

Axial deformation (mm)	Unit strain ϵ = ΔH/ΔHo	Axial strain (%)	Proving Ring reading	Load in [kN]	Cross - sectional Area A = Ao/1-ϵ	stress in [kN/m^2]
0.00	0.0000	0	0	0.0000	0.00100	0.0
0.20	0.0026	0.263158	15	0.0230	0.00100	22.9
0.40	0.0053	0.526316	29	0.0444	0.00101	44.1
0.60	0.0079	0.789474	36	0.0551	0.00101	54.6
0.80	0.0105	1.052632	45	0.0689	0.00101	68.1
1.00	0.0132	1.315789	57	0.0872	0.00101	86.1
1.20	0.0158	1.578947	71	0.1086	0.00102	106.9
1.40	0.0184	1.842105	87	0.1331	0.00102	130.7
1.60	0.0211	2.105263	97	0.1484	0.00102	145.3
1.80	0.0237	2.368421	110	0.1683	0.00102	164.3
2.00	0.0263	2.631579	120	0.1836	0.00103	178.8
2.20	0.0289	2.894737	126	0.1928	0.00103	187.2
2.40	0.0316	3.157895	132	0.2020	0.00103	195.6
2.60	0.0342	3.421053	135	0.2066	0.00104	**199.5**
2.80	0.0368	3.684211	133	0.2035	0.00104	196.0
3.00	0.0395	3.947368	132	0.2020	0.00104	194.0
3.20	0.0421	4.210526	127	0.1943	0.00104	186.1

Table I-15 UCS test result for (soil+1.5 % SF,10mm) uncured

Axial deformation (mm)	Unit strain ϵ = ΔH/ΔHo	Axial strain (%)	Proving Ring reading	Load in [kN]	Cross - sectional Area A = Ao/1-ϵ	stress in [kN/m^2]
0.00	0.0000	0	0.0	0.0000	0.00100	0.0
0.20	0.0026	0.263158	15	0.0230	0.00100	22.9
0.40	0.0053	0.526316	26	0.0398	0.00101	39.6
0.60	0.0079	0.789474	36	0.0551	0.00101	54.6
0.80	0.0105	1.052632	46	0.0704	0.00101	69.6
1.00	0.0132	1.315789	54	0.0826	0.00101	81.5
1.20	0.0158	1.578947	67	0.1025	0.00102	100.9
1.40	0.0184	1.842105	76	0.1163	0.00102	114.1
1.60	0.0211	2.105263	87	0.1331	0.00102	130.3
1.80	0.0237	2.368421	99	0.1515	0.00102	147.9
2.00	0.0263	2.631579	106	0.1622	0.00103	157.9
2.20	0.0289	2.894737	111	0.1698	0.00103	**164.9**
2.40	0.0316	3.157895	110	0.1683	0.00103	163.0

Table I-16 UCS test result for (soil+1.5 % SF,10mm) 7 days uncured

Axial deformation (mm)	Unit strain ϵ = ΔH/ΔHo	axial strain (%)	Proving Ring reading	Load in [kN]	Cross - sectional Area A = Ao/1-ϵ	stress in [kN/m^2]
0.00	0.0000	0	0	0.0000	0.00100	0.0
0.20	0.0026	0.263158	20	0.0306	0.00100	30.5
0.40	0.0053	0.526316	35	0.0536	0.00101	53.3
0.60	0.0079	0.789474	48	0.0734	0.00101	72.9
0.80	0.0105	1.052632	57	0.0872	0.00101	86.3
1.00	0.0132	1.315789	65	0.0995	0.00101	98.1
1.20	0.0158	1.578947	78	0.1193	0.00102	117.5
1.40	0.0184	1.842105	87	0.1331	0.00102	130.7
1.60	0.0211	2.105263	94	0.1438	0.00102	140.8
1.80	0.0237	2.368421	104	0.1591	0.00102	155.4
2.00	0.0263	2.631579	110	0.1683	0.00103	163.9
2.20	0.0289	2.894737	116	0.1775	0.00103	172.3
2.40	0.0316	3.157895	119	0.1821	0.00103	176.3
2.60	0.0342	3.421053	120	0.1836	0.00104	177.3
2.80	0.0368	3.684211	119	0.1821	0.00104	175.4

Table I-17 UCS test result for (soil+ 0.5 % SF,20mm) uncured

Axial deformation (mm)	Unit strain ϵ = ΔH/ΔHo	axial strain (%)	Proving Ring reading	Load in [kN]	Cross - sectional Area A = Ao/1-ϵ	stress in [kN/m^2]
0.00	0.0000	0	0.0	0.0000	0.00100	0.0
0.20	0.0026	0.263158	14	0.0214	0.00100	21.4
0.40	0.0053	0.526316	19	0.0291	0.00101	28.9
0.60	0.0079	0.789474	26	0.0398	0.00101	39.5
0.80	0.0105	1.052632	35	0.0536	0.00101	53.0
1.00	0.0132	1.315789	44	0.0673	0.00101	66.4
1.20	0.0158	1.578947	53	0.0811	0.00102	79.8
1.40	0.0184	1.842105	65	0.0995	0.00102	97.6
1.60	0.0211	2.105263	69	0.1056	0.00102	103.3
1.80	0.0237	2.368421	77	0.1178	0.00102	115.0
2.00	0.0263	2.631579	88	0.1346	0.00103	131.1
2.20	0.0289	2.894737	94	0.1438	0.00103	139.7
2.40	0.0316	3.157895	103	0.1576	0.00103	152.6
2.60	0.0342	3.421053	108	0.1652	0.00104	159.6
2.80	0.0368	3.684211	116	0.1775	0.00104	170.9
3.00	0.0395	3.947368	118	0.1805	0.00104	**173.4**
3.20	0.0421	4.210526	117	0.1790	0.00104	171.5
3.40	0.0447	4.473684	116	0.1775	0.00105	169.5

Table I-18 UCS test result for (soil+ 0.5 % SF,20mm) 7 days cured

Axial deformation (mm)	Unit strain ϵ = ΔH/ΔHo	axial strain (%)	Proving Ring reading	Load in [kN]	Cross - sectional Area A = Ao/1-ϵ	stress in [kN/m^2]
0.00	0.0000	0	0	0.0000	0.00100	0.0
0.20	0.0026	0.263158	12	0.0184	0.00100	18.3
0.40	0.0053	0.526316	18	0.0275	0.00101	27.4
0.60	0.0079	0.789474	28	0.0428	0.00101	42.5
0.80	0.0105	1.052632	39	0.0597	0.00101	59.0
1.00	0.0132	1.315789	46	0.0704	0.00101	69.5
1.20	0.0158	1.578947	57	0.0872	0.00102	85.8
1.40	0.0184	1.842105	64	0.0979	0.00102	96.1
1.60	0.0211	2.105263	79	0.1209	0.00102	118.3
1.80	0.0237	2.368421	86	0.1316	0.00102	128.5
2.00	0.0263	2.631579	93	0.1423	0.00103	138.5
2.20	0.0289	2.894737	98	0.1499	0.00103	145.6
2.40	0.0316	3.157895	108	0.1652	0.00103	160.0
2.60	0.0342	3.421053	114	0.1744	0.00104	168.5
2.80	0.0368	3.684211	120	0.1836	0.00104	176.8
3.00	0.0395	3.947368	124	0.1897	0.00104	182.2
3.20	0.0421	4.210526	127	0.1943	0.00104	**186.1**
3.40	0.0447	4.473684	126	0.1928	0.00105	184.2

Table I-19 UCS test result for (soil+ 1 % SF,20mm) uncured

Axial deformation (mm)	Unit strain ϵ = ΔH/ΔHo	axial strain (%)	Proving Ring reading	Load in [kN]	Cross - sectional Area A = Ao/1-ϵ	stress in [kN/m^2]
0.00	0.0000	0	0.0	0.0000	0.00100	0.0
0.20	0.0026	0.263158	13	0.0199	0.00100	19.8
0.40	0.0053	0.526316	22	0.0337	0.00101	33.5
0.60	0.0079	0.789474	32	0.0490	0.00101	48.6
0.80	0.0105	1.052632	42	0.0643	0.00101	63.6
1.00	0.0132	1.315789	52	0.0796	0.00101	78.5
1.20	0.0158	1.578947	61	0.0933	0.00102	91.9
1.40	0.0184	1.842105	70	0.1071	0.00102	105.1
1.60	0.0211	2.105263	79	0.1209	0.00102	118.3
1.80	0.0237	2.368421	87	0.1331	0.00102	130.0
2.00	0.0263	2.631579	96	0.1469	0.00103	143.0
2.20	0.0289	2.894737	104	0.1591	0.00103	154.5
2.40	0.0316	3.157895	112	0.1714	0.00103	165.9
2.60	0.0342	3.421053	118	0.1805	0.00104	174.4
2.80	0.0368	3.684211	122	0.1867	0.00104	179.8
3.00	0.0395	3.947368	125	0.1913	0.00104	183.7
3.20	0.0421	4.210526	128	0.1958	0.00104	**187.6**
3.40	0.0447	4.473684	127	0.1943	0.00105	185.6
3.60	0.0474	4.736842	125	0.1913	0.00105	182.2

Table I-20 UCS test result for (soil+ 1 % SF,20mm) 7 days cured

Axial deformation (mm)	Unit strain ϵ = ΔH/ΔHo	axial strain (%)	Proving Ring reading	Load in [kN]	Cross - sectional Area A = Ao/1-ϵ	stress in [kN/m^2]
0.00	0.0000	0	0	0.0000	0.00100	0.0
0.20	0.0026	0.263158	15	0.0230	0.00100	22.9
0.40	0.0053	0.526316	25	0.0383	0.00101	38.0
0.60	0.0079	0.789474	36	0.0551	0.00101	54.6
0.80	0.0105	1.052632	45	0.0689	0.00101	68.1
1.00	0.0132	1.315789	54	0.0826	0.00101	81.5
1.20	0.0158	1.578947	63	0.0964	0.00102	94.9
1.40	0.0184	1.842105	69	0.1056	0.00102	103.6
1.60	0.0211	2.105263	78	0.1193	0.00102	116.8
1.80	0.0237	2.368421	87	0.1331	0.00102	130.0
2.00	0.0263	2.631579	94	0.1438	0.00103	140.0
2.20	0.0289	2.894737	100	0.1530	0.00103	148.6
2.40	0.0316	3.157895	108	0.1652	0.00103	160.0
2.60	0.0342	3.421053	112	0.1714	0.00104	165.5
2.80	0.0368	3.684211	118	0.1805	0.00104	173.9
3.00	0.0395	3.947368	125	0.1913	0.00104	183.7
3.20	0.0421	4.210526	129	0.1974	0.00104	189.1
3.40	0.0447	4.473684	133	0.2035	0.00105	194.4
3.60	0.0474	4.736842	137	0.2096	0.00105	199.7
3.80	0.0500	5	140	0.2142	0.00105	203.5
4.00	0.0526	5.263158	143	0.2188	0.00106	207.3
4.20	0.0553	5.526316	147	0.2249	0.00106	**212.5**
4.40	0.0579	5.789474	146	0.2234	0.00106	210.4
4.60	0.0605	6.052632	144	0.2203	0.00106	207.0

Table I-21 UCS test result for (soil+ 1.5 % SF,20mm) un cured

Axial deformation (mm)	Unit strain ϵ = ΔH/ΔHo	axial strain (%)	Proving Ring reading	Load in [kN]	Cross - sectional Area A = Ao/1-ϵ	stress in [kN/m^2]
0.00	0.0000	0	0.0	0.0000	0.00100	0.00
0.20	0.0026	0.263158	12	0.0184	0.00100	18.31
0.40	0.0053	0.526316	22	0.0337	0.00101	33.48
0.60	0.0079	0.789474	35	0.0536	0.00101	53.13
0.80	0.0105	1.052632	41	0.0627	0.00101	62.07
1.00	0.0132	1.315789	46	0.0704	0.00101	69.45
1.20	0.0158	1.578947	53	0.0811	0.00102	79.81
1.40	0.0184	1.842105	62	0.0949	0.00102	93.11
1.60	0.0211	2.105263	67	0.1025	0.00102	100.35
1.80	0.0237	2.368421	75	0.1148	0.00102	112.03
2.00	0.0263	2.631579	83	0.1270	0.00103	123.65
2.20	0.0289	2.894737	92	0.1408	0.00103	136.69
2.40	0.0316	3.157895	99	0.1515	0.00103	146.69

2.60	0.0342	3.421053	108	0.1652	0.00104	159.59
2.80	0.0368	3.684211	112	0.1714	0.00104	165.05
3.00	0.0395	3.947368	115	0.1760	0.00104	**169.00**
3.20	0.0421	4.210526	114	0.1744	0.00104	167.08

Table I-22 UCS test result for (soil+ 1.5 % SF,20mm) 7 days cured

Axial deformation (mm)	Unit strain ϵ = ΔH/ΔHo	axial strain (%)	Proving Ring reading	Load in [kN]	Cross - sectional Area A = Ao/1-ϵ	stress in [kN/m^2]
0.00	0.0000	0	0	0.0000	0.00100	0.00
0.20	0.0026	0.263158	14	0.0214	0.00100	21.36
0.40	0.0053	0.526316	25	0.0383	0.00101	38.05
0.60	0.0079	0.789474	34	0.0520	0.00101	51.61
0.80	0.0105	1.052632	40	0.0612	0.00101	60.56
1.00	0.0132	1.315789	51	0.0780	0.00101	77.00
1.20	0.0158	1.578947	58	0.0887	0.00102	87.34
1.40	0.0184	1.842105	66	0.1010	0.00102	99.12
1.60	0.0211	2.105263	73	0.1117	0.00102	109.34
1.80	0.0237	2.368421	80	0.1224	0.00102	119.50
2.00	0.0263	2.631579	87	0.1331	0.00103	129.61
2.20	0.0289	2.894737	93	0.1423	0.00103	138.17
2.40	0.0316	3.157895	102	0.1561	0.00103	151.13
2.60	0.0342	3.421053	107	0.1637	0.00104	158.11
2.80	0.0368	3.684211	112	0.1714	0.00104	165.05
3.00	0.0395	3.947368	115	0.1760	0.00104	169.00
3.20	0.0421	4.210526	120	0.1836	0.00104	175.87
3.40	0.0447	4.473684	123	0.1882	0.00105	179.77
3.60	0.0474	4.736842	125	0.1913	0.00105	182.19
3.80	0.0500	5.000000	126	0.1928	0.00105	**183.14**
4.00	0.0526	5.263158	124	0.1897	0.00106	179.73

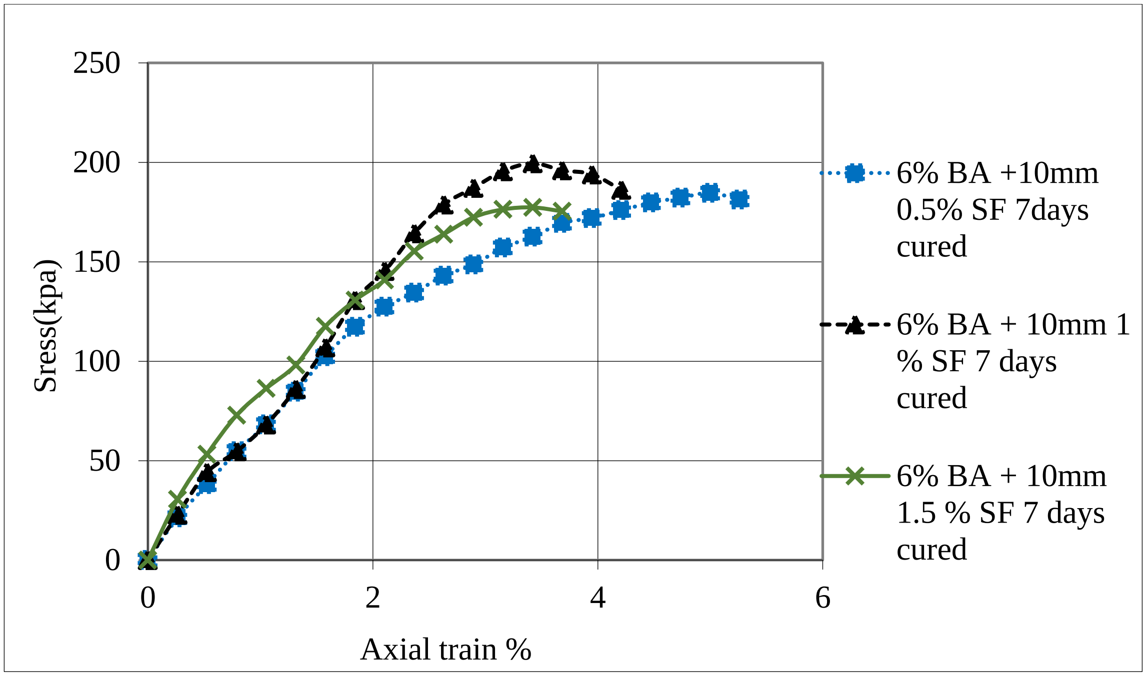

Figure I-1 UCS stress strain cure for soil+6BA+different percentages of SF (10mm), uncured

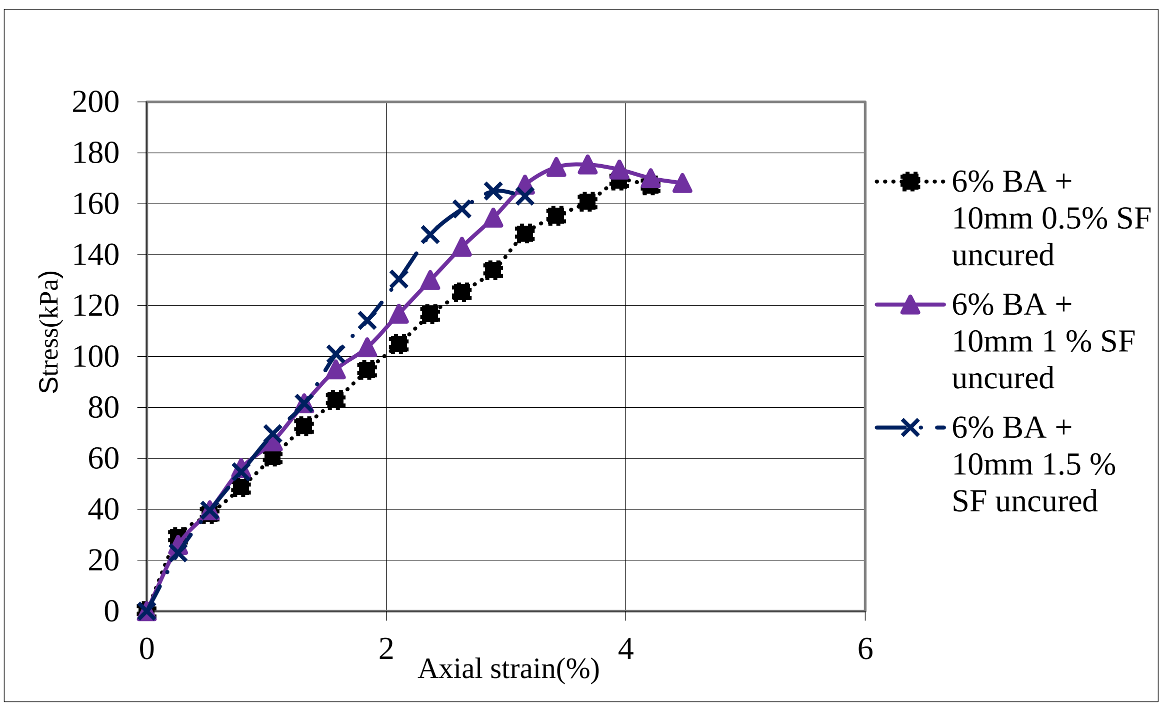

Figure I-2 UCS stress strain cure for soil+6BA+different percentages of SF (10mm),7 days cured

Table I-23 UCS test result for (soil+ 0.5 % SF,30mm) un cured

Axial deformation (mm)	Unit strain ϵ = ΔH/ΔHo	axial strain (%)	Proving Ring reading	Load in [kN]	Cross - sectional Area A = Ao/1-ϵ	stress in [kN/m^2]
0.00	0.0000	0	0.0	0.0000	0.00100	0.0
0.20	0.0026	0.263158	14	0.0214	0.00100	21.4
0.40	0.0053	0.526316	21	0.0321	0.00101	32.0
0.60	0.0079	0.789474	27	0.0413	0.00101	41.0
0.80	0.0105	1.052632	33	0.0505	0.00101	50.0
1.00	0.0132	1.315789	39	0.0597	0.00101	58.9
1.20	0.0158	1.578947	47	0.0719	0.00102	70.8
1.40	0.0184	1.842105	56	0.0857	0.00102	84.1
1.60	0.0211	2.105263	61	0.0933	0.00102	91.4
1.80	0.0237	2.368421	69	0.1056	0.00102	103.1
2.00	0.0263	2.631579	78	0.1193	0.00103	116.2
2.20	0.0289	2.894737	90	0.1377	0.00103	133.7
2.40	0.0316	3.157895	102	0.1561	0.00103	151.1
2.60	0.0342	3.421053	105	0.1607	0.00104	**155.2**
2.80	0.0368	3.684211	104	0.1591	0.00104	153.3
3.00	0.0395	3.947368	103	0.1576	0.00104	151.4

Table I-24 UCS test result for (soil+ 0.5 % SF,30mm) 7 days cured

Axial deformation (mm)	Unit strain ϵ = ΔH/ΔHo	axial strain (%)	Proving Ring reading	Load in [kN]	Cross - sectional Area A = Ao/1-ϵ	stress in [kN/m^2]
0.00	0.0000	0	0	0.0000	0.00100	0.0
0.20	0.0026	0.263158	15	0.0230	0.00100	22.9
0.40	0.0053	0.526316	23	0.0352	0.00101	35.0
0.60	0.0079	0.789474	29	0.0444	0.00101	44.0
0.80	0.0105	1.052632	36	0.0551	0.00101	54.5
1.00	0.0132	1.315789	42	0.0643	0.00101	63.4
1.20	0.0158	1.578947	47	0.0719	0.00102	70.8
1.40	0.0184	1.842105	54	0.0826	0.00102	81.1
1.60	0.0211	2.105263	62	0.0949	0.00102	92.9
1.80	0.0237	2.368421	67	0.1025	0.00102	100.1
2.00	0.0263	2.631579	78	0.1193	0.00103	116.2
2.20	0.0289	2.894737	90	0.1377	0.00103	133.7
2.40	0.0316	3.157895	102	0.1561	0.00103	151.1
2.60	0.0342	3.421053	107	0.1637	0.00104	158.1
2.80	0.0368	3.684211	112	0.1714	0.00104	165.0
3.00	0.0395	3.947368	116	0.1775	0.00104	170.5
3.20	0.0421	4.210526	117	0.1790	0.00104	**171.5**

3.40	0.0447	4.473684	116	0.1775	0.00105	169.5
3.60	0.0474	4.736842	115	0.1760	0.00105	167.6

Table I-25 UCS test result for (soil+ 1 % SF,30mm) 7 uncured

Axial deformation (mm)	Unit strain ϵ = ΔH/ΔHo	axial strain (%)	Proving Ring reading	Load in [kN]	Cross - sectional Area A = Ao/1-ϵ	stress in [kN/m^2]
0.00	0	0	0.0	0.0000	0.00100	0.0
0.20	0.002632	0.263158	16	0.0245	0.00100	24.4
0.40	0.005263	0.526316	23	0.0352	0.00101	35.0
0.60	0.007895	0.789474	29	0.0444	0.00101	44.0
0.80	0.010526	1.052632	36	0.0551	0.00101	54.5
1.00	0.013158	1.315789	43	0.0658	0.00101	64.9
1.20	0.015789	1.578947	52	0.0796	0.00102	78.3
1.40	0.018421	1.842105	61	0.0933	0.00102	91.6
1.60	0.021053	2.105263	71	0.1086	0.00102	106.3
1.80	0.023684	2.368421	80	0.1224	0.00102	119.5
2.00	0.026316	2.631579	89	0.1362	0.00103	132.6
2.20	0.028947	2.894737	98	0.1499	0.00103	145.6
2.40	0.031579	3.157895	104	0.1591	0.00103	154.1
2.60	0.034211	3.421053	106	0.1622	0.00104	156.6
2.80	0.036842	3.684211	108	0.1652	0.00104	159.2
3.00	0.039474	3.947368	109	0.1668	0.00104	**160.2**
3.20	0.042105	4.210526	108	0.1652	0.00104	158.3

Table I-26 UCS test result for (soil+ 1 % SF,30mm) 7 days cured

Axial deformation (mm)	Unit strain ϵ = ΔH/ΔHo	axial strain (%)	Proving Ring reading	Load in [kN]	Cross - sectional Area A = Ao/1-ϵ	stress in [kN/m^2]
0.00	0.000000	0	0	0.0000	0.00100	0.0
0.20	0.002632	0.263158	16	0.0245	0.00100	24.4
0.40	0.005263	0.526316	25	0.0383	0.00101	38.0
0.60	0.007895	0.789474	32	0.0490	0.00101	48.6
0.80	0.010526	1.052632	37	0.0566	0.00101	56.0
1.00	0.013158	1.315789	47	0.0719	0.00101	71.0
1.20	0.015789	1.578947	62	0.0949	0.00102	93.4
1.40	0.018421	1.842105	70	0.1071	0.00102	105.1
1.60	0.021053	2.105263	76	0.1163	0.00102	113.8
1.80	0.023684	2.368421	87	0.1331	0.00102	130.0
2.00	0.026316	2.631579	93	0.1423	0.00103	138.5
2.20	0.028947	2.894737	103	0.1576	0.00103	153.0
2.40	0.031579	3.157895	110	0.1683	0.00103	163.0
2.60	0.034211	3.421053	113	0.1729	0.00104	167.0
2.80	0.036842	3.684211	118	0.1805	0.00104	173.9
3.00	0.039474	3.947368	120	0.1836	0.00104	176.4

3.20	0.042105	4.210526	123	0.1882	0.00104	180.3
3.40	0.044737	4.473684	125	0.1913	0.00105	**182.7**
3.60	0.047368	4.736842	124	0.1897	0.00105	180.7
3.80	0.05	5	123	0.1882	0.00105	178.8

Table I-27 UCS test result for (soil+ 1.5 % SF,30mm) un cured

Axial deformation (mm)	Unit strain ϵ = ΔH/ΔHo	axial strain (%)	Proving Ring reading	Load in [kN]	Cross - sectional Area A = Ao/1-ϵ	stress in [kN/m^2]
0.00	0.0000	0	0.0	0.0000	0.00100	0.0
0.20	0.0026	0.263158	10	0.0153	0.00100	15.3
0.40	0.0053	0.526316	19	0.0291	0.00101	28.9
0.60	0.0079	0.789474	27	0.0413	0.00101	41.0
0.80	0.0105	1.052632	35	0.0536	0.00101	53.0
1.00	0.0132	1.315789	42	0.0643	0.00101	63.4
1.20	0.0158	1.578947	51	0.0780	0.00102	76.8
1.40	0.0184	1.842105	63	0.0964	0.00102	94.6
1.60	0.0211	2.105263	71	0.1086	0.00102	106.3
1.80	0.0237	2.368421	79	0.1209	0.00102	118.0
2.00	0.0263	2.631579	85	0.1301	0.00103	126.6
2.20	0.0289	2.894737	90	0.1377	0.00103	133.7
2.40	0.0316	3.157895	98	0.1499	0.00103	145.2
2.60	0.0342	3.421053	102	0.1561	0.00104	**150.7**
2.80	0.0368	3.684211	101	0.1545	0.00104	148.8

Table I-28 UCS test result for (soil+ 1.5 % SF,30mm) 7 days cured

Axial deformation (mm)	Unit strain ϵ = ΔH/ΔHo	axial strain (%)	Proving Ring reading	Load in [kN]	Cross - sectional Area A = Ao/1-ϵ	stress in [kN/m^2]
0.00	0.0000	0	0	0.0000	0.00100	0.0
0.20	0.0026	0.263158	14	0.0214	0.00100	21.4
0.40	0.0053	0.526316	24	0.0367	0.00101	36.5
0.60	0.0079	0.789474	32	0.0490	0.00101	48.6
0.80	0.0105	1.052632	38	0.0581	0.00101	57.5
1.00	0.0132	1.315789	47	0.0719	0.00101	71.0
1.20	0.0158	1.578947	56	0.0857	0.00102	84.3
1.40	0.0184	1.842105	65	0.0995	0.00102	97.6
1.60	0.0211	2.105263	73	0.1117	0.00102	109.3
1.80	0.0237	2.368421	85	0.1301	0.00102	127.0
2.00	0.0263	2.631579	92	0.1408	0.00103	137.1
2.20	0.0289	2.894737	100	0.1530	0.00103	148.6
2.40	0.0316	3.157895	106	0.1622	0.00103	157.1
2.60	0.0342	3.421053	109	0.1668	0.00104	161.1
2.80	0.0368	3.684211	115	0.1760	0.00104	**169.5**
3.00	0.0395	3.947368	114	0.1744	0.00104	167.5
3.20	0.0421	4.210526	113	0.1729	0.00104	165.6

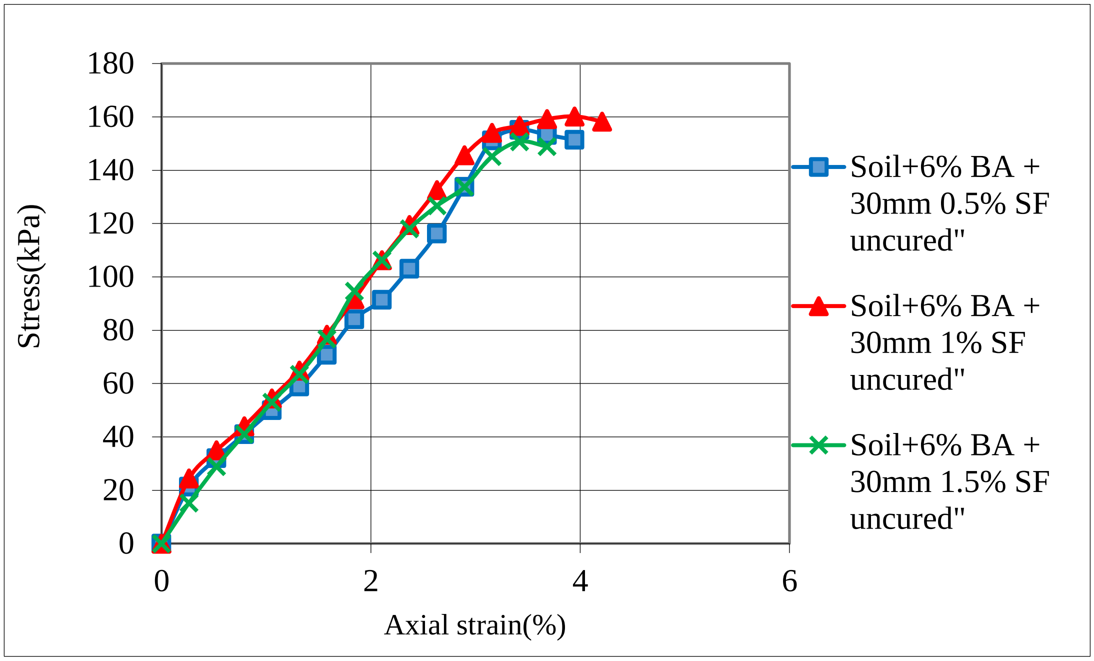

Figure I-3 Stress-Strain relationship of soil reinforced with 30mm length uncured

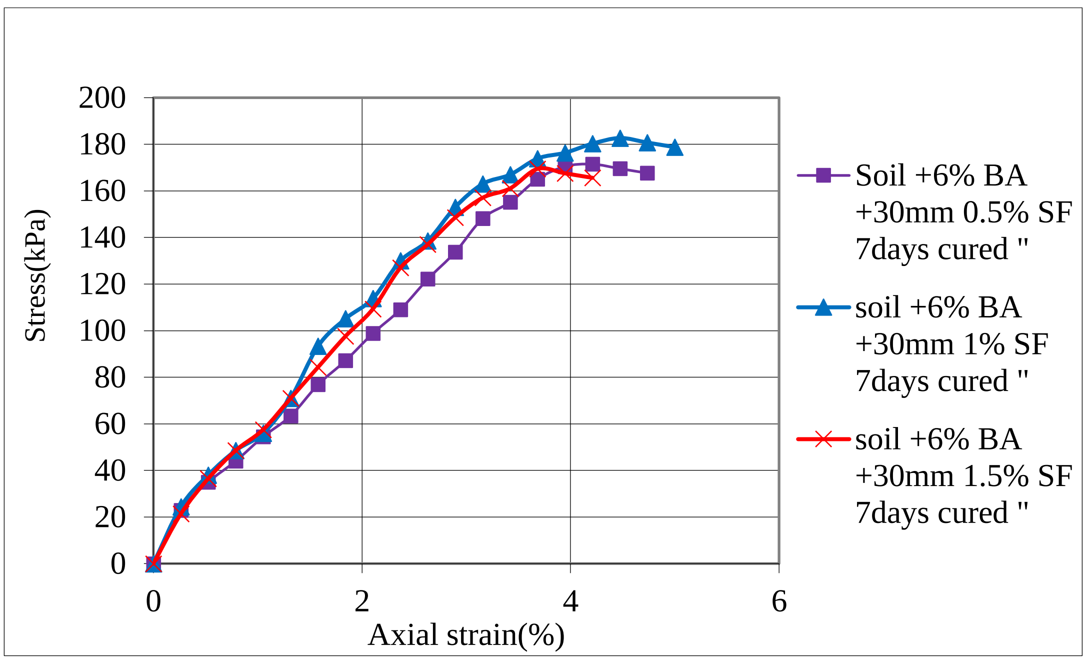

Figure I-4 Stress-Strain relationship of soil reinforced with 30mm length 7 days cured

Appendix : J One-Dimensional Consolidation Test Result

Table J-1 Specimen data before test and after test for expansive soil

Before test			
Weight of sample & Ring (gm)	252.05	Specific Gravity (G_s)	2.75
Weight of Ring (gm)	111.10	Sample Diameter (D) (mm)	75.00
Weight of sample (gm)	153.00	Sample Thickness (Ho) (mm)	20.00
Weight of Dry Sample (gm)	99.00	Area (A) (cm^2)	44.18
Weight of Initial Moisture (gm)	54.00	Volume (V) (cm^3)	88.37
Initial Moisture content (M_o) (%)	54.55	Bulk Density ($/\gamma_b$) (gm/cm^3)	1.731
		Dry Density ($/\gamma_d$) (gm/cm^3)	1.120
Initial Void Ratio: $e_o = (G_s/\gamma_d)-1$	1.455	`	
Height of Solids: $Hs = H_o/(1+e_o)$ (mm)	8.148		
Initial Saturation: $So = (M_o*G_s)/e_o$ (%)	103.11		
After test			
Weight of Sample + Ring +Can (gm)	257.10	Overall settlement (mm)	3.390
Weight of Dry Sample + Ring +Can (gm)	222.99	Volume change (cm^3)	14.98
Weight of Ring + Can (gm)	123.99	Final Volume (cm^3)	73.39
Weight of Wet Sample (gm)	133.11	Final Bulk Density (gm/cm^3)	1.814
Weight of Dry Sample (gm)	99.00	Final Dry Density (gm/cm^3)	1.349
Weight of Final Moisture (gm)	34.11	Final Void Ratio:(e_f)	1.039
Final Moisture Content (M_f) (%)	34.45	Final saturation (sf= Mf*Gs)/ef)	91.23

Table J-2 One-Dimensional consolidation test result for expansive soil

Sample diameter (D)=75mm					Height(H_O)			20 mm		
Height of solids $H_{S=}$8.148mm					Initial Voids ratio e_o			1.455		
Voids Ratio					Compressibility			Coefficient of consolidation		
					Incremental					
Increment	Pressure (kPa)	Cumulative compression (ΔH) mm	Consolidated height H = H_O-ΔH mm	Voids Ratio e=(H-HS)/Hs	Height change ΔH mm	Pressure change Δp kPa	M_v =(ΔH/H) *(1000/ Δp) m^2/MN	t_{90} min	H=1/2(H1+ H_2)	C_v=(0.848*H^2)/t_{90} m^2/year
0	0	0.000	20.000	1.455				-		-
					0.496	160	0.155			
1	160	0.496	19.504	1.394				144	19.75	2.30

					0.910	160	0.292			
2	320	1.406	18.594	1.282				256	19.05	1.20
					1.204	320	0.202			
3	640	2.610	17.390	1.134				400	17.99	0.69
					0.998	640	0.090			
4	1280	3.608	16.392	1.012				441	16.89	0.55
					0.990	1280	0.047			
5	2560	4.598	15.402	0.890				484	15.90	0.44
					0.558	1920	0.019			
6	640	4.040	15.960	0.959						
					0.650	480	0.085			
7	160	3.390	16.610	1.039						

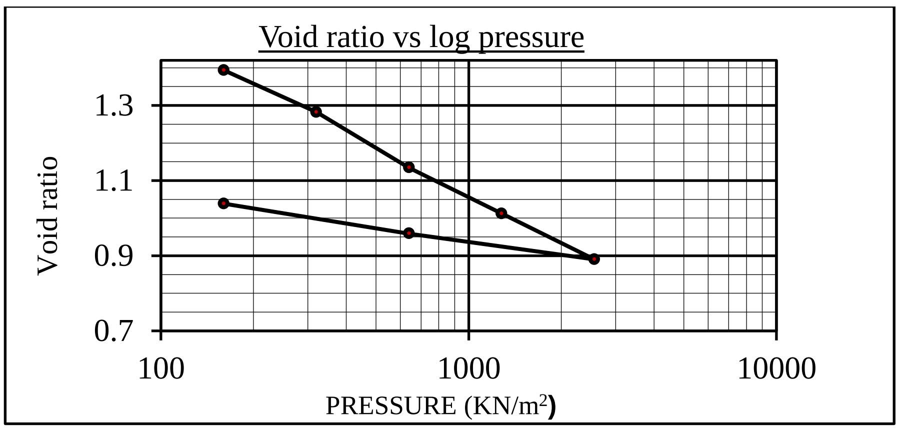

Figure J-1 Void ratio versus log pressure for natural soil

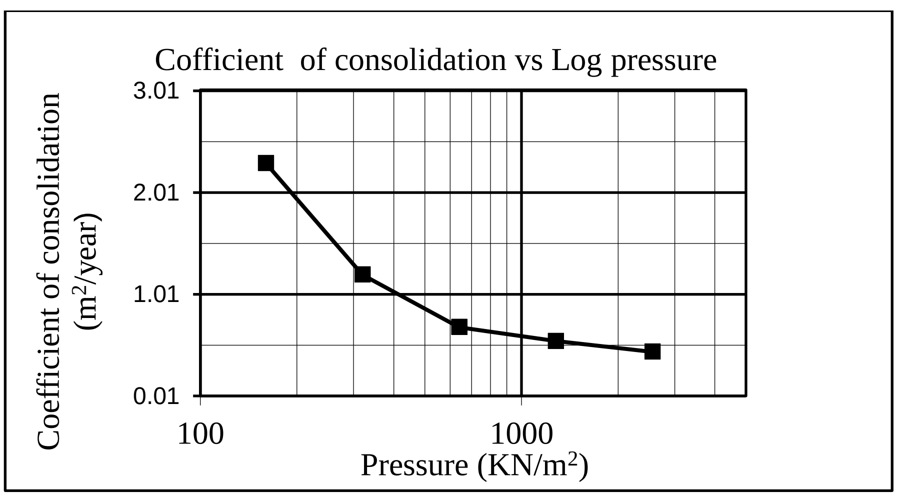

Figure J-2 Coefficient of consolidation vs Log pressure natural soil

Sample calculation for compression and recompression index

Compression index

e1 = 1.394 P1 = 160 P2 = 2560

e2 = 0.890 Cc=(e1-e2)/log(P2/P1) =0.418

Recompression index

e1 = 1.038617969 P1=160 Cr= (e1-e2)/log(P2/P1) =0.123

e2 = 0.890354844 P2= 2560

Table J-3 Specimen data before test and after test natural expansive soil with 3% BA

Before test			
Weight of sample & Ring (gm)	243.50	Specific Gravity (Gs)	2.68
Weight of Ring (gm)	115.10	Sample Diameter (D) (mm)	75.00
Weight of sample (gm)	128.40	Sample Thickness (H_o) (mm)	20.00
Weight of Dry Sample (gm)	96.99	Area (A) (cm^2)	44.18
Weight of Initial Moisture (gm)	31.41	Volume (V) (cm^3)	88.37
Initial Moisture content (M_o) (%)	32.38	Bulk Density (γb) (gm/cm^3)	1.453
		Dry Density (γd) (gm/cm^3)	1.098
Initial Void Ratio: $e_o = (G_s/\gamma d)-1$	1.442	`	
Height of Solids: $H_s = H_o/(1+e_o)$ (mm)	8.191		
Initial Saturation: $S_o = (M_o*G_s)/e_o$ (%)	60.20		
After test			
Weight of Sample + Ring +Can (gm)	269.00	Overall settlement (mm)	3.498
Weight of Dry Sample + Ring +Can (gm)	234.99	Volume change (cm^3)	15.46
Weight of Ring + Can (gm)	138.00	Final Volume (cm^3)	72.91
Weight of Wet Sample (gm)	131.00	Final Bulk Density (gm/cm^3)	1.797
Weight of Dry Sample (gm)	96.99	Final Dry Density (gm/cm^3)	1.330
Weight of Final Moisture (gm)	34.01	Final Void Ratio:(e_f)	1.015
Final Moisture Content (M_f) (%)	35.07	Final Saturation: $S_f = (M_f*G_s)/e_f$ (%)	92.61

Table J-4 One-Dimensional consolidation test result for natural expansive soil with 3 %BA

Sample diameter (D)=75mm				Height (H_O)			20 mm			
Height of solids H_{S}=8.148mm				Initial Voids ratio e_o			1.455			
Voids Ratio					Compressibility			Coefficient of consolidation		
					Incremental					
Increment N°	Pressure kPa	Cumulative compression (ΔH) mm	Consolidated height H = H_O-ΔH mm	Voids Ratio e=(H-HS)/Hs	Height change ΔH mm	Pressure change Δp kPa	m_v =(ΔH/H1)*(1000/Δp) m^2/MN	t_{90} min	H = 1/2(H1+ H2)	C_v = (0.848 *H^2)/t_{90} m^2/year
0	0	0.000	20.000	1.442				-		-
					0.732	160	0.229			
1	160	0.732	19.268	1.352				117	19.634	2.79
					0.898	160	0.291			
2	320	1.630	18.370	1.243				237	18.819	1.27
					1.170	320	0.199			
3	640	2.800	17.200	1.100				324	17.785	0.83
					0.942	640	0.086			
4	1280	3.742	16.258	0.985				361	16.729	0.66
					0.910	1280	0.044			
5	2560	4.652	15.348	0.874				400	15.803	0.53
					0.598	1920	0.020			
6	640	4.054	15.946	0.947						
					0.556	480	0.073			
7	160	3.498	16.502	1.015						

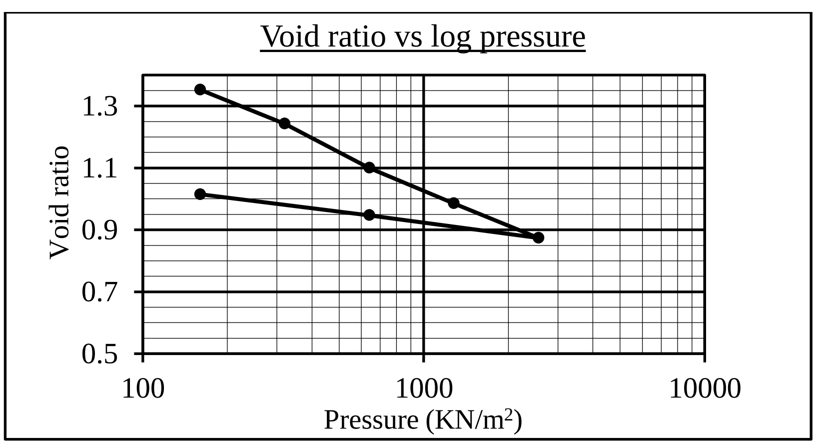

Figure J-3 Void ratio versus log pressure for soil with 3 %BA

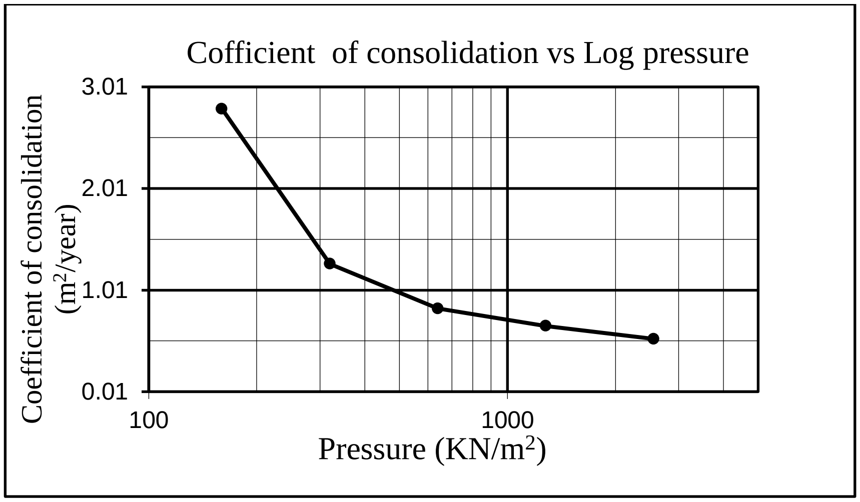

Figure J-4 Coefficient of consolidation vs Log pressure soil with 3 %BA

Table J-5 Specimen data before test and after test soil with 6 %BA

Before test			
Weight of sample & Ring (gm)	241.50	Specific Gravity (G_s)	2.65
Weight of Ring (gm)	112.10	Sample Diameter (D) (mm)	75.00
Weight of sample (gm)	129.40	Sample Thickness (Ho) (mm)	20.00
Weight of Dry Sample (gm)	97.90	Area (A) (cm^2)	44.18
Weight of Initial Moisture (gm)	31.50	Volume (V) (cm^3)	88.37
Initial Moisture content (M_o) (%)	32.18	Bulk Density (γ_b) (gm/cm^3)	1.464
		Dry Density (γ_d) (gm/cm^3)	1.108
Initial Void Ratio: $e_o = (G_s/\gamma_d)-1$	1.392		
Height of Solids: $Hs = H_o/(1+e_o)$ (mm)	8.361		
Initial Saturation: $So = (M_o*G_s)/e_o$ (%)	61.25		
After test			
Weight of Sample + Ring +Can (gm)	262.50	Overall settlement (mm)	3.798
Weight of Dry Sample + Ring +Can (gm)	232.00	Volume change (cm^3)	16.78
Weight of Ring + Can (gm)	134.10	Final Volume (cm^3)	71.59
Weight of Wet Sample (gm)	128.40	Final Bulk Density (gm/cm^3)	1.794
Weight of Dry Sample (gm)	97.90	Final Dry Density (gm/cm3)	1.368
Weight of Final Moisture (gm)	30.50	Final Void Ratio:(ef)	0.938
Final Moisture Content (M_f) (%)	31.15	Final saturation($Sf=M_f*G_s)/e_f$ (%)	88.04

Table J-6 One-Dimensional consolidation test result for natural expansive soil with 6 %BA

Sample diameter (D) =75mm					Height H_O			20mm		
Height of solids H_S=8.361					Initial Voids ratio (e_o)			1.392		
Voids Ratio					Compressibility			Coefficient of consolidation		
					incremental					
Increment N°	Pressure kPa	Cumulative compression (ΔH) mm	Consolidated height H = H_O-ΔH mm	Voids Ratio e=(H-HS)/Hs	Height change ΔH mm	Pressure change Δp kPa	m_v =(ΔH/H1) *(1000/Δp) m²/MN	t_{90} min	H = 1/2(H1+H2)	C_v = (0.848*H²)/t_{90} m²/year
0	0	0.000	20.000	1.392				-		-
					0.998	160	0.312			
1	160	0.998	19.002	1.273				100.0	19.501	3.22
					0.862	160	0.284			
2	320	1.860	18.140	1.170				169.0	18.571	1.73
					1.032	320	0.178			
3	640	2.892	17.108	1.046				213.2	17.624	1.24
					0.908	640	0.083			
4	1280	3.800	16.200	0.938				317.0	16.654	0.74
					0.922	1280	0.044			
5	2560	4.722	15.278	0.827				342.2	15.739	0.61
					0.548	1920	0.019			
6	640	4.174	15.826	0.893						
					0.376	480	0.049			
7	160	3.798	16.202	0.938						

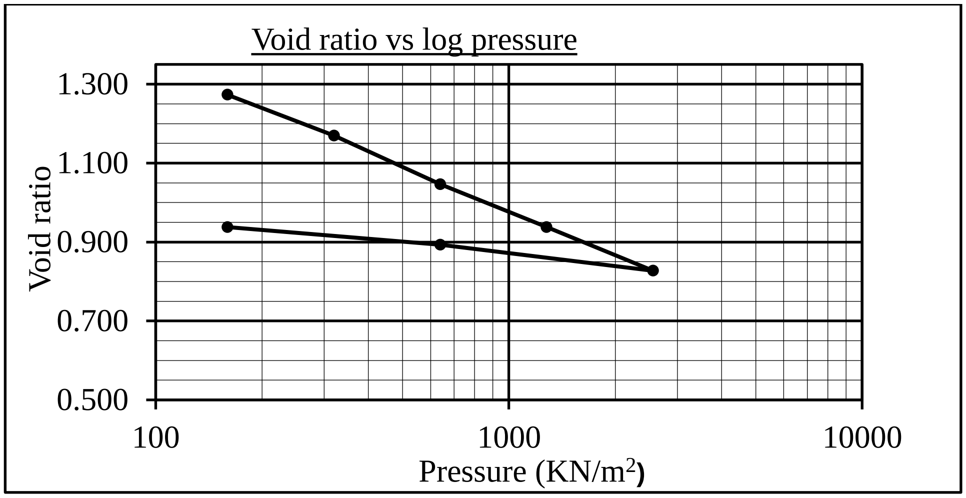

Figure J-5 Void ratio vs log pressure

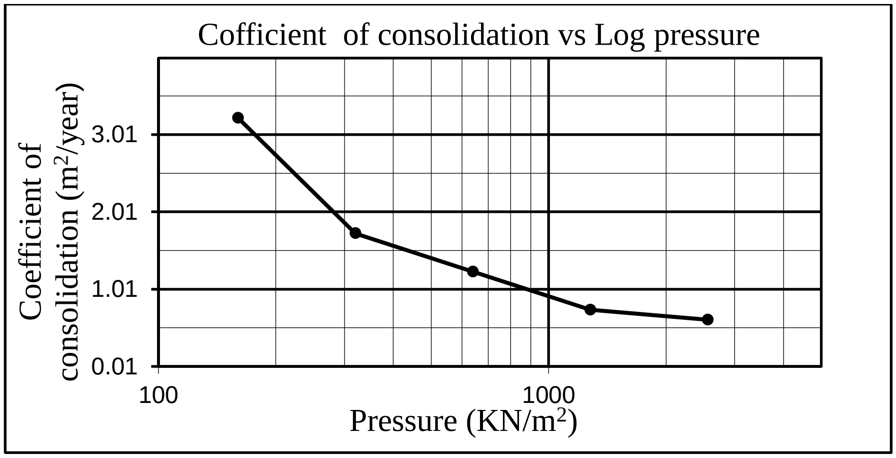

Figure J-6 Coefficient of consolidation vs log pressure

Table J-7 Specimen data before test and after test for soil with 9% BA

Before test			
Weight of sample & Ring (gm)	268.50	Specific Gravity (G_s)	2.64
Weight of Ring (gm)	113.10	Sample Diameter (D) (mm)	75.00
Weight of sample (gm)	155.40	Sample Thickness (H_o) (mm)	20.00
Weight of Dry Sample (gm)	97.20	Area (A) (cm^2)	44.18
Weight of Initial Moisture (gm)	58.20	Volume (V) (cm^3)	88.37
Initial Moisture content (M_o) (%)	59.88	Bulk Density (γ_b) (gm/cm^3)	1.759
		Dry Density (γ_d) (gm/cm_3)	1.100
Initial Void Ratio: $eo = (Gs/\gamma_d)-1$	1.400	`	
Height of Solids: $Hs = Ho/(1+e_o)$ (mm)	8.333		
Initial Saturation: $So = (Mo*G_s)/e_o$ (%)	112.90		
After test			
Weight of Sample + Ring +Can (gm)	284.50	Overall settlement (mm)	3.408
Weight of Dry Sample + Ring +Can (gm)	251.30	Volume change (cm^3)	15.06
Weight of Ring + Can (gm)	154.10	Final Volume (cm^3)	73.31
Weight of Wet Sample (gm)	130.40	Final Bulk Density (gm/cm^3)	1.779
Weight of Dry Sample (gm)	97.20	Final Dry Density (gm/cm^3)	1.326
Weight of Final Moisture (gm)	33.20	Final Void Ratio:(e_f)	0.991
Final Moisture Content (M_f) (%)	34.16	Final Saturation: $S_f = (M_f*G_s)/e_f$ (%)	90.98

Table J-8 One-Dimensional consolidation test result for soil with 9% BA

Sample diameter(D)=75mm					Height (H_0)=			20mm		
Height of solids H_S=8.333mm					Initial Void ratio e_0=			1.400mm		
Voids Ratio					Compressibility			Coefficient of consolidation		
					Incremental					
Increment N°	Pressure p kPa	Cumulative compression (ΔH) mm	Consolidated height $H = H_O - \Delta H$ mm	Voids Ratio $e = (H - H_S)/Hs$	Height change ΔH mm	Pressure change Δp Kpa	$m_v = (\Delta H/H_1)*(1000/\Delta p)$ m^2/MN	t_{90} min	$H = 1/2(H_1 + H_2)$	$Cv = (0.848*H^2)/t_{90}$ m^2/year
0	0	0.000	20.000	1.400				-		-
					0.692	160	0.216			
1	160	0.692	19.308	1.317				121	19.654	2.71
					0.890	160	0.288			
2	320	1.582	18.418	1.210				219	18.863	1.38
					1.150	320	0.195			
3	640	2.732	17.268	1.072				282	17.843	0.96
					0.970	640	0.088			
4	1280	3.702	16.298	0.956				328	16.783	0.73
					0.900	1280	0.043			
5	2560	4.602	15.398	0.848				361	15.848	0.59
					0.578	1920	0.020			
6	640	4.024	15.976	0.917						
					0.616	480	0.080			
7	160	3.408	16.592	0.991						

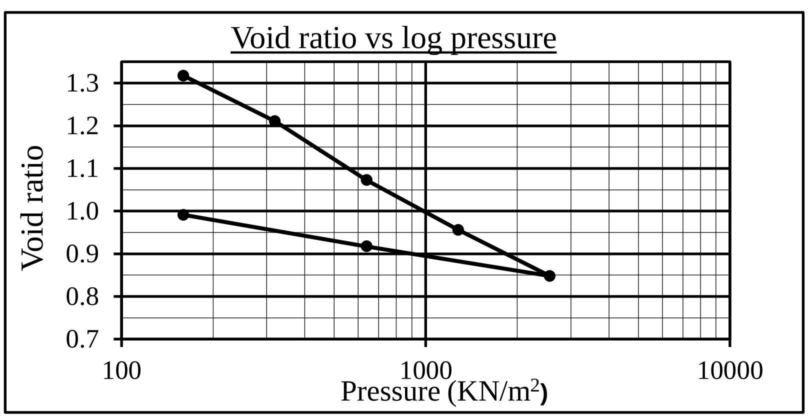

Figure J-7 Void ratio vs log pressure graph for soil+ 9% BA

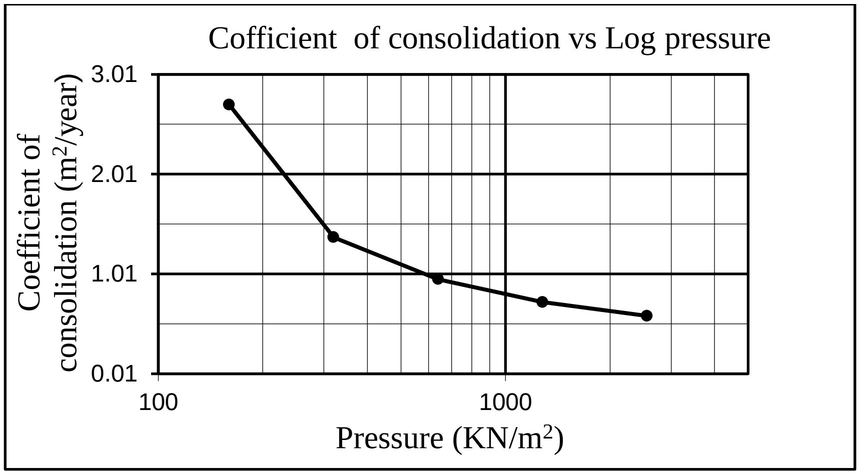

Figure J-8 coefficient of consolidation vs log pressure graph for soil+ 9% BA

Table J-9 Specimen data before test and after test BA stabilized soil with 20mm length 0.5% SF

Before test			
Weight of sample & Ring (gm)	260.50	Specific Gravity (G_s)	2.63
Weight of Ring (gm)	112.10	Sample Diameter (D) (mm)	75.00
Weight of sample (gm)	148.40	Sample Thickness (H_o) (mm)	20.00
Weight of Dry Sample (gm)	97.37	Area (A) (cm^2)	44.18
Weight of Initial Moisture (gm)	51.03	Volume (V) (cm^3)	88.37
Initial Moisture content (Mo) (%)	52.41	Bulk Density (γ_b) (gm/cm^3)	1.679
		Dry Density (γ_d) (gm/cm^3)	1.102
Initial Void Ratio: $e_o = (G_s/\gamma_d)-1$	1.387	`	
Height of Solids: $Hs = Ho/(1+e_o)$ (mm)	8.379		
Initial Saturation: $So = (Mo*G_s)/e_o$ (%)	99.38		
After test			
Weight of Sample + Ring +Can (gm)	255.50	Overall settlement (mm)	3.720
Weight of Dry Sample + Ring +Can (gm)	221.21	Volume change (cm^3)	16.44
Weight of Ring + Can (gm)	123.84	Final Volume (cm^3)	71.93
Weight of Wet Sample (gm)	131.66	Final Bulk Density (gm/cm^3)	1.830
Weight of Dry Sample (gm)	97.37	Final Dry Density (gm/cm^3)	1.354
Weight of Final Moisture (gm)	34.29	Final Void Ratio:(e_f)	0.943
Final Moisture Content (Mf) (%)	35.22	Final saturation (sf= Mf*Gs)/ef)	98.23

Table J-10 One-Dimensional consolidation test result for BA stabilized soil with 20mm length 0.5% SF

Sample diameter(D)=75mm					Height (H_o) = 20 mm					
Height of solid (H_s)=8.379mm					Initial void ratio (e_o) = 1.387					
Voids Ratio					Compressibility			Coefficient of consolidation		
					Incremental					
Increment N^o	Pressure p kPa	Cumulative compression (ΔH) mm	Consolidated height H = H_O-ΔH mm	Voids Ratio e=(H-HS)/Hs	Height change ΔH mm	Pressure change Δp kPa	M_v =(ΔH/H_1) *(1000/Δp) m^2/MN	t_{90} min	H = 1/2(H_1+H_2)	C_v =(0.848 *H^2)/t_{90} m^2/year
0	0	0.000	20.00	1.387				-		-
					1.098	160	0.343			
1	160	1.098	18.90	1.256				96	19.45	3.34
					0.888	160	0.294			
2	320	1.986	18.01	1.150				145	18.46	1.99
					0.982	320	0.170			
3	640	2.968	17.03	1.033				230	17.52	1.13
					0.740	640	0.068			
4	1280	3.708	16.29	0.944				301	16.66	0.78
					0.890	1280	0.043			
5	2560	4.598	15.40	0.838				334	15.85	0.64
					0.282	1920	0.010			
6	640	4.316	15.68	0.872						
					0.596	480	0.079			
7	160	3.720	16.28	0.943						

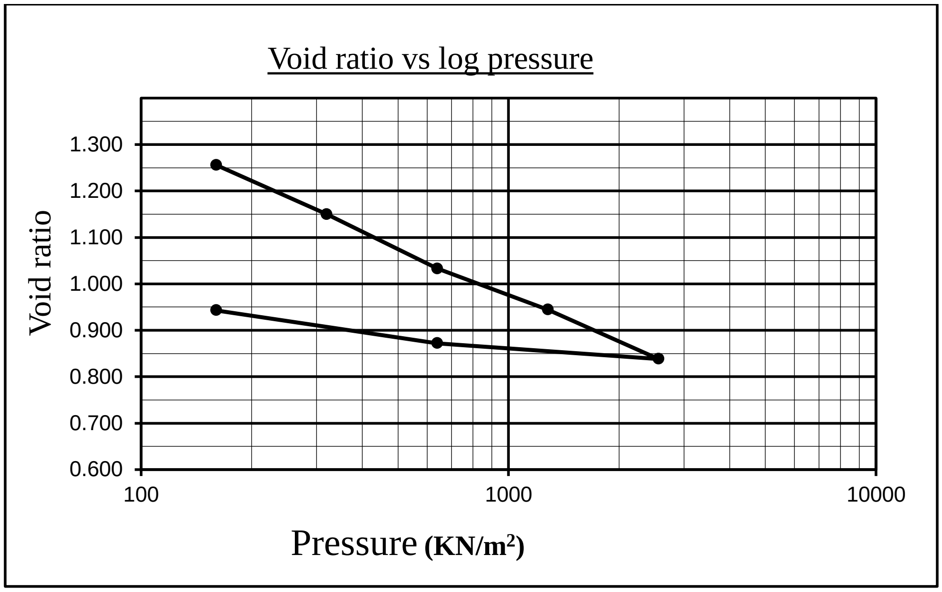

Figure J-9 Void ratio vs log pressure graph for 6% BA with 0.5% SF ,20mm

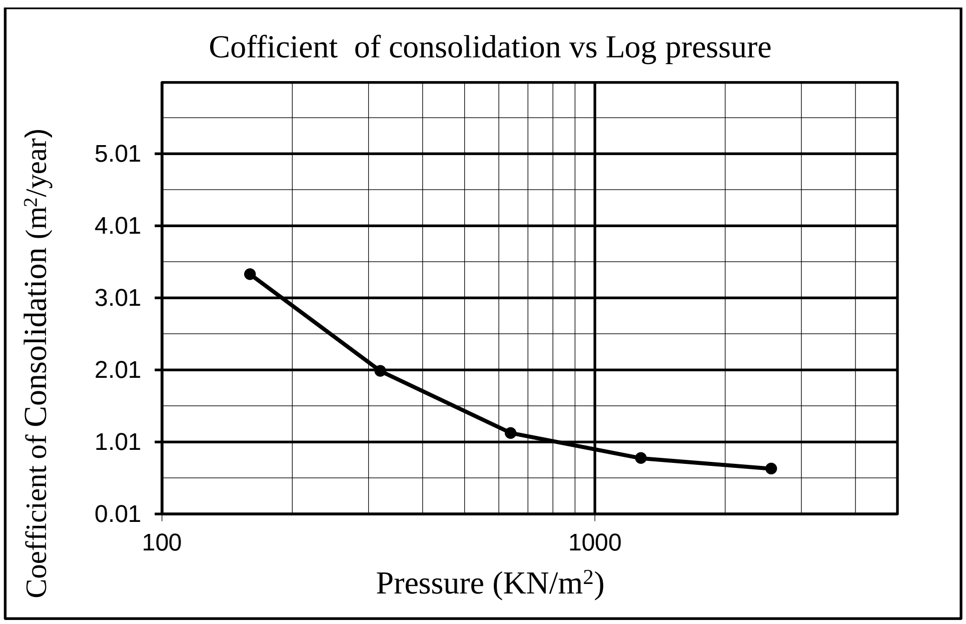

Figure J-10 coefficient of consolidation vs log pressure graph for 6% BA with 0.5% SF ,20mm

Table J-11 Specimen data before test and after test for BA stabilized soil with 20mm length 1 % SF

Before test			
Weight of sample & Ring (gm)	261.50	Specific Gravity (G_s)	2.62
Weight of Ring (gm)	113.10	Sample Diameter (D) (mm)	75.00
Weight of sample (gm)	148.40	Sample Thickness (Ho) (mm)	20.00
Weight of Dry Sample (gm)	102.89	Area (A) (cm^2)	44.18
Weight of Initial Moisture (gm)	45.51	Volume (V) (cm^3)	88.37
Initial Moisture content (M_o) (%)	44.23	Bulk Density (γ_b) (gm/cm^3)	1.679
		Dry Density (γ_d) (gm/cm^3)	1.164
Initial Void Ratio: $e_o = (Gs/\gamma_d)-1$	1.250	`	
Height of Solids: $Hs = H_o/(1+e_o)$ (mm)	8.888		
Initial Saturation: $So = (M_o*G_s)/e_o$ (%)	92.69		
After test			
Weight of Sample + Ring +Can (gm)	295.50	Overall settlement (mm)	3.194
Weight of Dry Sample + Ring +Can (gm)	255.90	Volume change (cm^3)	14.11
Weight of Ring + Can (gm)	153.01	Final Volume (cm^3)	74.26
Weight of Wet Sample (gm)	142.49	Final Bulk Density (gm/cm^3)	1.919
Weight of Dry Sample (gm)	102.89	Final Dry Density (gm/cm^3)	1.386
Weight of Final Moisture (gm)	39.60	Final Void Ratio:(e_f)	0.891
Final Moisture Content (M_f) (%)	38.49	Final saturation (sf= Mf*Gs)/ef)	113.19

Table J-12 One-Dimensional consolidation test result for BA stabilized soil with 20mm length 1 % SF

Sample diameter(D)=75mm					Height (H_o) = 20 mm					
Height of solid (H_s)=8.888mm					Initial void ratio (e_o) = 1.250					
Voids Ratio					Compressibility			Coefficient of consolidation		
Increm ent N°	Pressu re p kPa	Cumula tive compre ssion (ΔH) mm	Consoli dated height H = H_O- ΔH mm	Voids Ratio e=(H-HS)/Hs	Incremental Heigh t chang e ΔH mm	Incremental Pressur e change Δp kPa	m_v =($\Delta H/H_1$) *(1000/ Δp) m^2/MN	t_{90} min	H = 1/2(H_1+ H_2)	C_v=(0.848 *H^2)/t_{90} m^2/year
0	0	0.000	20.00	1.250				-		-
					0.998	160	0.312			
1	160	0.998	19.00	1.138				81	19.501	3.98
					0.838	160	0.276			
2	320	1.836	18.16	1.044				100	18.583	2.93
					0.912	320	0.157			
3	640	2.748	17.25	0.941				144	17.708	1.85
					0.722	640	0.065			
4	1280	3.470	16.53	0.860				210	16.891	1.15
					0.642	1280	0.030			
5	2560	4.112	15.89	0.788				296	16.209	0.75
					0.434	1920	0.014			
6	640	3.678	16.32	0.836						
					0.484	480	0.062			
7	160	3.194	16.81	0.891						

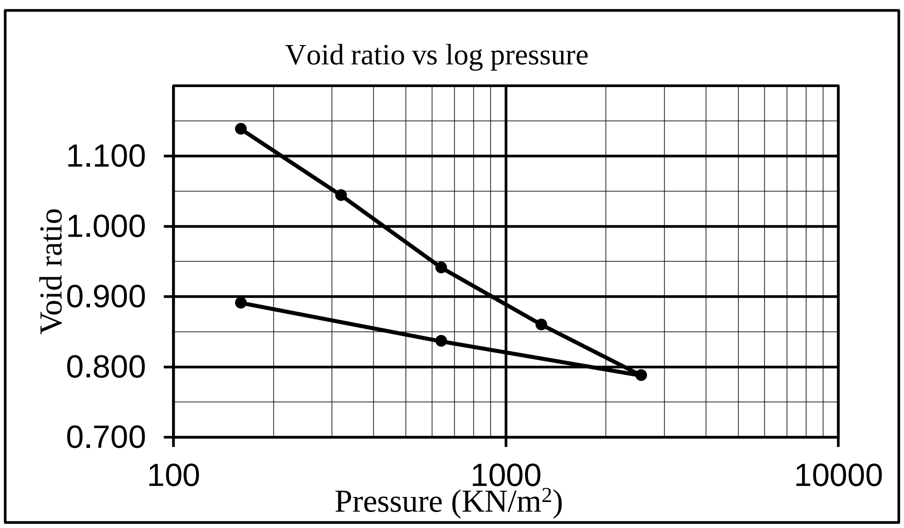

Figure J-11 Void ratio vs log pressure graph for 6% BA with 1 % SF ,20mm

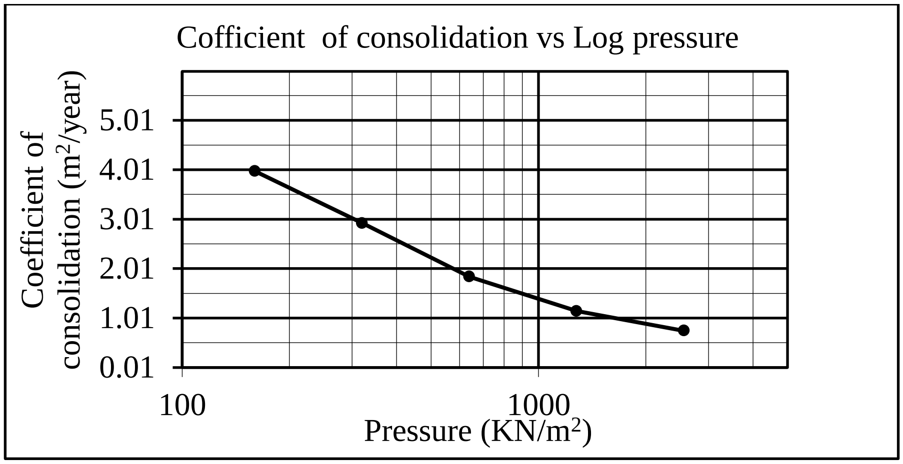

Figure J-12 coefficient of consolidation vs log pressure graph for 6% BA with 0.5% SF ,20mm

Table J-13 Specimen data before and after test for BA stabilized soil, 20mm length 1.5% SF

Before test			
Weight of sample & Ring (gm)	241.50	Specific Gravity (G_s)	2.61
Weight of Ring (gm)	112.10	Sample Diameter (D) (mm)	75.00
Weight of sample (gm)	128.95	Sample Thickness (Ho) (mm)	20.00
Weight of Dry Sample (gm)	96.83	Area (A) (cm^2)	44.18
Weight of Initial Moisture (gm)	32.12	Volume (V) (cm^3)	88.37
Initial Moisture content (Mo) (%)	33.17	Bulk Density (γb) (gm/cm^3)	1.459
		Dry Density (γd) (gm/cm^3)	1.096
Initial Void Ratio: $e_o = (G_s/\gamma_d)-1$	1.382	`	
Height of Solids: $Hs = H_o/(1+e_o)$ (mm)	8.397		
Initial Saturation: $So = (M_o*Gs)/e_o$ (%)	62.65		
After test			
Weight of Sample + Ring +Can (gm)	254.50	Overall settlement (mm)	3.870
Weight of Dry Sample + Ring +Can (gm)	221.84	Volume change (cm^3)	17.10
Weight of Ring + Can (gm)	125.01	Final Volume (cm^3)	71.27
Weight of Wet Sample (gm)	129.49	Final Bulk Density (gm/cm^3)	1.817
Weight of Dry Sample (gm)	96.83	Final Dry Density (gm/cm^3)	1.359
Weight of Final Moisture (gm)	32.66	Final Void Ratio:(e_f)	0.921
Final Moisture Content (M_f) (%)	33.73	Final saturation(sf= Mf*Gs)/ef)	95.58

Table J-14 One-Dimensional consolidation test result for BA stabilized soil , 20mm 1.5% SF

Sample diameter (D)=75 mm					Height $H_{O=}$			20.0 mm		
Height of solids H_S =8.397 mm					Initial Voids ratio e_o =			1.382		
Voids Ratio					Compressibility			Coefficient of consolidation		
Increment	Pressure p kPa	Cumulative compression (ΔH) mm	Consolidated height H = H_O- ΔH mm	Voids Ratio e=(H-HS)/Hs	Incremental: Height change ΔH mm	Incremental: Pressure change Δp kPa	m_v =($\Delta H/H_1$)*(1000/Δp) m^2/MN	t_{90} min	H = 1/2(H_1+ H_2)	c_v =(0.848*H^2)/t_{90} m^2/year
0	0	0.000	20.000	1.382				-		-
					1.350	160	0.422			
1	160	1.350	18.650	1.221				95	19.32	3.33
					0.980	160	0.328			
2	320	2.330	17.670	1.104				130	18.16	2.15
					0.874	320	0.155			
3	640	3.204	16.796	1.000				216	17.23	1.17
					0.802	640	0.075			
4	1280	4.006	15.994	0.905				280	16.39	0.81
					0.754	1280	0.037			
5	2560	4.760	15.240	0.815				320	15.62	0.65
					0.200	1920	0.007			
6	640	4.560	15.440	0.839						
					0.690	480	0.093			
7	160	3.870	16.130	0.921						

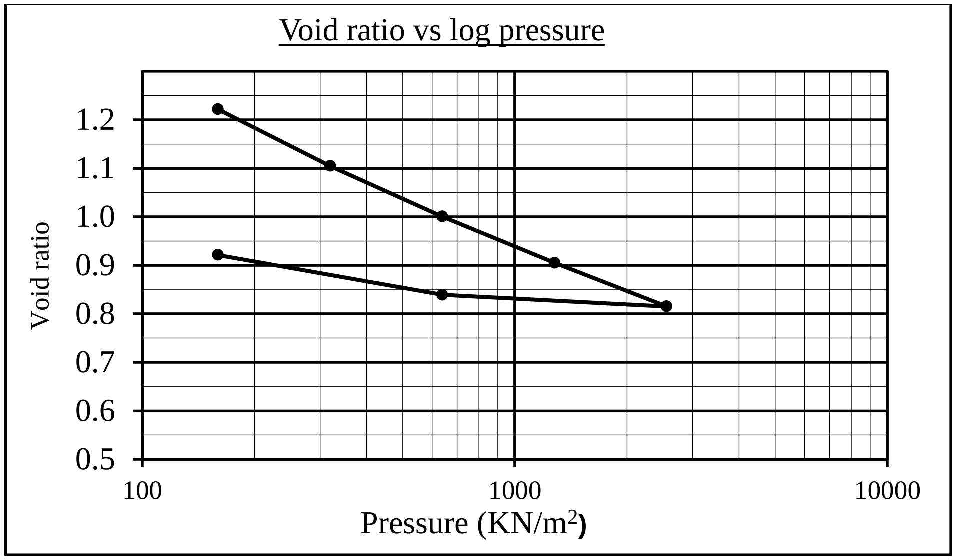

Figure J-13 Void ratio vs log pressure graph for 6% BA with 1.5% SF ,20mm

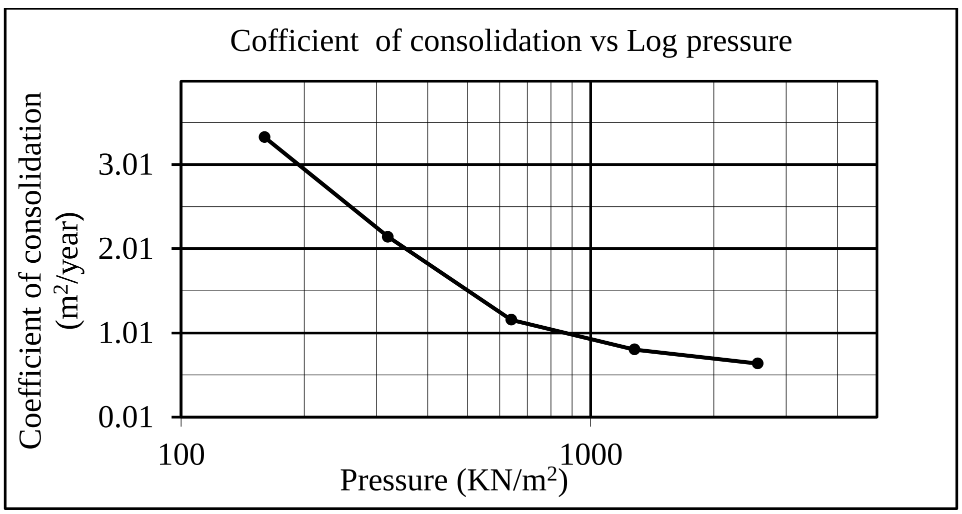

Figure J-14 Coefficient of consolidation vs log pressure graph for 6% BA with 1.5% SF,20mm